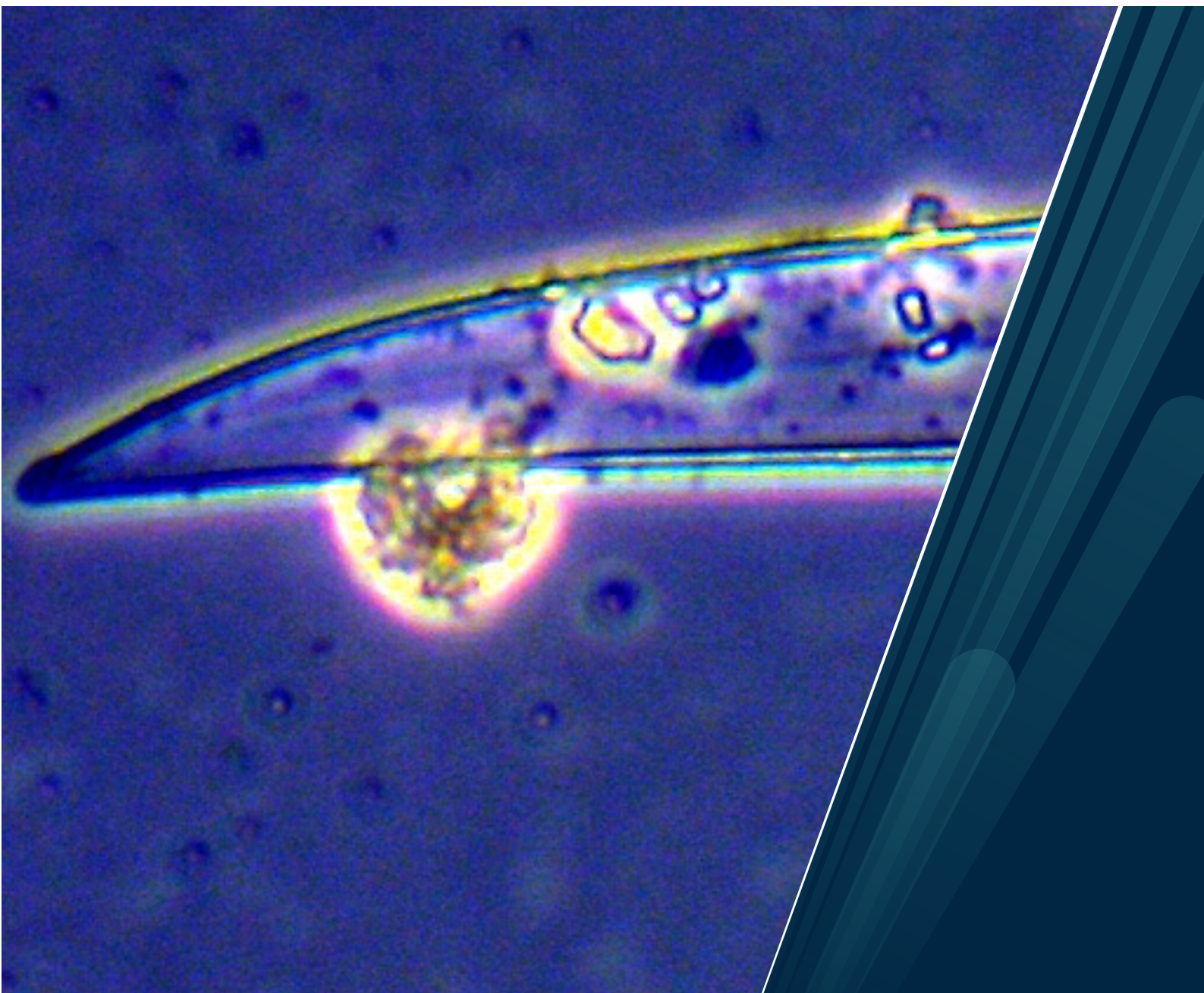**UiT** The Arctic University of Norway

The Norwegian College of Fishery Science

The Role of Silicate in the Parasitism of *Pleurosigma sp.* Diatoms by the Thraustochytrid *Phycophthorum isakeiti*

Daniel Jerome Finley Powers
Master's thesis in Marine Biotechnology (May 2020)
60 credits

UiT

Table of Contents

List of Tables

List of Figures

Forward

Abbreviations

AAPH	2,2′-azobis (2-methylpropionamide) dihydrochloride
AUC	Area under the curve
BHI	Brain heart infusion medium
BSA	Bovine serum albumin
CFU	Colony forming units
CO_2	Carbon dioxide
dH2O	Distilled water
DMSO	Dimethyl sulfoxide
DNA	Deoxyribonucleic acid
ELISA	Enzyme-linked immunosorbent assay
EN	Ectoplasmic net
ESI	Electrospray ionization
EU	Endotoxin units
FBS	Fetal bovine serum
FSW	Filtered seawater
GLM	General linear model
GPY	Glucose-peptone-yeast extract medium
H	Honda medium
HPLC	High performance liquid chromatography
ITS	Internal transcribed spacer
KMV	Modified Vishniac's medium
LC	Liquid culture
LPG	Labyrinthulea Phylogenetic Group
LPS	Lipopolysaccharides
MC	Mar Chiquita medium
MC-BHB	Mar Chiquita—brain heart broth
MeOH	Methanol
MH	Mueller Hinton Broth
MIC	Minimum inhibitory concentration

Ms	Mass spectrometry
N	Nitrogen
NO_3	Nitrate
OD	Optical Density
P	Phosphorus
PCR	Polymerase chain reaction
PMA	Phorbol 12-myrisate 13-acetate
PUFA	Polyunsaturated fatty acids
RPMI	Roswell Park Memorial Institute growth media
rRNA	Ribosomal ribonucleic acid
SiO_2	Silicate
SSA	Serum seawater agar medium,
SSU rRNA	Small subunit ribosomal ribonucleic acid
TBS	Tris-buffered saline
TC	Tissue culture
TE	Trolox equivalent standard units
TNF-α	Tumor necrosis factor
TPG	Thraustochytrid Phylogenetic Group
UHPLC/Q-TOF-MS	Ultra-high performance liquid chromatography-quadrupole time-of-flight mass spectrometry

Abstract

The recently described thraustochytrid diatom parasite *Phycophthorum isakeiti* has been isolated from the marine system of northern Norway (Hassett, 2020). Protist *P. isakeiti's* ecological role, biodiscovery potential, and interactions with a possible diatom host, *Pleurosigma* sp. remain largely unexplored. Here I present culturing experiments to test whether *P. isakeiti* is an obligate parasite. To supplement this analysis, incidence of infection and division was explored in a *P. isakeiti-Pleurosigma* sp. model system and assessed as a function of time in the presence of standard and reduced silicate conditions. Nutrient analysis and cell counting experiments spanning 15 to 31 days were conducted to investigate rates of free silicate uptake, free nitrate uptake, and the effect of *P. isakeiti* on rates of *Pleurosigma sp.* division and infection. Resin and ethyl acetate extractions were performed to characterize and screen for allelopathic chemicals involved in diatom defense or thraustochytrid parasitism. Lastly, bioassays were undertaken to detect whether any primary or secondary metabolites produced during host parasitism had biotechnologically relevant activities. Contrary to my hypothesis that *P. isakeiti* would be able to grow in the absence of its diatom host due to its presence in highly seasonal, light limited climates like northern Norway, I found no evidence to support a facultative strategy of *P. isakeiti* in a variety of tested medium. In coculturing experiments, the proportion of host *Pleurosigma* sp. cells dividing increased over time in the presence of the parasite, *P. isakeiti*. The silicate was depleted in media to a greater extent in parasitized cultures compared to non-parasitized cultures suggesting greater uptake of silicate in parasitized diatom populations. Two compounds, $C_{17}H_{27}NO_2$ (4.2422 min; 278.20923 m/z) and $C_{23}H_{16}O_2$ (9.2357min, 325.12084 *m/z*), were detected through liquid chromatography mass spectrophotometry exclusively in *Pleurosigma* sp. cultures parasitized by *P. isakeiti.* Limited bioactivity was detected in anti-bacterial assays against gram-positive *Staphylococcus aureus* and in the inhibition of TNF-a production during the anti-inflammation screening. No bioactivity was observed in the anti-cancer or biofilm assays. Experiments and observations in this thesis characterize the role of silicate in the parasitism of *Pleurosigma* sp. by *P. isakeiti.* The present research is multidisciplinary, spanning the fields of ecology and biodiscovery to yield novel, fundamental knowledge on a newly described species, *P. isakeiti* and to describe the interaction with its host, *Pleurosigma* sp., an ecologically important diatom species.

Keywords: Thraustochytrid, Pleurosigma, Silicate, Parasitism, Infection, Defense, Bioprospecting, Microalgae, Diatom, Marine, Coastal

1 Introduction

Twenty percent of the photosynthesis on Earth is carried out by microscopic, eukaryotic phytoplankton known as diatoms (Field et al. 1998). These photosynthetic organisms are found in waters throughout the world wherever sufficient light and nutrients persist. The word Diatom stems from the Greek diatomos, referring to the symmetry of their characteristic two-part silica cell walls (Kooistra et al. 2007). Annually, photosynthesis by marine diatoms (*Bacillariophyceae*) generates the same amount of organic carbon as all terrestrial rainforests combined (Armbrust 2009). Organic carbon photosynthesized by diatoms is consumed quickly in pelagic marine food webs (Okafor 2011). Organic carbon from bacterial and phytoplankton is transferred to protozooplankton, mesozooplankton, and gelatinous predators where it becomes available to mesopredators (Vargas 2007), supporting fisheries in coastal waters (Sime-Ngando 2012). In the open ocean, most of the organic matter transformed by diatoms sinks from the surface, a process known as vertical flux, and thus becomes available for consumption by organisms living in deeper-waters and remineralization (Spilling 2018; Rapp et al. 2018). A fraction of sinking organic matter eludes consumption and accumulates on the sea floor, (Armbrust 2009) where it is degraded and metabolized by a variety of microorganisms -- including thraustochytrids (Rapp et al. 2018). Thraustochytrids are protists present throughout the Earth's oceans (Raghukumar 2002; Pernice et al. 2015). Novel molecular diversity of Thraustochytrids has been found in heterotrophic microbial communities in the coastal waters of Hawaii, southern China, Greenland, Norway, Japan, India, and throughout the littoral zones of the world (Naganuma et al. 2006; Damare and Raghukumar 2008; Li et al. 2013; Liu et al. 2017).

Phytoplankton production is, in part, controlled by parasitism (Chambouvet et al. 2008; Alves-de-Souza et al. 2015). The focus of this thesis centers on the relationship between the first known thraustochytrid diatom parasite *Phycophthorum isakeiti* and its diatom host *Pleurosigma* sp. The observations presented in this thesis builds on the culturing and identification efforts of B. Hassett (2020). The unicellular, heterotrophic, eukaryotic parasite was isolated on the southern shore of Tromsøya, Norway with the diatom *Pleurosigma* sp. (Hassett 2020). Diatom hosts rely on silica for cell wall construction (Raven and Waite 2004), buoyancy (Gemmell et al. 2016), and key cues to initiate cell division (Dell'Aquila et al. 2017). Consequently, I hypothesized that silicate concentrations may play a role in diatom susceptibility to infection by parasites like *P. isakeiti*.

Changes in local and global silicate will likely adversely impact diatom biomass and primary productivity (Smetacek 1998). Thraustochytrid parasites, such as *P. isakeiti,* may produce metabolites specifically to aid in the infection of *Pleurosigma* sp. Similarly, diatoms can synthesize defense compounds in order to defend themselves against parasites (Raghukumar 1992; Pohnert et al. 2000). Bioactive compounds have been isolated from both thraustochytrids and diatoms (Rowland et al. 2001; Grossi et al. 2004; Byreddy 2016). Extractions and bioassays can illuminate whether potentially novel products generated by the interaction between the *P. isakeiti* parasite and its *Pleurosigma* sp. host have biotechnological relevance. Bioassays can be used effectively to screen for cytotoxicity and other medical application potential of the primary and secondary metabolites extracted from cocultures (Haefner 2003). Undertaking bioactivity assays can prevent long arduous culture upscaling for compound isolation and detailed chemical analysis. By generating preliminary bioassay results, future bioprospecting efforts can narrow in on specific activities and assess their value, before committing valuable time prolonged isolation procedures. Bioactive compounds have been found in both diatoms (Bhattarai et al. 2009) and thraustochytrids (Xie et al. 2017), thus bioactivity screening of *isakeiti* and *Pleurosigma* sp. infected cocultures of *Pleurosigma* sp. with *P. isakeiti* are prime candidates for bioprospecting.

1.1 Parasite Host Relationship

Thraustochytrids are almost exclusively considered saprobes of decaying organic matter and opportunistic parasites of marine animals (Scholz et al. 2016). Reports of pathogenic species of thraustochytrids on marine mollusks (McLean and Porter 1982, Bower et al. 1989, Whyte et al. 1994) seagrasses (Muehlstein et al. 1988) and flatworms (Schärer 2007) have raised interest in their relevance to ecosystems, especially under forecasted climate change. While parasitism of healthy diatoms is rarely reported, other protists closely related with *P. isakeiti* are regularly observed in other parasitic relationships with microalgae (Pan et al. 2017). While previous attempts to isolate *P. isakeiti* from its host have suggested it may be an obligate parasite, it is unknown if *P. isakeiti* has the capacity to live as a facultative parasite during winter seasons (Hassett 2020). Diatoms are well known to be highly infected in nature by stramenopilian zoosporic parasites (Rad-Menéndez et al. 2018) and parasitism among dense populations of the diatom *Guinardia flaccida* have been recorded as high as 65% (Tillmann et al. 2020) by *Pirsonia* and *Cryothecomonas*.

Thraustochytrid growth marginally decreases with chlorophyll *a* (Kimura et al. 2001, Raghukumar et al. 2001, Ueda et al. 2015). Marginal declines in chlorophyll *a* and thraustochytrid abundances may be explained by prevalent thraustochytrid parasitism (Hassett 2020). The identification of *P. isakeiti*-related sequences in sediment traps and at >200 m depth suggests diatom-associated vertical flux, as reported by Rapp et al. (2018). Parasites are known to physically follow their hosts in upwelling events (Gutiérrez 2016); however, their presence also suggests that the diatoms persist, survive, and scavenge throughout long dark winter months until spring-time blooms in Arctic regions (Hassett 2020). Thraustochytrid persistence within their diatom host population through extended seasonal variance suggest they may be facultative parasites, capable of a non-parasitic mode of survival.

1.1.1 Thraustochytrid Isolation

Isolation of parasites, outside of the presence of their hosts, is essential to tracing the origin of chemicals detected in parasitic coculture by techniques like mass spectrometry. A common method for isolating thraustochytrid zoospores, the flagellate asexual spore stage, involves baiting environmental substrate with sterile pine pollen in sterile seawater (Gupta 2013). Thraustochytrids break the hard sporopollenin layer of the pollen grain using ectoplasmic net (EN) elements (Damare 2019). The protists colonize the pollen and get their nutrition from the pollen interior (Bennett et al. 2017). Once the thraustochytrid cells are visible under the microscope, a pollen grain is plated on antibacterial agar medium to promote growth. Antibacterial agents are added to limit common contaminants (Damare 2019).

Within the coculture, compounds used by *Pleurosigma* sp. to defend against pathogens or *P. isakeiti* to parasitize are not distinguishable between the host and thraustochytrid because, without a juxtaposition of the profile of the metabolites the thraustochytrid produces when monocultured, no comparison with its host can be made. Determining the origin of primary or secondary metabolites extracted from a coculture requires monoculture analysis of both organisms, *Pleurosigma* sp. and *P. isakeiti,* individually.

1.1.2 Zoosporic Settlement

Elucidating the lifecycle of thraustochytrids and how specific life history events are synchronized with the diatom host is necessary for understanding ecological dynamics and assessing possible biodiscovery avenues. Parasitic thraustochytrids lose their flagella on contact with their host (Bowler et al. 1989). Shortly after settlement in the host cell wall, prior to the complete development of the endoplasmic net (EN), bothrosomes form, and extracellular lytic activity interferes with the host cell walls (Bowler et al. 1989). The damaged cells are lysed, and the parasite zoospores enter holes in the cell wall (Figure 1). The ENs of the bothrosomes develop and can release lytic agents (Iwata et al. 2017). Some EN elements have been observed deep within the cytoplasm of host cells (Coleman and Vestal 1987).
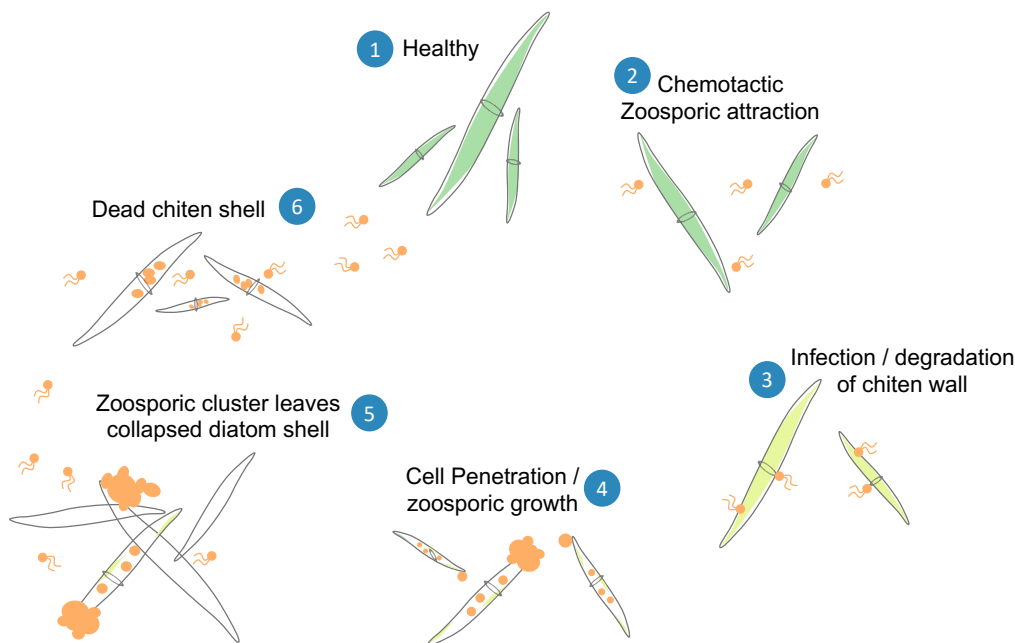
Figure 1 General sequence of *P. isakeiti* infection and proliferation among *Pleurosigma sp.* host. 1.) Healthy *Pleurosigma sp.* divide regularly and adhere to surfaces. 2.) Chemotactic zoosporic attraction brings *Pleurosigma sp.* host and parasite *P. isakeiti* close in proximity 3.) Parasite *P. isakeiti* attaches to the girdle band, valve or silica wall of host *Pleurosigma sp.* and penetrates the cell wall 4.) *P. isakeiti,* once attached to the cell wall, loses its whiplash flagellum, begins to form sporangium, zoospores begin to form, cleave away from their cohort and new whiplash flagellum gain motility 5.) Zoospores begin to stray away from their original host *Pleurosigma sp.* cell, seeking out new hosts. The original diatom host *Pleurosigma sp.* is fully lysed and is no longer viable. Zoospores can assume an amoeboid vegetative form 6.) Dead *Pleurosigma sp.* cell remains, while the sporangium continues to occupy the host cell while zoospores move on to infect new hosts.

EN elements originate from one or more points on the thraustochytrid cell, generating a branched network of extensions associated with the bothrosome along the periphery of the cell (Bongiorni et al. 2005). The EN expands surface area of the thraustochytrid and secretes surface-bound

hydrolytic enzymes enabling the digestion of organic material (Harel 2008). The EN attaches to surfaces and penetrates organic particles. Once entering the host by way of attachment and penetration of the girdle belt, *P. isakeiti* produces oil globules, forms sporangia, destroys chloroplasts, and eventually ruptures the entire cell wall structure, where upon zoospores are diffused and move freely among the host community (Hassett 2020). Secondary metabolites that relax the cell wall structure may be at play in zoosporic settlement of thraustochytrids on their hosts (Iwata 2017).

The evolutionary history of the bothrosome – a characteristic feature of thraustochytrids – remains unclear (Iwata and Honda 2018). Zoospore transformation into a vegetative cell in *Schizochytrium aggregatum* leads to the disappearance of the whiplash flagellum during zoospore attachment and settlement. After attachment, the bothrosome, emerging from the anterior-ventral pole, draws closer to the Golgi (Iwata and Honda 2018). Iwata et al. (2017) described actin co-locating with the bothrosome within the EN, implying that actin filaments tug the endoplasmic reticulum toward the bothrosome and instigate evagination of the membrane within the ENs (Tsui et al. 2009; Iwata et al 2017).

Freshly encysted zoospores are 4 to 5 mm in diameter (Bongiorni et al. 2005). Two different types of development have been observed – zoosporic formation and an amoeboid mode (Fossier Marchan et al. 2018). In zoosporic formation, the zoospores appear first in the outer margins of the zoosporangia (Bahnweg and Sparrow 1974). Cleavage of zoospores away from the sporangia occurs quickly and an empty sporangium sac is left behind as zoospores move through tears in the host's cell wall via the whiplash flagellum (Appendix 1; Schnepf et al. 1978; Dick 2001). Release of the zoospores takes about a minute and they can persist up to a month (Bongiorni et al. 2005).

In the amoeboid mode, motile zoospores transform to vegetative cells and undergo binary fission (Bower et al. 1989). Vegetative stages of thraustochytrids are globulose and sub-globulose single cells ~12-15 μm found growing on substrata epibiontically (*i.e.,* living on the surface of another organism) (Bower et al. 1987). Thalli begin to assume an amoeboid shape about 30 μm in length and 20 μm in width (Honda et al 1999; Bongiorni et al. 2005). "Prominent, hyaline, and sheath-like ectoplasm" with dense granular cells transform quickly back into the same dimensions as

normal zoosporangia (Bongiorni et al. 2005). The morphological ambiguity and transformation of thraustochytrid zoospores into a vegetative state, or ameboid mode, suggest a possible means of a non-parasitic existence.

1.1.3   Associations with Bacteria

Spring blooms cause succeeding microorganismic communities that cohabitate with diatoms enhancing and controlling their population growth (Garvetto et al. 2018). Open-ocean diatoms can live with nitrogen-fixing cyanobacteria under their silicate cell wall, while others fasten to silicate spines protruding out of the diatom cell walls. Observations have reported bacteria existing within the outside of the third and fourth membranes of freshwater diatom plastids (Schmid 2003). Such a coexistence could have evolved because metabolites are shared, both actively and coincidentally, across kingdoms in the diluted marine realm. Transferability, reliability, and redundancy of metabolic components among different environments likely predicts whether a cross-kingdom interaction is opportunistic or obligate symbiosis (Armbrust 2009).

1.1.4   Taxonomy of Thraustochytrids

The mode of production of zoospores varies between genera and forms the major taxonomic criterion distinguishing thraustochytrids (Fossier Marchan et al. 2018). As a group, the labyrinthulomycetes are saprotrophic, or less frequently, parasitic stramenopilan protists, typically occupying marine ecosystems. The taxonomic placement of labryinthmycota and thraustochytrids has been an ongoing question (Cavalier-Smith, 1998). F.K Sparrow Jr. first described thraustochytrids in Woods Hole, Massachusetts when studying the role of fungi in the decomposition of organic complexes in the ocean (Sparrow 1936). Since then, thraustochytrid lineages have been proposed to be both fungal and algal (Leyland 2017). Despite their past taxonomic association with fungi, thraustochytrids diverge from members of the Kingdom Fungi in myriad ways. Thraustochytrid cell walls are multi-lamellate and consisting of sulphated polysaccharides circular scales, rather than of chitin microfibrils (Darley et al. 1973; Chamberlain 1980; Chamberlain and Moss 1988;). Thraustochytrids evolutionarily cluster closer with diatoms than with fungi (Baldauf 2003); however, thraustochytrids are genetically and ecologically distinctive from algae. Most fundamentally, algae rely on photosynthesis for energy while thraustochytrids are saprotrophic, absorbing and metabolizing nutrients for their core function

using a system of endoplasmic nets, gliding bodies and a distinct organelle known as the bothrosome (Song et al. 2018).

Leander and Porter (2001) broadly characterized thraustochytrids as non-interconnected single cells with ENs and zoosporic reproduction. Thraustochytrid cell wall composition also suggests that the thraustochytrids and labyrinthuloids may form two distinct groups (Bahnweg and Jäckle 1986). The thraustochytrid cell wall consists of mostly carbohydrate (Darley et al 1973), while species of Labyrinthuloides build cell walls of mostly fucose (Bahnweg and Jäckle 1986). Honda et al. (1999) proposes the Labyrinthulomycota consists of two phylogenetic groups, a Labyrinthula Phylogenetic Group (LPG) and Thraustochytrid Phylogenetic Group (TPG). Leander and Porter (2001) distinguishes Labyrinthulomycota in three groups: the labyrinthulids, the thraustochytrids, and the labyrinthuloids evidenced with small subunit ribosomal ribonucleic acid (SSU rRNA) sequence data (Pan et al. 2017; Bennett et al. 2017).

Phylogenetic analysis confirmed three broad lineages of the compared taxa, namely the labyrinthulids, aplanochytrids, and the thraustochytrids (Honda et al. 1998; Leander and Porter 2001). The phylogenetic tree (Pan et al. 2017; Figure 2) illustrates the placement of *P. isakeiti*, within the thraustochytrids, among the major polyphyletic genus *Thraustochytrium* and the monophyletic *Schizochytrium* genus. Similar observation had been made previously by Honda et al. (1999). Binary division, the amoeboid stage, or division of zoosporangia could have evolved within the thraustochytrids independently, making the classification based exclusively on morphological characters challenging (Sparmann et al. 2004). Working with a taxonomically complicated organism clouds the implications of measured effects – since morphology and life strategies within the thraustochytrids are not easily assigned to sections of a phylogenetic tree (Damare and Raghukumar 2016).

Thraustochytrid *P. isakeiti,* the focus of the present work, was partially identified by observation of ectoplasmic threads penetrating diatoms frustules. The parasite reproduced through both binary division inside and outside the diatom, and epibiotically with biflagellated zoospores. Amorphic cells were observed migrating across the diatom cell wall at the girdle band. Bothrosomes, small absorption organelles, were also detected. Upon phylogenetic analysis of DNA sequences, the

protist clustered within the Thraustochytriidae on a novel branch within the environmental sequence clade Lab19 (Figure 2; Pan et al. 2017; Hassett 2020)
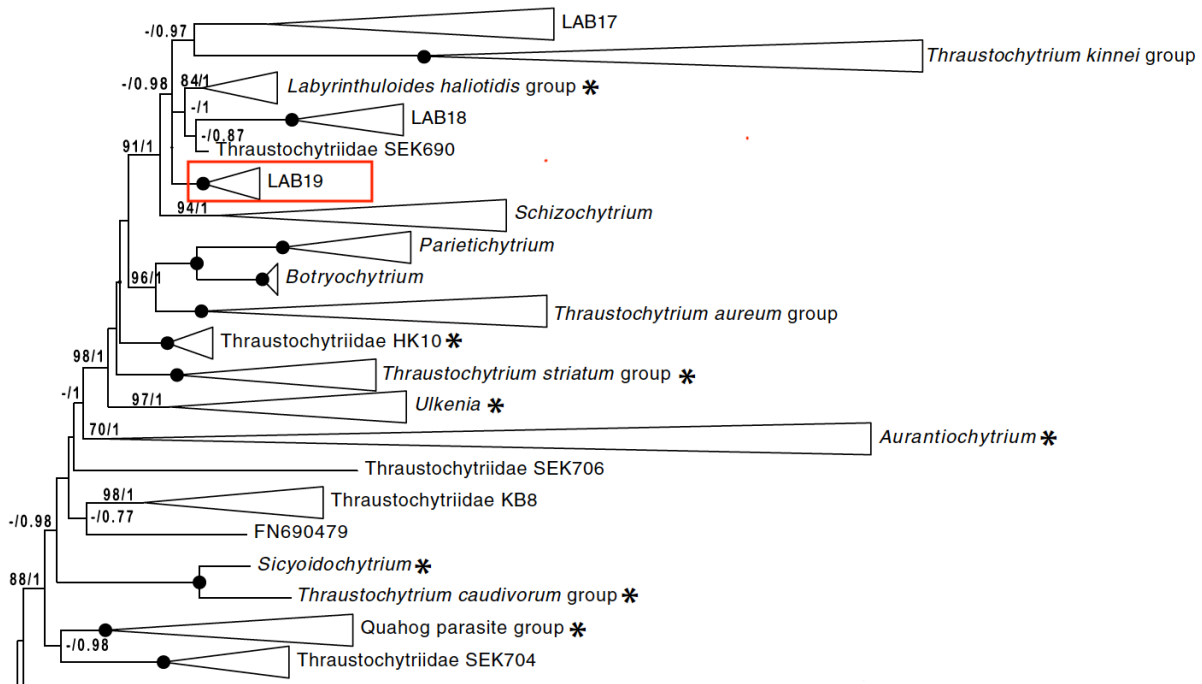
Figure 2 Taxonomic placement of thraustochytrid *P. isakeiti* among the labyrinthulomycota shown in red; Groups containing host-associated sequences are indicated by * (Adapted from Pan et al. 2017)

1.2 Role of Silicate Limitation on Parasitism

While considerable attention has been given to the relationship between iron levels in the ocean and diatom growth (Roncel et al. 2016), other elements like nitrogen (N), phosphorus (P), and dissolved silicate (SiO_2) are also essential to diatom proliferation (Amo and Brzezinski 1999). Nearly all diatoms show a clear dependence on silica for growth and normal metabolism (Martin-Jézéquel and Lopez 2003). Diatoms take up dissolved SiO_2 and transform it into an amorphous form known as biogenic silica to construct cell walls (frustules) – their primary defense against antagonists (Smetacek 1998). If concentrations of dissolved SiO_2 are low or depleted in the environment, diatom growth is limited and other phytoplankton species less reliant on SiO_2 bloom in their place (Dutkiewicz 2020). Silicate is crucial for cell division and healthy immunosystems of diatoms (Smetacek 1998).

Evolutionarily, the use of silica as a cell wall material prevented photosynthetic metabolism from becoming dominated by cell growth. Diatom communities evolved with the constant need to replenish silica, thus linking cell division and silica concentration (Darley & Volcani 1969);

however, under parasitism, it is unclear what role silicate has in cell division. The diatom cell wall evolved as a waste management mechanism for silica metabolism and was ultimately retained due to other advantages (Medlin 2002). Eventually, silica catalyzed diatom metabolic activities by providing surfaces with bioactive compounds (Lechner and Becker 2015).

Sensing and transport of silicic acid are key aspects of understanding diatom SiO_2 utilization (Hildebrand 1998). At low silicic acid concentrations (less than 30 µM), transport into the cell occurs via silicic acid transport proteins, and at higher concentrations, silicate enters the cell through diffusion (Hildebrand 1994). The transport role of the silicic acid transport proteins is relatively insignificant under conditions with adequate silicic acid. The primary role of silica transport proteins is to sense silicic acid levels concentrations and establish whether the cell can undertake cell wall formation and division processes (Shrestha and Hildebrand 2015). Modelers examining silicate in diatoms predict synthesis of valves exclusively during growth II, interphase, and metaphase, while setae and girdles are synthesized during growth phase I (Lee et al. 2014). Stress from reduced silicate results in a loss of setae, followed by thinning of valves in successive later generations until a minimum silicate cell quota is achieved to initiate division; after this point, the duration of growth phase II is prolonged, and growth is silicate-limited (Flynn and Martin-Jézéquel 2000) Zoosporic parasitism, at the cell wall, could disrupt silicate sensing silicic transport proteins, potentially sending altered signals prompting division.

Primary production in the ocean is limited by upwelling dissolved silicate (Smetacek 1998). Diatom blooms initiate a cascade of life; however, this cascade cannot be initiated without sufficient silicate to commence binary division. Nitrogen and phosphorus discharged into coastal zones have globally increased 2.5X and 2.0X (Oelsner and Stets 2019), respectively, from nitrogen fertilizer and phosphate mining (Bouwman et al. 2009). Global silicate in the ocean has been decreasing in recent years (Wasmund et al. 2013). Dramatic changes in nutrient loads and composition ($NO_3:SiO_2:P$ ratios) entering coastal seas will have lasting effects on coastal ecosystems (Humborg et al. 2000) and limit the total primary production output of diatom blooms.

Around the world, dissolved biogenic silica moves to estuaries by riverways (Tréguer and Rocha 2013). Inputs of silicate into the ocean have been declining recently as river dams have hindered

natural discharge (Conley et al. 1993; Gupta et al. 2012). Diatom growth, from N and P induced eutrophication and consumption of fixed biogenic silica through sedimentation from the water column (Billen et al. 1991) could explain observed reduction in silicate (Ittekkot et al. 2000). The stoichiometric changes in nutrient elements (NO_3:SiO_2) result in observable changes in phytoplankton populations in marine and freshwater water (Admiral et al. 1990; Ittekkot et al. 2000; Choudhury and Bhadury 2015; Käse and Geuer 2018).

Marine diatoms have been ecologically successful despite their additional requirement for silicate; however, silicate limitation may offer some advantages to diatoms. Nitrogen and silicate metabolism models in diatoms (Flynn and Martin- Jézéquel 2000; Flynn et al. 2012) suggest silicate-starved diatoms recover faster than nitrogen-starved diatoms upon nutrient resupply. Diatoms descended from nitrate starved cultures never catch-up to cultures descended from silicate starved populations when both groups are simultaneously supplied with nutrients pulses (Flynn and Martin-Jézéquel 2000). The more time lapses between nutrient supply and growth in the nitrate-starved cells, the higher the proportion of nutrients are taken in by descendants of silicate starved diatoms. In the model, the silicate-starved cells took in more than three quarters of all the nutrients added while nitrate-starved diatoms consumed the remainder. Silicate limitation may allow diatoms to respond faster than other phytoplankton to nutrients in upwelling waters in the euphotic zone (Rocha and Passow 2004).

Determining the infection rate of parasite *P. isakeiti* under standard and reduced silicate culturing conditions may shed light on the role of silicate in the primary metabolism of diatom *Pleurosigma* sp. under infection pressures. Measuring the free silicate and nitrate uptake in healthy and parasitized cultures of *Pleurosigma* sp., can further characterize the host response and its effect on critical cellular functions related to parasitism and nutritional uptake. While growth rate of thraustochytrids have been recorded (Jain et al. 2005), little information exists about host growth under infection pressures from thraustochytrids, warranting further time-series experiments of host infection and growth.

1.2.1 Silica Cell Wall of Diatom *Pleurosigma* sp.

Diatom silicate utilization sustains debate (Simpson and Volcani 1981; Sumper Kröger 2002; Brunner et al. 2004; Bondoc et al. 2016). Defense is the primary suggestion (Pančić et al. 2019). Silicate metabolism and cell wall production was retained in diatoms due to the tensile strength of silica polymers and the protection it offered against enzymatic attack (Hamm et al. 2003). In a hypothetical intervening or temporary terrestrial habitat (Harwood et al. 2017), a silica wall could prevent desiccation thus allowing cells to enter a resting state. Raven and Waite (2004) have concluded that the externalization of silicate to the cell wall accelerated sinking, helping to move parasitized cells away from the population, ensuring species survival (Simms et al. 2006).

Ancestral diatoms accumulated silica in the endoplasmic reticulum, where it was polymerized and packed into acidic vacuoles, where it would be eventually extruded from the cell (Sims et al. 2006). Consequently, diatoms developed a need to replenish their internal silicate, explaining the observed absolute silica requirement diatoms have for division (Darley and Volcani 1969). The silicified two-part cell walls of diatoms originate in intracellular compartments precipitated from supersaturated $Si(OH)_4$ where they are externalized (Lechner and Becker 2015). Whatever the initial evolutionary advantage may have been, silicification increases density and sinking rates which can be offset by the regulation of solute content according to resource supply. Parasitism moves cells into resource supply conditions causing them to sink away from uninfected surface populations. If the earliest silicified diatoms were planktonic, increasing the sinking rate may have been an original defensive mechanism against parasites (Raven and Waite 2004).

Drawing nutrients from diatom hosts via the EN element exposes thraustochytrids to the defense chemicals of algae (Raghukumar 1990; Sholtz et al. 2017). Thraustochytrids have been observed growing directly on the diatom cuticle, avoiding penetration of epidermal cells, and circumnavigating algal antagonism. Diatoms of the Arabian Sea harbor thraustochytrid *Ulkenia visurgensis* (Raghukumar 1986). The protist parasite failed to infect healthy cells, rather it dwelled on senescent cultures. Thraustochytrid parasite *Schizochytrium* has been observed disintegrating the diatom cell wall; however, it could not be isolated with pine pollen-sea water medium for further study (Raghukumar 1986).

1.2.2 Cell Cycle of the Host *Pleurosigma* sp.

Pleurosigma sp., studied in this thesis, is a benthic diatom. *Pleurosigma* sp. cells are several times longer than they are wide. The chromatophores appear as bright green ribbons under the microscope. The central nucleus forms the core of the cytoplasm. During anaphase, the daughter chromosomes congregate at the poles of the spindle and daughter chromosomes move farther apart. In telophase, the daughter nuclei organize. Similar to other observations (Subrahmanyan 1945), *Pleurosigma* sp. cytokinesis has been observed commencing during anaphase as a small cleavage furrow slices the cytoplasm into two parts along the valvar plane.

1.3 Silicate and Nitrate Uptake Under Pressures of Parasitism

The main driver of composition, diversity, and biomass of diatoms in coastal waters is nitrogen concentration and its temporal and spatial changes (Kafouris et al. 2019). While nitrogen is the major driver of diatoms in the ecosystem, silicate is also an essential inorganic nutrient necessary for growth. Most research on diatom metabolism has focused on nitrogen limitation; however, increasing $NO_3:SiO_2$ ratios in the environment may results in widespread silicate limitation (Gilpin et al. 2004).

Consensus has built around the proposition that $NO_3:SiO_2$ ratios less than one, result in N limitation of diatom biomass accumulation and ratios greater than one, result in silicate limitation (Levasseur and Therriault, 1987; Dortch and Whitledge, 1992). The assumption of an approximate 1:1 N: SiO_2 ratio in diatom biomass (Officer and Ryther, 1980; Egge and Aksnes, 1992; Flynn and Martin-Jézéquel, 2000) was generally accepted after Brzezinski (1985) compared the N:SiO_2 ratios of 27 different diatom species.

1.4 Parasitism as a Bioprospecting Strategy

The suspected scavenging and nutritional cycling roles of thraustochytrids suggest they may synthesize interesting extracellular enzymes (Raghukumar et al., 1994; Sharma et al. 1994; Bremer and Talbot 1995; Raghukumar 2008). Degradation and penetration of the diatom cell wall may be the result of thraustochytrid enzymatic activity synthesized by *P. isakeiti* during opportunistic encounters with diatoms like *Pleurosigma* sp. Nagano et al. (2010) detected cellulolytic activity in the genera *Botryochytrium, Oblongichytrium, Parietichytrium, Schizochytrium, Sicyoidochytrium,*

Thraustochytrium, Aplanochytrium and *Ulkenia*, but not in *Aurantiochytrium.* Taoka et al. (2009) did not observe any cellulolytic activity in *Thraustochytrium, Schizochytrium* and *Aurantiochytrium*. Other hydrolase activities have been detected in thraustochytrids, including agarase, amylase, proteinase, gelatinase, urease, lipase, α-glucosidase, phosphatase and xylanase. Chitinase, carrageenase, alginate lyase, and pectinase have been found less frequently (Raghukumar et al. 1994; Sharma et al. 1994; Taoka et al. 2009; Kanchana et al. 2011; Devasia and Muraleedharan, 2012). Kanchana et al. (2011) discovered a lipase with optimum activity at alkaline pH showing biotechnological potential as an additive in detergent, while Brevnova et al. (2013) patented cellobiohydrolase type I derived from *Schizochytrium aggregatum* (Fossier Marchan et al. 2018). Clearly, some thraustochytrids, demonstrate enzymatic function, and *P. isakeiti* has visible penetration capacity against its *Pleurosigma* sp. host's cell wall (Hassett 2020), suggesting its prospect as a bioactivity compound producing organism.

Just as a thraustochytrids may use novel extracellular enzymes to absorb nutrients and invade hosts, diatoms may produce its own compliment of bioactive molecules to defend themselves. Both organisms are known to produce polyunsaturated fatty acids (PUFAs) (Li et al. 2014; Patel 2020). This coevolved mechanism of extracellular predation and defense may characterize the relationship between *P. isakeiti* and its host *Pleurosigma sp.;* however, determining the precise biochemical relationship associating the diatom and its host remains outside the scope of this thesis. The aim, presented here, is to detect whether any bioactive enzymes or metabolites involved in *P. isakeiti* invasion of *Pleurosigma* sp. are bioactive and potentially biotechnologically relevant.

Bioactive polysaccharides, synthesized by marine unicellular algae, released into the surrounding medium have been used in a myriad of technical applications (Rasposo et al. 2013). Diatoms, known to defend themselves against copepods, also produce bioactive metabolites to compete for resources and defend themselves from other predators (Pohnert 2005; Leflaive and Ten-Hage 2009). Algae have coexisted longer with protists and fungi than with copepods (Knoll et al. 2006; del Campo et al. 2016;) and have been exposed to longer periods of extracellular competition with protists like *P. isakeiti*.

Triacylglycerides (TAGs) are typically synthesized during nutrient starvation because they constitute important energy storage compounds that prolong diatom cell survival in unfavorable conditions (Abida et al. 2013). Alternatively, oxylipin production by diatoms can be induced as a defense mechanism against their principal predators, crustacean copepods (Cadwell 2009; Fontana et al. 2007). Oxylipin production by diatoms also constitutes a system for allelopathic communication between diatom cells (Meyer et al. 2018), a cellular cross-talk mechanism thought to be essential to such marine communities (Abida et al. 2013). The cytotoxic effects of some of these diatom-derived aldehydes were also found in organisms belonging to different phyla ranging from bacteria to marine invertebrates (Adolph 2004). Furthermore, some molecules may even be generated as the result of cooperative chemistry between host and microbial photo-symbionts or bacterial symbionts. For example, it was demonstrated in *Dysidea avara* that the level of metabolites produced was dependent on co-locating bacteria (De Caralt 2013). It is therefore crucial to consider a variety of planktonic organisms for bioprospecting, rather than narrow the search down to a specific clade or size fraction (Abida et al. 2013).

1.5 Bioassays of Diatoms and Thraustochytrids

Numerous examples of case studies that initially started with ecological investigations of microorganisms have resulted in biotechnological leads as a result of discovery of new compounds with specific industrial or research applications (Lewis et al. 1999). Marine bioprospecting aims to uncover and commercialize novel products found in the sea (Svenson 2013). The ocean represents a highly competitive environment with longer evolutionary history and under-exploited biodiversity in comparison to terrestrial environments. Marine environments are characterized by constant dilution thus requiring organisms to produce highly potent bioactive molecules to be effective against antagonists, competitors, prey, hosts, and parasites making marine organisms suitable targets for bioprospecting research (Abida et al. 2013). Secondary metabolites are not strictly obligatory for survival, growth, development, or reproduction (Liu et al. 2010). Techniques have been developed to extract and isolate bioactive secondary metabolites efficiently (Abida et al 2013). Bioassay guided purifications detect bioactivity to inform the isolation process and reduce unnecessary characterization of compounds unsuited to target research areas (Svenson et al. 2013).

Thraustochytrids have piqued the interest of bioprospectors in recent years (Sholz et al. 2016). Thraustochytrids are increasingly being used to produce long chain omega-3 or omega-6 fatty acids, such as docosahexaenoic acid (Zhou et al. 2010), eicosatetraenoic acid, or arachidonic acid for nutraceutical, food additive, and aquaculture industries (Gupta et al. 2012). Carotenoids, including β-carotene, astaxanthin, zeaxanthin, cantaxanthin, phoenicoxanthin, and echinenone have been found in thraustochytrids and have been demonstrated to be useful in skin protection and the inhibition of adverse processes induced or mediated by solar ultraviolet radiation (Corinaldesi et al. 2017). While thraustochytrids have demonstrated their potential as research organisms, understanding their role in fundamental marine ecological processes may lead to unforeseeable discoveries.

2 Objectives & Hypotheses

2.1 Objectives

The overall objective of this thesis is to study the relationship between the parasite *P. isakeiti* and its diatom host, *Pleurosigma* sp. *P. isakeiti* may disintegrate the silica cell wall enzymatically or restrict host silica uptake, thin the host cell walls (Figure 3), prior to zoospore settlement. This thesis is comprised of five primary objectives to describe and document the novel diatom parasite and its means of infection:

To determine whether *P. isakeiti* is an obligate parasite or whether it can live as a facultative parasite saprotrophically without its host.

1. To determine the proportion of cells under division and infection by thraustochytrid parasite *P. isakeiti* under standard and reduced silicate culturing conditions among host *Pleurosigma* sp. cells.

2. To investigate how the proportion of dividing host diatom *Pleurosigma* sp. cells is affected by SO_2 and NO_3 uptake in healthy and parasitized cultures.

3. To detect chemical indicators of parasitism or defense.

4. To perform bioassays to understand whether any primary or secondary metabolites produced under parasitism have biological activities with potential medical application.

2.2 Hypotheses

Hypothesis 1: *P. isakeiti* is an obligate parasite of diatom *Pleurosigma* sp.

Hypothesis 2: (A) The infection rate of *Pleurosigma* sp. by *P. isakeiti* increases under reduced-silicate treatment, and (B) the rate of division decreases under reduced silicate conditions.

Hypothesis 3: (A) The division rate of *Pleurosigma* sp. increases as uptake of silicate decreases in parasitized *Pleurosigma* sp. cultures, and (B) available nitrate decreases over time.

Hypothesis 4: Chemical variance can be detected among healthy and parasitized *Pleurosigma* sp. cultures.

Hypothesis 5: Extracts from parasitized *Pleurosigma* sp. cultures have measurable effectiveness in cytotoxicity assays.

2.3 Testing the Null

Each hypothesis has been evaluated by testing the null hypothesis using a variety of experiments:

1) To test whether *P. isakeiti* is not an obligate parasite, culturing experiments were performed to isolate *P. isakeiti*. After culturing experiments, and detecting the presence of bacteria, follow-up 16S sequencing was performed to identify other prokaryotic organisms found associated with the parasitic protist and its diatom host.

2) To determine whether there was no effect of silicate on the infection and division rates of *Pleurosigma* sp. – time-series counting experiments were conducted (Figure 4). Observations were made of healthy, parasitized, dividing and dead *Pleurosigma* sp. cells and recorded. Observations were made by counting 500 living *Pleurosigma* sp. cells and recording the proportion of parasitized to healthy cells. Dividing cells were recorded as a subset of the healthy cells. Dead cells were recorded independently of the proportion of healthy to parasitized cells and the dividing cells. Each sample was counted twice, and the values were averaged. Counts were taken at each time-point using three biological replicates. The time-series experiment was performed over 31 days. The infection rate of cultures using standard and silicate-reduced media were compared (Figure 3).
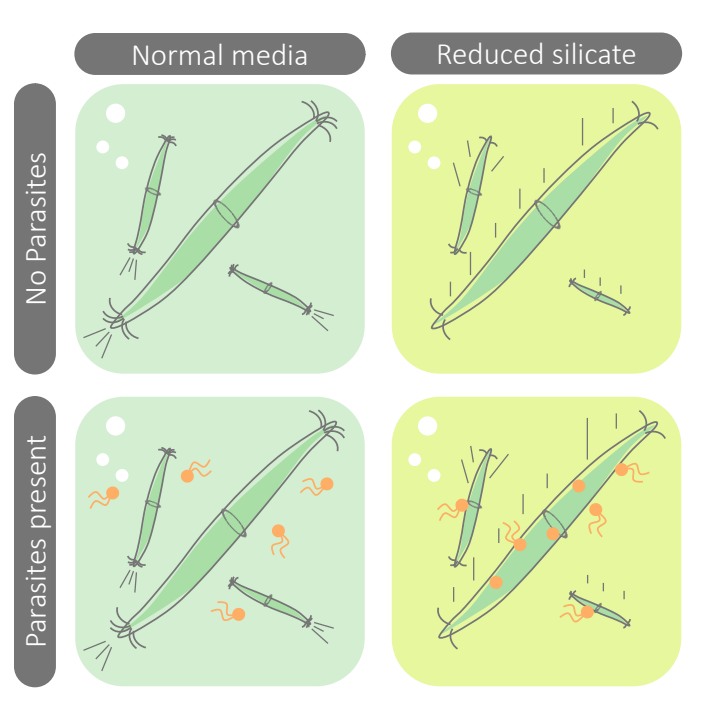
Figure 3 Hypothesized impact of reduced silicate and parasitism on diatom buoyancy

2) To determine whether there was no effect of silicate on the infection and division rates of *Pleurosigma* sp. – time-series counting experiments were conducted. Observations were made of healthy, parasitized, dividing, and dead *Pleurosigma* sp. cells and recorded. Observations were made by counting 500 living *Pleurosigma* sp. cells and recording the proportion of parasitized to healthy cells. Dividing cells were recorded as a subset of the healthy cells. Dead cells were recorded independently of the proportion of healthy to parasitized cells and the dividing cells. Each sample was counted twice, and the values were averaged. Counts were taken at each time-point using three biological replicates. The time-series experiment was performed over 31 days. The infection rate of cultures using standard and silicate-reduced media were compared.

3) To evaluate whether the uptake of silicate decreases in parasitized cultures of *Pleurosigma* sp., free silicate and nitrogen was measured in concert with the same counting procedure as described in (2) over a two-week period. Nutrient analysis, like the counting experiments, was performed in triplicate biological sampling and triplicate machine replicates. Non-parasitized healthy *Pleurosigma* sp. cultures were compared to parasitized *Pleurosigma* sp. cells. $NO_3:SO_2$ was plotted over time to compare the parasites physiological impact on its host.

4) To test whether measurable chemical differences in parasitized and healthy culture was detectable, extracts were made from both the parasitized and non-parasitized *Pleurosigma* sp. cultures, as well as media controls and were analyzed using a mass spectrometer. Principal component analysis was performed to identify the primary chemical signatures driving the differences between the three samples.

5) To test whether parasitized *Pleurosigma* sp. cultures produce bio-active molecules effective in cytotoxic and anti-cancer screening, two primary experiments were conducted. Furthermore, anti-inflammation, anti-oxidant, and biofilm assays were also conducted using extracts from parasitized and non-parasitized *Pleurosigma* sp. cultures and media controls.

3 Materials and Methods

3.1 Culturing

The study organisms were provided by B. Hassett (UiT The Arctic University of Norway). Non-parasitized *Pleurosigma* sp. cultures and cocultures of *Pleurosigma* sp. with thraustochytrid *P. isakeiti* were maintained in the extraction laboratory at Marbio– an analytical platform for natural products in Forskingsparken, in Tromsø, Norway. The cultures were held at 10 °C on a 10-14-hour light cycle. Cultures were raised and maintained in Sigma-Aldrich F/2 media (Guillard 1975). The cocultures were periodically shaken for 30 minutes every two days.

3.1.1 Agar Cultures

The purpose of further isolating the thraustochytrid parasite in absence of its *Pleurosigma* sp. host was to 1) determine if the *P. isakeiti* is an obligate or facultative parasite, and 2) to compare with healthy diatom and coculture LC-MS data to trace the origin of chemical variances between host and parasite. Isolation of the thraustochytrid was attempted using six different media (Table 1; Rosa et al. 2011). Agar and filtered seawater were used as controls. Each media was plated with and without kanamycin and penicillin.

Table 1 List of media ingredients for isolation of thraustochytrid *P. isakeiti* into monoculture

Components	Media Composition (% w/v)					
	GPY[b]	H[b]	KMV[c]	SSA[d]	MC[d]	MC-BHB
D-Glucose; Sigma D9434-1KG	2.00	0.20	0.1	-	0.20	0.10
Peptone; Sigma 82303-5KG-F	1.00	-	0.01	-	0.10	0.05
Yeast extract; Sigma 09182-1KG-F	0.50	0.02	0.01	-	0.10	0.05
Monosodic glutamate; Sigma G1626-500G	-	0.05	-	-	0.10	0.05
Gelatine hydrolysate; Sigma G0262-500G	-	-	0.10	-	0.20	0.10
Corn-steep liquor –a; Sigma C4648-500G	-	-	-	-	0.10	0.05
Artificial sea salt; Sigma S9883-1KG	1.75	1.75	1.75	1.75	1.75	1.75
Horse serum; Sigma H1270-500ML	-	-	-	1.00	-	-
Brain–heart broth; Sigma 53286-500G	-	-	-	-	-	1.75
Agar; VRW 20767.298	2.00	2.00	1.20	1.20	2.00	2.00

GPY glucose-peptone-yeast extract medium, H Honda medium, KMV modified Vishniac's medium, SSA serum seawater agar medium, MC Mar Chiquita medium, MC-BHB Mar Chiquita—brain heart broth

[a] Concentration expressed as % (v/v)

[b] Media used for Aurantiochytrium limacinum SR21 (Honda et al. 1998)

[c] Current media used for thraustochytrids (Porter 1990)

3.1.2 Characterization of Fungal and Bacterial Strains

To determine whether any contaminants or partner associated microbes were present in the cocultures, growth strains were sequenced. The internal transcribed spacer (ITS) region of the nuclear ribosomal repeat unit was used to identify potential fungi while the 16S rRNA gene sequence was used for potential bacteria strains. These methods are quite similar, involving three general steps; polymerase chain reaction (PCR), purification of the amplicon, and finally sequencing. This analysis is possible with a small sample size and is cost-effective.

3.1.2.1 PCR

Firstly, a small amount of the organisms to be characterized were collected using a swab from the KMV and Honda agar plates. Then amplification of the DNA using a PCR reaction was conducted following the procedure in the DreamTaq kit (Thermo Scientific). Briefly, a 25 µl reaction mixture

was prepared using 12.5 μl of the 2x DreamTaq Master Mix (Thermo Scientific, Cat no K1081/82), 1 μl of both forward and reverse primers (either ITS4 and ITS5 for fungi or 27F primer and 1429R primer for bacteria (Table 2)) and 10.5 μl of double distilled water. This mixture was then cycled through the scheme outlined in Table 3 for amplification in an Eppendorf AG 22331 PCR thermocycler. The PCR product was determined through gel electrophoresis. The gel was prepared using a 1% solution of agarose (1 g, Life technologies, UltraPure™ Agarose, Cat # 15510-027) with 1x TBE buffer (100 ml, Life technologies, Cat # 15581-044) mixed with 10 μl of 10.000x GelRed (BioTium, Cat # 41003). Gels were left to set up in trays before loading with 6 μl of 1kb ladder solution (Life technologies, Cat # 10787-018.) and 6 μl of the amplified sample. Gels were run for 15 min at 180 V in the gel electrophoresis system (OWI separation system Inc, B2 model). Finally, gels were exposed to ultraviolet light and photographed (GeneFlash®, SYNGENE Bio imaging) to determine the success of the amplification.

Purification of the amplified PCR sample was conducted following manufacturer's instructions and the QIAquick PCR Purification Kit (QIAGEN, Cat no 28104). The concentration and quality of the purified PCR products was measured using the NanoVue® (NanoVue Plus™, GE Healthcare). The final stage of sequencing was performed using a mixture of 1 μl of BigDye 3.1, 2 μl of 5x sequencing buffer, 1 μl of the forward or reverse primer for fungi or bacteria (Table 2) and 6 μl of double distilled water together with the PCR sample swab. This new mixture was run through the cycle outlined in Table 3 in the PCR machine Eppendorf AG22331.

Table 2 Fungal and Bacterial Primers for PCR Reactions

Organism	Primer Pair	Sequence	Product
Fungi	ITS5	5'-GGAAGTAAAAGTCGTAACAAGG-3'	~500-1100bp
Fungi	ITS4	5'-TCCTCCGCTTATTGATATGC-3'	~500-1100bp
Bacteria	27F	5' - AGAGTTTGATCMTGGCTCAG-3'	~1500bp
Bacteria	1492R	5'- TACCTTGTTACGACTT-3'	~1500bp

Table 3 DNA Amplification Program

Initial Denaturation		95 °C	3min (bacteria), 5 min (fungi)
Cycle	Denature	95 °C	30sec

x 35	Annealing	47 °C*	30sec
	Elongation	72 °C	1min (1min <2kb products)
Final Extension		72 °C	10min
Hold		4 °C	∞

Table 4 16S DNA Sequencing Program

Initial Denaturation		96 °C	1min
Cycle x30	Denature	96 °C	10sec
	Annealing	47 °C*	5sec
	Elongation	60 °C	2min (45 sec for <700bp)
Hold		4 °C	∞

3.1.2.2 16S Ribosomal DNA Sequencing

Successful PCRs were purified using either QIAquick PCR purification kit clean-up treatment per the manufacturer's manual. Purified PCR products were prepared for two directional Sanger sequencing reaction using BigDye3.1 and a PCR program shown in Table 4. The sequencing was performed by the sequencing platform at the University Hospital of North Norway utilizing Applied Biosystems 3130xl Genetic Analyzer (Life Technologies/Applied Biosystems). The returned chromatograms were imported into Geneious v10.2.3 (https://www.geneious.com/), trimmed to 0.05 error probability assembled into consensus sequences and proofread according to guidelines proposed by Nilsson et al. (2012)

3.1.2.3 Nucleotide Basic Local Alignment Search Tool

Consensus sequences from UiT UNN were assembled in fasta format and blasted using the NCBI nucleotide BLAST National Center for Biotechnology Information (NCBI)[Internet]. Bethesda (MD): National Library of Medicine (US), National Center for Biotechnology Information; [1988] – [cited 2020 Apr 06]. Available from: https://www.ncbi.nlm.nih.gov/

3.2 Counting Methods

40 ml flasks were inoculated with 38 ml of *Pleurosigma* sp. at ~500 cells/ml concentration and 2 ml of *Pleurosigma* sp./ *P. isakeiti* cocultures at a concentration of ~500 cells/ml at a ~90% rate of infection. Cells were counted using a hemocytometer to estimate density. Counts of health status were taken daily for one month (healthy, parasitized, dividing, and dead). Each flask was counted twice for internal control. For time-series experiments, each timepoint was taken in triplicate. The health status (healthy, parasitized, dead, and dividing) *Pleurosigma* sp. cells were defined as (Appendix 1):

1. Healthy cells included diatoms that did not show reduced chloroplasts. There were no visible penetrations of the cell wall. They demonstrated some motility.

2. Parasitized cells showed reduced and irregular chloroplast shape and discoloration. Parasitized cells also showed clear signs of penetration by zoospores; however, they remained motile.

3. Dead cells were recorded when they were empty of chloroplasts, their chloroplasts were dead, showed no sign of motility, had a ruptured cell wall or there was sporangium growing within the cell wall (Appendix 1).

4. Dividing cells were recorded when anaphase had cytokinesis commenced and a cleavage was visible cutting the cytoplasm in two.

Cell health status counts were enumerated using a light microscope (see section 4.1.3). Culture flasks were counted by using randomized fields of view. Each field of view was tallied and recorded until the total healthy + infected equaled 500. Dividing cells were recorded only among livings cells, (two sister silica shells void of life were not recorded). Dead cells were recorded concurrently as the healthy, infected, and dividing cells were observed and totaled.
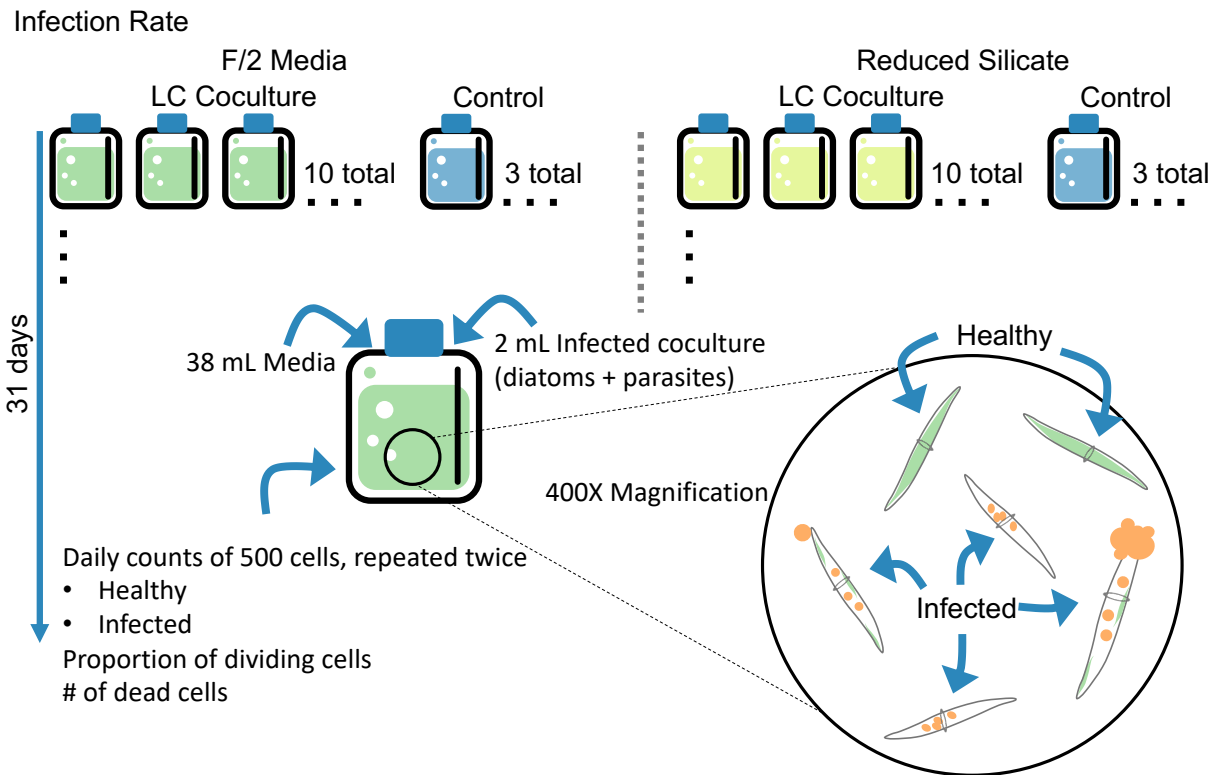
Figure 4 Infection and division rate time-series in 1:50 F/2 and 1:50 F/2 reduced silicate media over 31 days. Host *Pleurosigma* sp. cells were recorded as parasitized, healthy, dead, and dividing
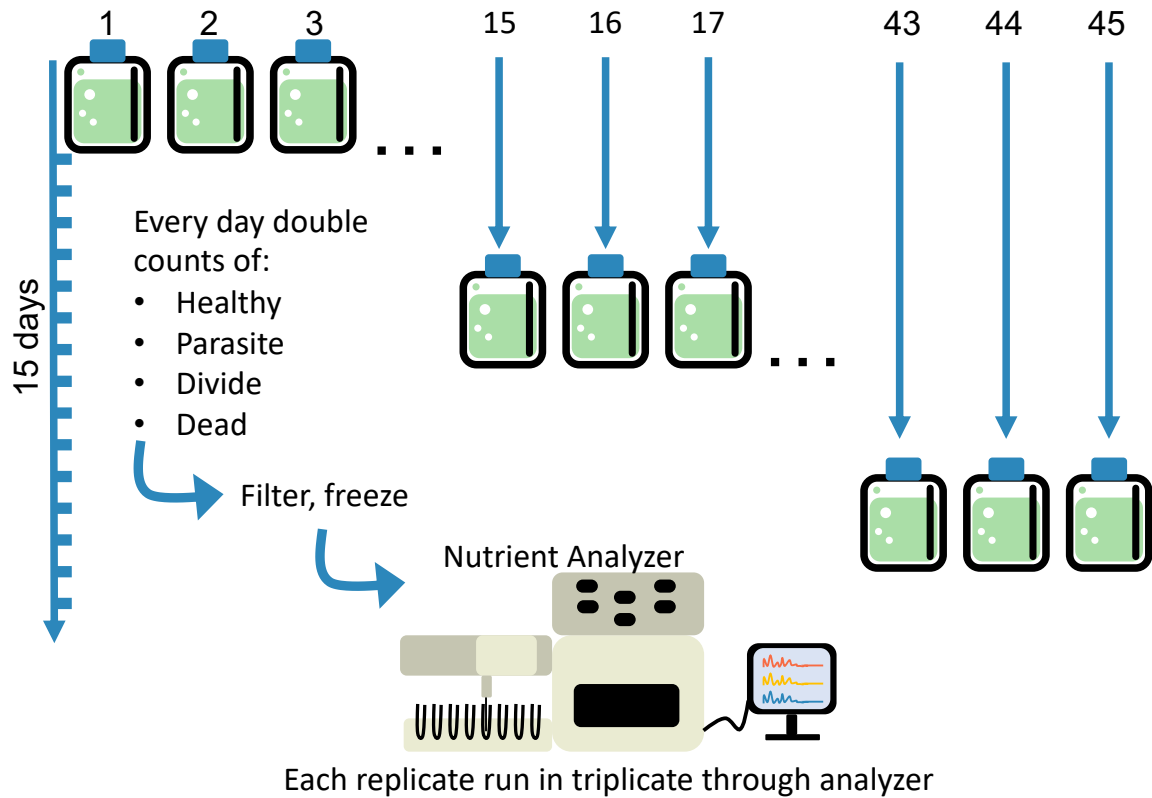
Figure 5 Infection and division rate with nutrient analysis of *Pleurosigma* sp. and *P. isakeiti* coculture time-series in 1:50 F/2 media over 15 days
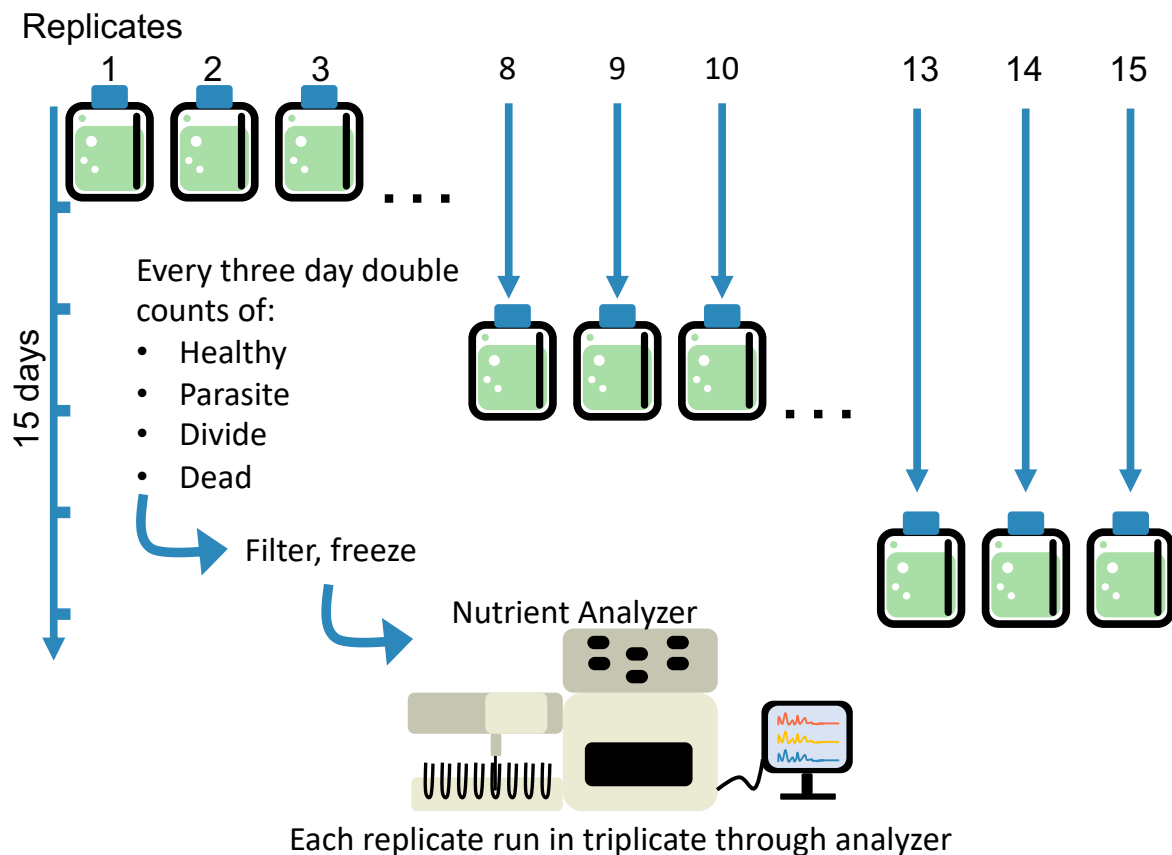
Figure 6 Division rate with nutrient analysis of *Pleurosigma* sp. time-series in 1:50 F/2 media over 15 days

3.2.1 Light Microscopy

A Zeiss[2] primo inverted microscope was used to visualize the cultures at 200X and 400X. Photographs were taken using a Zeiss AxioCam ERc5s.

3.3 Nutrient Analysis

Samples from time-series experiments of parasitized and healthy *Pleurosigma* sp. were tested (Figure 5 and 6). Silicate and nitrate depletion are attributed primarily to *Pleurosigma* sp. metabolism due to the greater relative size of the diatom cell compared to the parasite. Healthy and parasitized cultures were frozen at pre-determined time points. After sample flasks were counted, FSW + silicate reduced and standard F/2 media containing the diatoms and their parasites were filtered using a 0.2 μm filter. These samples were frozen at -20°C. At the end of the experiment the samples were collected. Nutrient analysis (silicate (SiO_2), nitrate (NO_3^-), and nitrite

(NO_2^-)) was performed on 120 samples. Samples were analyzed colorimetrically with a QuAAtro analyzer from SEAL Analytical, UK using a method developed by the Royal Netherlands Institute for Sea Research, Den Hoorn (Texel), The Netherlands. The analyzer was calibrated using synthetic seawater and analytical reagent grade standards for each nutrient. Briefly, nutrient determination was based on the reduction of the compound in an acidic environment to form a dye (either molybdenum blue or reddish-purple azo dye for silicate and nitrite / nitrate, respectively). The absorbance was then measured at a specific wavelength (820 or 520 nm, respectively) under an LED photometer. Samples were diluted 1:10 & 1:100 to fall into the range of the standards run. The analysis and calibration were performed by Paul Dubourg (AMB, UiT).

3.4 Chemical Differences in Healthy and Infected *Pleurosigma* sp. Cultures

3.4.1 Extractions

Extractions were preformed using ethyl acetate and resin to test which method had the most appropriate capacity to capture primary and secondary metabolites in lysed media from cultures of *Pleurosigma* sp., cocultures of *Pleurosigma* sp., and *P. isakeiti* and F/2 media as a control (Figure 7).

3.4.1.1 Ethyl Acetate Extraction

The ethyl acetate extraction was performed by mixing 1 mL ethyl acetate and 1 mL of the concentrated culture sample. The samples were placed on the sonicator for 1.5 hours. The samples stood until a phase separation took place and the ethyl acetate slowly rose to the top. The ethyl acetate phase was collected. The ethyl acetate was evaporated under reduced pressure in a Laborota 4011, Heidolph™ rotavapor system. The remaining samples were dissolved in dimethyl sulfoxide (DMSO) and prepared for liquid chromatography—mass spectrometry (LCMS) analysis.

3.4.1.2 Resin Extraction

The nonionic resin Amberlite® XAD7HP (Sigma Aldrich) was used to extract the content from the supernatant after centrifugation to get rid of cell residue. 60 g of Amberlite® XAD7HP was prepared by rinsing with 2 L distilled water (dH2O) thrice, sufficient 100% Methanol (MeOH)

was used to cover the resin grains and left to sit for 30 minutes. The resin was washed with 2 L dH2O another three times. Once the Amberlite® XAD7HP was washed thoroughly, it was left to air-dry and covered with aluminum foil to prevent dust from combining with the sample. The dry Amberlite® XAD7HP was distributed to three 250 mL Erlenmeyer flasks. The supernatant was centrifuged to remove remaining cell residue and combined with flasks containing 60 g dry Amberlite® XAD7HP. Flasks were covered with aluminum foil. Supernatant-resin mixture was agitated at low pace (150 rpm) overnight. Compounds present in the media adhere to the Amberlite® XAD7HP grains; however, the most polar and charged compounds will not absorb into the resin.

The supernatant-resin mix was filtered on a porcelain filter holder with a Whatman® quality 1 filter paper. Amberlite® XAD7HP was gathered and added to a 250 mL Erlenmeyer flask containing 50 mL of 100% MeOH and mixed slowly overnight. MeOH washed out and replaced the organic compounds attached to the Amberlite® XAD7HP grains. A rotary evaporation device (Laborota 4011, Heidolph™ rotavapor system) was employed at 40°C and reduced pressure to dry the solution. The dried matter was first dissolved in 3.3 mL of MilliQ, then 3.3 mL 50% MeOH followed by 3.3 mL 100% MeOH, and the fractions were mixed. The combined solution was aliquoted into 10 mL glass tubes and evaporated to dryness in SpeedVac Plus SC210A (Savant™) coupled with Refrigerated Condensation Trap RT400 (Savant™). When dry the solids were washed out with 250 µL MilliQ, 250 µL 50% MeOH and then 250 µL 100% MeOH, before being collected in High Performance Liquid Chromatography (HPLC) vials. The total dissolved matter is 750 µL in 1:1 MeOH:MQ.

Extraction / MS
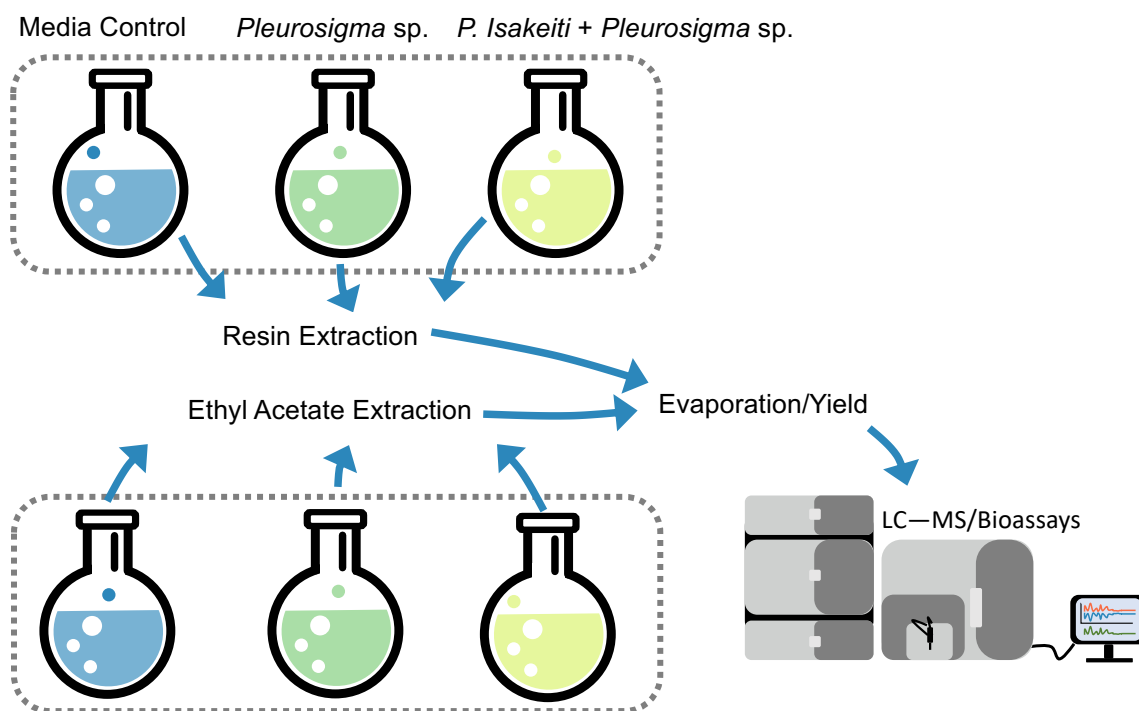
Figure 7 General scheme of resin and ethyl acetate extractions for LCMS and bioassay experiments. Media controls (blue), healthy *Pleurosigma* sp. (green), and cocultures of *Pleurosigma* sp. and *P. isakeiti* (yellow)

3.4.2 Mass Spectrometry

Ethyl acetate and resin extracts were analyzed using ultra-high-performance liquid chromatography-quadrupole time-of-flight mass spectrometry (UPLC-QToF-MS). Before injection, the extracts were diluted 1:10 in 80% methanol and transferred to HPLC glass vials. The injection volume used was 1 µL and the samples were run on the Acquity UPLC I-class system with a C18 column, followed by the VION IMS QToF. All samples were run on ESI+ mode (electrospray ionization), and complex samples were also run on ESI- mode.

15 µL of the different extracts were placed in two UPLC tubes with 100 µL 50% MeOH to dilute the samples. UPLC-HR-MS analysis was performed on the samples using a Waters Acquity I-class UPLC system (Milford, MA, USA) interfaced with a PDA Detector and a VION IMS-qTOF, using ESI in positive mode, wavelengths from 190-500 nanometers were detected. VION IMS-qTOF conditions for UPLC-HR-MS analysis included capillary voltage (0.80 kV), cone gas (50

L/h), desolvation temperature (350°C), desolvation gas (800 L/h), source temperature (120°C), and acquisition range (*m/z* 50–2000). The system was controlled, and data was processed using UNIFI 1.8.2 (Waters). Chromatographic separation was performed with an BEH C18 1.7 μm (2.1 × 100 mm) column (Waters) maintained at 40°C. Selected peaks were dereplicated using MarinLit, ChemSpider, and Dictionary of Natural Products, as well as extensive literature searches.

Waters UNIFI and Progenesis software was used conduct variance analyses between *Pleurosigma* sp*., Pleurosigma* sp. *i*nfected with *P. isakeiti,* and media control extracts from ethyl acetate and resin methods by analysis of variance (ANOVA) tests and principal component analysis (PCA; Appendix 5).

3.5   Testing for Bioactivity

3.5.1   Anti-cancer Assay

The cytotoxic activity of the extracted metabolites from the diatom culture samples was determined using the CellTiter96 ® Aqueous One Solution Cell Proliferation assay. Firstly, melanoma cells (A2058) were incubated in a 96 well plate overnight at 37°C, 5% carbon dioxide (CO_2), and a density 2000 cells/well in RPMI-1640 media with 10% fetal bovine serum (FBS, Biochrom, FG1385). Following incubation, the media was removed and replaced with 100 μL new media together with extract samples in triplicate. Plates with samples were incubated for 72 h at 37°C and 5 % CO_2 before 10 μl Aqueous One Solution Reagent (Promega, G3581) was added to each well. Positive controls were 10% DMSO and negative controls contained media only. Plates were further incubated for 1 h. Absorbance at ~490 nm was measured in a spectrophotometer (Multimode detector DTX 880). This absorbance value is directly proportional to the number of living cells in the culture which can reduce the tetrazolium compound (yellow color) to a formazan product (blue color) and, as such, exhibit cytotoxicity against proliferating melanoma cancer cells.

3.5.2   Anti-oxidant Assay

The antioxidant potential of extracted metabolites from the diatom culture samples was assessed using the oxygen radical absorbance capacity (ORAC) assay. This assay measures the oxidative degeneration of fluorescein, an organic dye compound, by 2,2′-azobis (2-methylpropionamide) dihydrochloride (AAPH), which forms peroxyl free radicals with the addition of heat. These free

radicals decrease the fluorescence of fluorescein and antioxidants provide protection of fluorescein from the free radicals. 10.5 µL of the sample was combined with 14.5 µL of MilliQ water in duplicates of a black 96-well microtiter plate. A 6-point standard curve containing 25 µL of Trolox standard solution (stock solution prepared using 25 mg of Trolox (Sigma Aldrich, 53188-07-1) in 10 mL of phosphate buffer (10.649 g $Na_2HPO_4*2H_2O$ dissolved in 1000 mL of MilliQ water with pH adjusted to 7.4) diluted to 18, 12.5, 6.25, 3.125 and 1.563 µM). Phosphate buffer was used in 0 µM Trolox wells. 125 µL fluorescein (55 nM dilution of the stock solution prepared by dissolving 33 mg of fluorescein (Sigma Aldrich, 2321-07-5) in 10 mL of phosphate buffer) was added to each well and the plate was incubated for 15 minutes at 37°C. 60 µL of 57 mM AAPH (Sigma Aldrich, cat: 44,091-4, prepared using 705 mg AAPH dissolved in 13 mL of phosphate buffer) reagent was added to all sample wells before the plate was set in the Victor 3 plate reader set at 485 nm excitation, 520 nm emission for 45 minutes at 37°C. Samples were compared against the Trolox standard curve. For all the samples, the area under the curve (AUC) is calculated. The area between the curves (ABC) = AUC_{sample} - $AUC_{standard}$. Ethyl acetate extraction samples from healthy *Pleurosigma* sp., cocultures of *Pleurosigma* sp. and *P. isakeiti*, and media controls far exceeded the standard TE calibration curve (Figure 8).
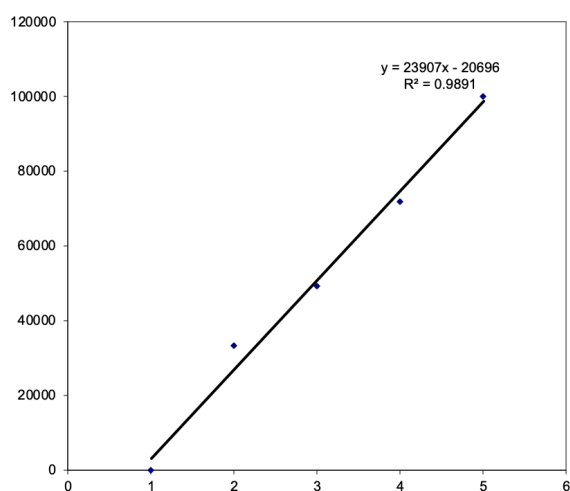
Figure 8 Calibration curve using Trolox Equivalent (TE) standard units

3.5.3 Anti-bacterial MIC Assay

The antibacterial potential of the extracted secondary metabolites was tested using a minimum inhibitory concentration (MIC) assay against different bacteria strains. Bacteria strains (*S. aureus,*

ATCC 25923; *E. coli,* ATCC 25922; *E. faecalis,* ATCC 29212; *P. aeruginosa,* ATCC 27853; *Streptococcus b.,* ATCC 12386) are maintained in the Marbio lab for these tests. To prepare the bacteria for testing, an agar plate (ordered from UNNs media kitchen) was inoculated with a scoop of the bacteria stock taken from the freezer. The blood agar plate was incubated overnight at 37ºC. Mueller Hinton Broth (MH, Becton Dickinson, 275730) and brain heart infusion (BHI, Becton Dickinson, 237500) growth media was prepared according to the manufacturer's instructions and then autoclaved for 60 min at 121°C before use. Bacteria from blood agar plates were added to the growth media according to Table 5 and incubated at 37°C overnight. Following incubation, 2 mL of the bacterial suspension was transferred into 25 mL of the growth medium.

Table 5 Bacteria, growth medium, and incubation period

Bacteria	Growth medium	Incubation	Bacterial density (colony forming units)
S. aureus	MH	2,5 h	$0,5\text{-}3\times10^5$ CFU/ml (2500-15000 CFU/well)
E. coli	MH	1,5 h	$0,5\text{-}3\times10^5$ CFU/ml (2500-15000 CFU/well)
E. faecalis	BHI	1,5 h	$0,5\text{-}3\times10^5$ CFU/ml (2500-15000 CFU/well)
P. aeruginosa	MH	2,5 h	$3\text{-}7\times10^4$ CFU/ml (1500-3500 CFU/well)
Streptococcus b	BHI	1,5 h	$0,5\text{-}3\times10^5$ CFU/ml (2500-15000 CFU/well)

Extract samples of 40 μg/ml were added in parallel to 5 microtiter plates (Nunc, 734-2097) together with 50 μl diluted (1:1000) bacteria growth medium solution and incubated overnight at 37ºC. Negative controls were comprised of growth medium (without bacteria) and autoclaved MilliQ water. Positive controls were growth medium (with bacteria) and autoclaved MilliQ water. A dilutions series of Gentamicin (Amresco, E737), a known antibacterial compound, was run in a separate plate at a concentration between 0.01- 32 μg/ml together with 50 μl of bacterial suspension. Plates were run with a Victor3 plate reader.

3.5.4 Anti-bacterial Biofilm Assay

The antibacterial activity of extracted secondary metabolites was tested using *Staphylococcus epidermidis* and this bacteria's ability to potentially form a biofilm. Firstly, a scoop of bacteria (*Staphylococcus epidermidis*, RP62A 42-77; *Staphylococcus haemolyticus* (clinical isolate 8-7A)

was transferred from the blood agar (detailed in MIC assay) into 5 mL of Tryptic soy broth (prepared according to manufacturer's instructions, Merk, 1.05459) and incubate at 37°C overnight on a shaker. Dilute bacterial solution further in 1:100 Tryptic soy broth with 1% glucose (Sigma, D9434). Then 50 µl of the samples 40 µg/ml in triplicates were pipetted into microtiter plates together with 50 µl bacteria. The negative control was comprised of 50 µl *S. haemolyticus* and 50µl MilliQ water. The positive control was comprised 50 µl *S. epidermidis* and 50 µl MilliQ water. A medium blank was included made of 50 µl Tryptic soy broth and 50 µl MilliQ water. Plates were incubated overnight at 37°C.

Following the 2nd incubation, bacteria was removed from the plates using cell paper and the plates were rinsed with tap water 2-3 times. The biofilm now on the inside of the plate wells was allowed to fixate for 1 hr at 65°C before adding 70 µl 0.1 % crystal violet solution (Merck, 1.15940) into each well then incubating for 10 min. The crystal violet solution was then removed from the wells with cell paper and plates were again washed with tap water 2-3 times. Plates were set to dry for 1 hr at 65°C. Finally, 70 µl 70 % ethanol was added to each well and plates were incubated on a shaker for 5-10 min. The antibacterial potential of the extract was measured at 600 nm using the Victor3 plate reader and the WorkOut 2.5 software. Samples that inhibit biofilm formation will results in wells with little or no violet color.

3.5.5 Anti-inflammation Assay

The purpose of this method is to find compounds, fractions, or extracts that inhibit lipopolysaccharides (LPS) induced secretion of tumor necrosis factor (TNF-α). Thp-1 cells (human acute monocytic leukemia cell line**)** differentiated from monocytes to macrophages are added compounds, fractions or extracts. After one hour of incubation LPS is added and the cells are incubated for 6 hours. TNF-α secreted into the cell culture media is measured by a TNF-α enzyme-linked immunosorbent assay (ELISA) assay. Endotoxin levels are measured in Endotoxin units per milliliter (EU/mL). One EU equals approximately 0.1-0.2 ng endotoxin/mL of solution. Thp-1 cells are very sensitive to endotoxins.

Thp-1 cells grow in suspension as single cells or small lumps of cells. Split cells twice a week to maintain the culture by transferring 2-3 x 10^5 cells/mL to a new tissue culture (TC) flask. Cells grow exponentially 3-8 x 10^5 cells/ml. Cell density must be kept over 1 x 10^5 cells/ml.

Thp-1 cells will be differentiated from monocytes to macrophages when stimulated with phorbol 12-myrisate 13-acetate (PMA). Microtiter plates had negative and positive control duplicates with growth media and 1 ng/ml LPS, respectively.

3.5.5.1 Cell Line Maintenance

To maintain and seed cells, growth media was pre-heated to 37°C. TC-flasks and microtiter plates were labeled with cell line, passage number, date and initials. Cells were observed under a microscope. TC-flasks were wiped with 70% ethanol and placed in a laminar flow hood. Cells were transferred from the TC-flask to 50 mL centrifuge tubes. Cells were spun at 150 g for 5 min. Old media was removed and cells were re-suspended in 25-30 mL of fresh growth media. 50 µl of cell suspension was transferred to a tube containing 450 µl trypan blue and stirred. 10 µl of cells was transferred in trypan blue to a cell-counting chamber. Living cells were counted under the microscope. Dead cells were blue. The cells were counted in two squares and the number of cells in cell suspension was determined. The volume of cell-suspension needed to maintain and seed cells in microtiter plates by using the formula C_1 x V_1 = C_2 x V_2 was found. Cells were maintained in 175 cm^2 TC-flask at a density of 2-3 x 10^5 cells/mL in 50-60 mL growth media. Cells were incubated at 37°C with 5 % CO_2 for 3-4 days. Cells were split every 3-4 days. A cell suspension was made at a density of 1 x 10^6 cells/mL for seeding cells in microtiter plates. 50 ng/mL PMA was added to the cell suspension (0.5 µl PMA stock solution per 10 ml) to differentiate cells from monocytes to macrophages. A 10 mL cell suspension was made for each microtiter plate plus 5 mL extra. 100 µl cell suspension was added to each well in a microtiter plate. Cells were incubated at 37°C with 5 % CO_2 for 48 hours. Cells were observed under the microscope after 24 hours. Cells were washed with endotoxin tested PBS and add new growth media. Cells were incubated at 37°C with 5 % CO_2 for 24 hours.

3.5.5.2 Anti-inflammation Assay Prep

Endotoxin tested phosphate-buffered saline (PBS), new growth media, and cell suspension were pre-heated to 37°C. Old media was removed and 80 µl RPMI (Roswell Park Memorial Institute)

growth media was added to each well. 90 µl RPMI media was added to LPS controls and 100 µl RPMI media to cell controls. 10 µl of extracts from *Pleurosigma* sp., cocultures with *P. isakeiti,* and media controls was added to each well. Each sample was made in duplicate. Samples and controls were added. Cells were then incubated at 37°C with 5 % CO_2 for 1 hour.

10 ng/mL LPS solution was prepared and 10 µl was added to each well except the cell control. LPS concentration will be 1 ng/ml. LPS was diluted in two steps; 1) 10 µL LPS was added to 990 µL RPMI and mixed well. 2) LPS was diluted to 1:1000, mixed well and added to cells. Cells were incubated at 37°C with 5 % CO_2 for 6 hours. Plates were incubated at -80°C freezer for storage.

3.5.5.3 Human TNF-α ELISA Assay:

Affinity purified anti-human TNF-α was diluted to 2 µg/mL in 10 mM Tris-buffered saline (TBS). 100 µL was added to each well in a 96-well Maxisorp plate and incubated at 4°C overnight. The blocking buffer, assay diluent, and wash buffer were prepared. The plate was washed with the Aquamax plate washer. 200 µl 10 mM TBS with 2 % bovine serum albumin (BSA) was added to each well and incubated for 1 hour on the shaker. Plate was washed with the Aquamax plate washer. Samples and standards were diluted in assay diluent directly in ELISA plate. The plate was incubated for two hours on shaker. Biotin anti-human TNF-α was diluted to 3 µg/mL in assay diluent.100 µl was added to each well and incubated for 1 hour on shaker. Plate was washed with the Aquamax plate washer. ExtrAvidin-Alkaline phosphatase was diluted 1:20000 in assay diluent. 100 µl was added to each well and incubated for 30 min on shaker. Para-nitrophenylphosphate in 1 M diethanolamin buffer was diluted to 1 mg/ml. 100 µL was added to each well for 30-45 minutes. Absorbance was read at 405 nm.

3.6 Statistical Analysis of Silicate Treatments and Nutrient Levels on Parasitism

Data collected was imported into Rstudio version 1.2.5003 running R 3.5.1 GUI 1.70 El Capitan build (7543) written by Simon Urbanek, Hans-Jörg Bibiko, Stefano M. Iacus. Quasi-binomial generalized linear models (glm) in the base R "stats" package were used to model the proportion of infected cells were calculated as infected / (health + infected cells) and dividing cells were calculated as dividing / healthy cells. The data was cleaned by removing the control replicates.

Generalized linear models were created to explore the relationship between percent infected and percent under division over time (Day) by silicate treatment. The quasi-binomial distribution was chosen for the glm as counts were done by categorizing cells as either healthy or infected, dividing and dead, a natural choice for a binomial distribution. Furthermore, the quasi-binomial distribution allows for greater variation in the data without losing statistical power (Consul, 1990).

The nutrient analysis dataset was divided into culture groups. Quasi-binomial generalized linear models were generated to test the effect of SiO_2, NO_3, and $NO_3:SiO_2$ on the proportion of infected and dividing *Pleurosigma* sp. *i*nfected with *P. isakeiti* over time. $NO_3:SiO_2$ was calculated by dividing NO_3/SiO_2 at the dilution concentrations used. Quasi-binomial generalized linear models were also generated for healthy *Pleurosigma* sp. cells over time to test the effect of SiO_2, NO_3, and $NO_3:SiO_2$ on the proportion of dividing cells. The models were visualized and extracted using the l*attice* (Sarkar 2008) and *ggplot2* (Wickham 2019) packages. Models and estimated values and t-values for each model parameter are presented for each test. T-values represent the magnitude of the departure of the estimated value from the predicted value for each parameter relative to its standard error. Significance was set to $\alpha=0.05$ for model outputs (Appendix 6).

4   Results

4.1   Isolation of the Thraustochytrid *P. isakeiti* into Monoculture

None of the common thraustochytrid isolation media (Rosa et al. 2011) used to attempt a transfer and monoculture of parasite *P. isakeiti* in the present study were successful (Table 1). Unsuccessful media isolation experiments conducted in this thesis limit the ability to accept the hypothesis that *P. isakeiti* is an obligate parasite of *Pleurosigma* sp.; however, no evidence presented here supports any other life strategy. No growth was found on GPY[b], KMV[c], H[b], SSA[d], MC[d], and MC-BHB media. Plates were checked every three days for three weeks and only bacterial growth was observed on select media. Two different bacteria were responsible for bacterial growth on KMV[c] and H[b] media. Bacteria were stained and visualized on a light field microscope and inverted light microscope. FSW was lightly added to visualize the movement of bacterial cells.

4.1.1 Characterization of Cocultured Bacterial Strains

Colony PCR was conducted, amplifying 16S DNA directly from the PCR reaction from two bacterial colonies. Fungal primers failed to amplify the DNA. Bacterial sequencing and BLAST (NCBI) revealed two distinct bacteria (clear and red pigments) present. Nucleotide BLAST hit tables from DNA sequencing of PCR reaction products of bacterial colonies growing on KMV revealed that bacterium present was an *Alteromonas* species closely affiliated with *A. genoviensis* (Table 6). On the Honda media, nucleotide BLAST hit tables from DNA sequencing of PCR reaction products of bacterial colonies revealed that samples represented a *Marinobacter* species (Table 7).

Table 6 BLAST hit table of DNA sequence from PCR reaction products of bacteria colonies picked from KMV media.

Description	Max Score	Total Score	Query Cover	E value	Per. Ident	Accession
Marine bacterium IVA014 16S ribosomal RNA gene, partial sequence	2540	2540	99%	0.0	99.57%	KJ814566.1
Marine bacterium IIIA014 16S ribosomal RNA gene, partial sequence	2531	2531	99%	0.0	99.35%	KJ814565.1
Uncultured bacterium clone L4-B38 small subunit ribosomal RNA gene, partial sequence	2529	2529	100%	0.0	99.28%	KJ549053.1
Uncultured bacterium clone L4-B105 small subunit ribosomal RNA gene, partial sequence	2529	2529	100%	0.0	99.28%	KJ549025.1
Uncultured marine bacterium clone TU27 16S ribosomal RNA gene, partial sequence	2529	2529	100%	0.0	99.28%	JN717177.1
Alteromonas genoviensis strain I96 16S ribosomal RNA gene, partial sequence	2529	2529	100%	0.0	99.28%	FJ040187.1
Alteromonas genovensis partial 16S rRNA gene, strain LMG 24079	2529	2529	100%	0.0	99.28%	AM887686.1
Alteromonas genovensis strain LMG 24078 16S ribosomal RNA, partial sequence	2525	2525	100%	0.0	99.21%	NR_042667.1
Alteromonas genovensis strain TC12 16S ribosomal RNA gene, partial sequence	2523	2523	100%	0.0	99.21%	KF472189.1
Uncultured bacterium clone L4-B81 small subunit ribosomal RNA gene, partial sequence	2521	2521	100%	0.0	99.21%	KJ549092.1
Uncultured bacterium clone L5n-B75 small subunit ribosomal RNA gene, partial sequence	2518	2518	100%	0.0	99.14%	KJ549205.1
Uncultured bacterium clone L4-B63 small subunit ribosomal RNA gene, partial sequence	2518	2518	100%	0.0	99.14%	KJ549075.1

Table 7. Blast hit table of DNA sequence from PCR reaction products of bacteria colonies picked from Honda media.

Description	Max Score	Total Score	Query Cover	E value	Per. Ident	Accession
Marinobacter sp. SW2104 partial 16S rRNA gene, isolate SW_2_104	987	987	100%	0.0	98.92%	LR722857.1
Marinobacter litoralis strain SW-45 16S ribosomal RNA gene, partial sequence	987	987	100%	0.0	98.92%	MN186602.1
Marinobacter litoralis strain SW45 16S ribosomal RNA gene, partial sequence	987	987	100%	0.0	98.92%	MN186593.1
Marinobacter sp. strain CB08016 16S ribosomal RNA gene, partial sequence	987	987	100%	0.0	98.92%	MH420596.1
Uncultured bacterium clone AB-4 16S ribosomal RNA gene, partial sequence	987	987	100%	0.0	98.92%	KX651417.1
Marinobacter litoralis strain NIOSSK056#96 16S ribosomal RNA gene, partial sequence	987	987	100%	0.0	98.92%	KY926903.1
Marinobacter litoralis strain NIOSSK056#91 16S ribosomal RNA gene, partial sequence	987	987	100%	0.0	98.92%	KY678484.1
Marinobacter litoralis strain NIOSSK079#51 16S ribosomal RNA gene, partial sequence	987	987	100%	0.0	98.92%	KY604813.1
Marinobacter sp. H1-125 16S ribosomal RNA gene, partial sequence	987	987	100%	0.0	98.92%	KM979118.1
Marinobacter sp. DM06 BPH 16S ribosomal RNA gene, partial sequence	987	987	100%	0.0	98.92%	KT348327.1
Marinobacter sp. EK6D gene for 16S ribosomal RNA, partial sequence	987	987	100%	0.0	98.92%	LC053420.1
Marinobacter sp. M3-11 16S ribosomal RNA gene, partial sequence	987	987	100%	0.0	98.92%	KP058417.1

4.2 Rate of Infection and Division

The infection rate experiment (Figure 9) revealed that the parasitism of *Pleurosigma* sp. by *P. isakeiti* is significantly affected by silicate (Table 8). Time significantly impacts both infection and division with higher proportions of both occurring later in the incubation period (Table 8 and 9, respectively). Time agonistically interacts with the silicate treatment to lower the proportion of infected cells as the incubation period progresses (Table 8; Figure 9A). The infection rate of *Pleurosigma* sp. by *P. isakeiti* increases under reduced-silicate treatment although not visually different until day 10 (Figure 9A). While the infection rate difference with silicate treatment is subtle, it is statistically significant (Table 8; Appendix 2). Notably, the initial rate of infection for the silicate treatment started slightly higher than the reduced silicate treatment. The reduced silicate treatment resulted in a slightly faster infection, however the increase in infection rate did not have dramatic impact on the outcome of the infection process. By the twentieth day, the total proportion of infected to healthy cells was not different and by the end of the experiment both cultures were nearly 99% infected. Therefore, the hypothesis 2A which states the infection rate of *Pleurosigma* sp. by *P. isakeiti* is affected by silicate treatment can be accepted.
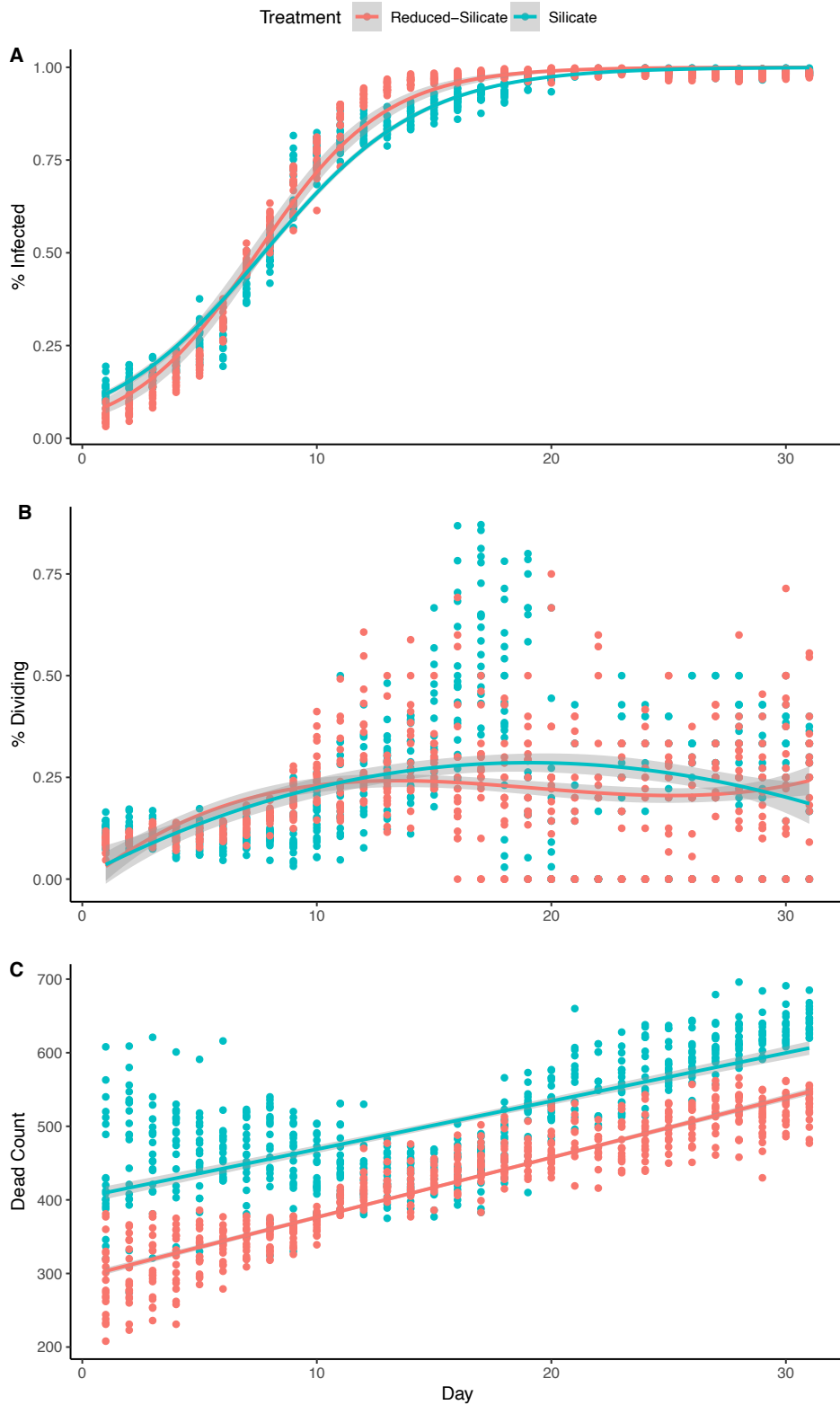
Figure 9 A) Incidence of parasitism and B) division of pennate diatom *Pleurosigma* sp. cultures by thraustochytrid parasite *P. isakeiti* over 31 days. Total dead enumerated during counting observations (C). Quasi-binomial generalized linear models are transposed over the data points. Cultures treated with reduced-silicate media are shown in green while non-silicate-reduced media are shown in red. Grey ribbons around lines are the 95% confidence intervals around the predicted value from the glm

Table 8 Statistical variance of generalized linear model of the interaction between incidence of host infection on day and treatment

Model: glm(proportion of Infected cells ~ Day * Treatment)

Model Parameters	Estimate	t value	p value
Intercept	-2.73526	-24.977	< 2e-16
Day	0.36670	30.731	**< 2e-16**
Silicate Treatment	0.43341	2.993	**0.00282**
Day*Silicate Treatment	-0.06926	-4.572	**5.35e-06**

The proposed hypothesis (2B) that the rate of division of infected *Pleurosigma* sp. would decrease in response to reduced silicate treatment was rejected (Table 9; Figure 9B). Cocultures of thraustochytrid *P. isakeiti* and *Pleurosigma* sp. incubated in the reduced silicate treatment had slightly lower rates of division than those reared in the abundant silicate media although not significantly different statistically. The rate of division clearly increased over time in both cultures observed in standard and reduced silicate media. The response of division to infection was more immediate in reduced silicate samples. The incidence of division in samples with more available silicate visibly reached greater total proportions by day 20. By the end of the 31-day experiment, the rate of division in both treatments converged on roughly 30% with no significant difference between the two treatments.

Table 9 Statistical variance of generalized linear model of the interaction between the incidence of host division on day and treatment

Model: glm(proportion of Dividing cells ~ Day * Treatment)

Model Parameters	Estimate	t value	p value
Intercept	-1.750838	-20.579	< 2e-16
Day	0.024691	5.564	**3.25e-08**
Silicate Treatment	-0.027083	-0.226	0.822
Day*Silicate Treatment	0.007261	1.159	0.247

4.3 Effect of Free Silicate and Nitrate on Division Over Time

The third objective, to assess the uptake of silicate and nitrate nutrients under healthy and parasitic conditions, resulted in confounding results. The initial hypothesis, that the uptake of silicate decreases in parasitized *Pleurosigma sp.* cultures, could not be rejected (Figure 10B; Figure 11A). Silicate abundance in the media decreased over time (Figure 11), and thus uptake by diatoms increased in response to parasitism. The ratio of nitrate to silicate increased over the course of a two-week period as the infection rate rose steadily and rate of division increased (Figure 11). This

ratio increased as a result of increasing nitrogen abundance in both cultures and decreasing silicate abundance in infected cultures (Figure 11). Plotting raw silicate and nitrate over time demonstrates the impact of increased silicate uptake during parasitism on nitrate:silicate ratio (Figure 10; Figure 11). Slight increases in nitrate were observed in both healthy and infected *Pleurosigma* sp. culture mediums.

In infected cultures, the proportion of infected cells increased significantly with increasing nitrate levels, increasing nitrate to silicate ratios, and over time (Table 10). The proportion of dividing cells in infected cultures was significantly affected by the interaction of time and nitrate levels (Table 10). In healthy *Pleurosigma* sp. cultures, the proportion of dividing cells was negatively affected by silicate levels, the interaction between time and silicate levels, and time (Table 11). The nitrate to silicate ratio positively affected the proportion of dividing cells in healthy cultures independent of time (Table 11). Silicate concentration decreased faster over time in the coculture including *P. isakeiti* in comparison with the healthy *Pleurosigma* sp. cultures (Table 10).

4.3.1   *Pleurosigma* sp. Division Over Time

Pleurosigma sp. cocultured with thraustochytrid *Phycophthorum isakeiti* divided at an increased rate over the course of the experiment when compared to healthy *Pleurosigma* sp. cells (Figure 10 C).

Table 10 Statistical variance of generalized linear model of the interaction between incidence of host infection on day and silicate level, host division on day and silicate level, host infection on day and nitrate level, host division on day and nitrate level, host infection on day and nitrate: silicate level, and host division on day and nitrate: silicate level

Model: glm(proportion of **Infected** cells in Coculture~ Day * Silicate Level)

Model Parameters	Estimate	t value	p value
Intercept	-1.760268	-15.116	< 2e-16
Day	0.248591	17.729	**< 2e-16**
Silicate Level	-0.024659	-0.872	0.38509
Day*Silicate Level	0.012915	2.711	**0.00767**

Model: glm(proportion of **Dividing** cells in Coculture ~ Day * Silicate Level)

Model Parameters	Estimate	t value	p value
Intercept	-2.333688	-16.007	< 2e-16
Day	0.103879	6.820	**3.74e-10**
Silicate Level	0.035656	1.054	0.294
Day*Silicate Level	-0.006581	-1.285	0.201

Model: glm(proportion of **Infected** cells in Coculture~ Day * Nitrate Level)

Model Parameters	Estimate	t value	p value
Intercept	-2.320532	-12.368	< 2e-16
Day	0.368657	14.499	**< 2e-16**
Nitrate Level	0.149341	3.134	**0.00216**
Day* Nitrate Level	-0.023762	-4.253	**4.16e-05**

Model: glm(proportion of **Dividing** cells in Coculture ~ Day * Nitrate Level)

Model Parameters	Estimate	t value	p value
Intercept	-1.877246	-8.826	9.48e-15
Day	-0.006440	-0.252	0.80134
Nitrate Level	-0.069263	-1.227	0.22229
Day* Nitrate Level	0.019184	3.286	**0.00133**

Model: glm(proportion of **Infected** cells in Coculture~ Day * Nitrate:Silicate ratio)

Model Parameters	Estimate	t value	p value
Intercept	-1.864089	-21.523	< 2e-16
Day	0.292928	23.882	**< 2e-16**
Nitrate:Silicate ratio	0.060321	2.004	**0.04727**
Day* Nitrate:Silicate ratio	-0.008835	-2.856	**0.00505**

Model: glm(proportion of **Dividing** cells in Coculture ~ Day * Nitrate:Silicate ratio)

Model Parameters	Estimate	t value	p value
Intercept	-2.125474	-20.178	< 2e-16
Day	0.072244	5.542	**1.75e-07**
Nitrate:Silicate ratio	-0.047708	-1.251	0.213
Day* Nitrate:Silicate ratio	0.005685	1.619	0.108

Table 11 Statistical variance of generalized linear model of the interaction between incidence of host division on day and silicate level, incidence of host division on day and nitrate level, incidence of host division on day and nitrate:silicate level

Model: glm(proportion of Dividing cells in Pleurosigma culture~ Day * Silicate Level)			
Model Parameters	Estimate	t value	p value
Intercept	-1.085690	-4.418	7.13e-05
Day	-0.075000	-2.229	**0.03139**
Silicate Level	-0.094247	-3.472	**0.00123**
Day* Silicate Level	0.008104	2.174	**0.03551**

Model: glm(proportion of Dividing cells in Pleurosigma culture ~ Day * Nitrate Level)			
Model Parameters	Estimate	t value	p value
Intercept	-1.924547	-5.306	4.18e-06
Day	0.021629	0.471	0.640
Nitrate Level	-0.001182	-0.036	0.971
Day* Nitrate Level	-0.001828	-0.470	0.641

Model: glm(proportion of Dividing cells in Pleurosigma culture ~ Day * Nitrate:Silicate ratio)			
Model Parameters	Estimate	t value	p value
Intercept	-2.37003	-12.393	1.89e-15
Day	0.03552	1.462	0.1514
Nitrate:Silicate ratio	0.34685	2.440	**0.0191**
Day*Nitrate:Silicate ratio	-0.02979	-1.705	0.0957
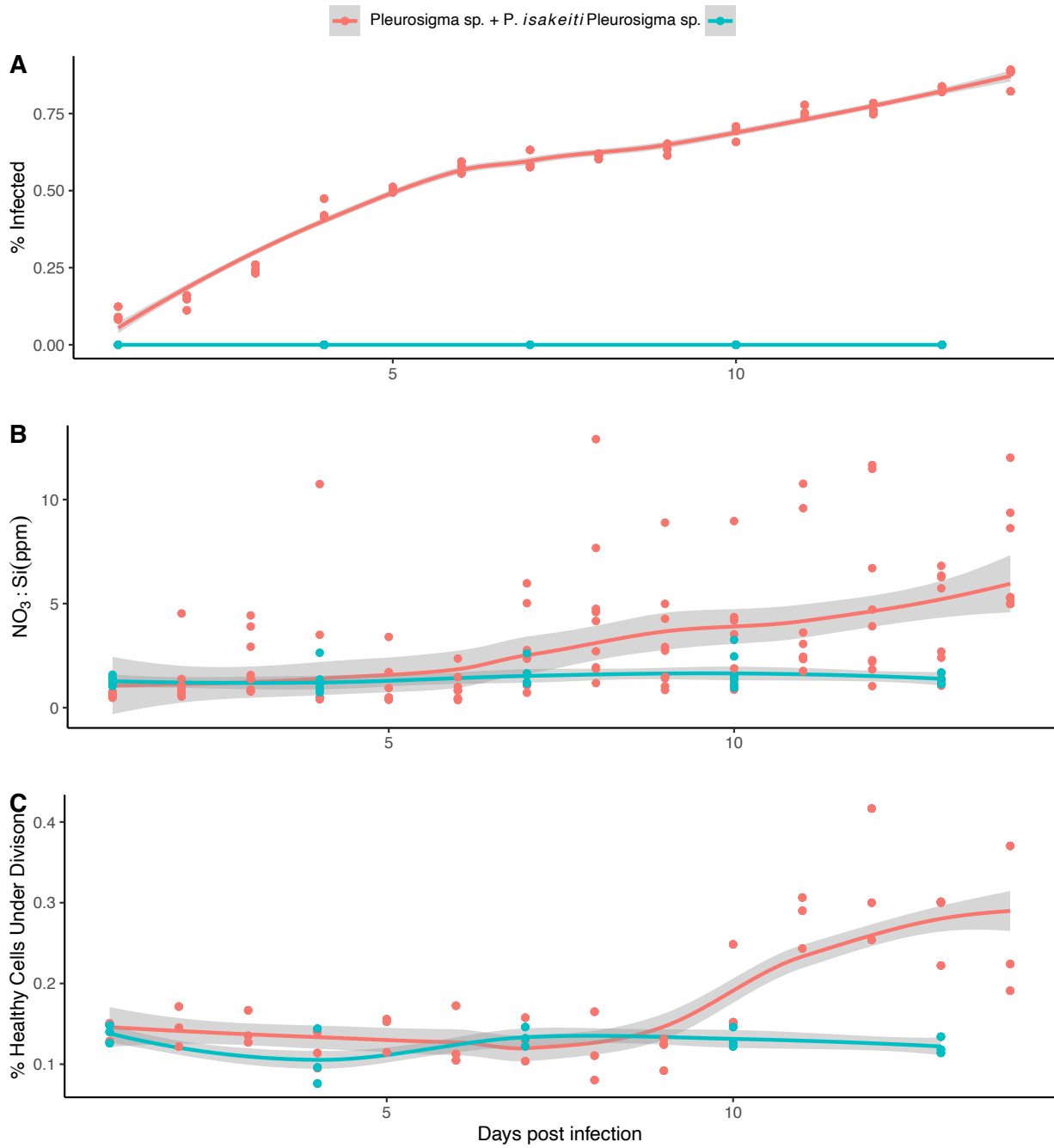
Figure 10 Incidence of A) parasitism, B) abundance of free $NO_3:SO_2$ and C) incidence of division of pennate diatom *Pleurosigma* sp. cultures by thraustochytrid parasite *P. isakeiti* over 15 days. Quasi-binomial generalized linear models are transposed over the data points. Healthy *Pleurosigma* sp. cultures are shown in green while *Pleurosigma* sp + *P. isakeiti* cocultures are shown in red. Grey ribbons around lines are the 95% confidence intervals around the predicted value from the glm
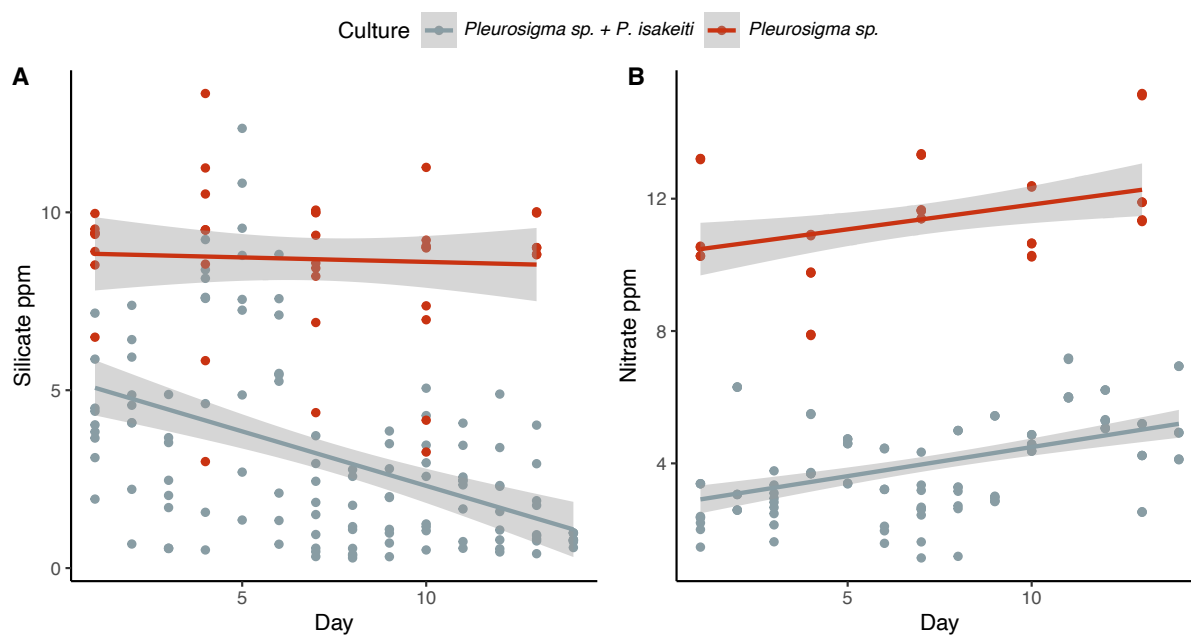
Figure 11 Silicate (A) and nitrate (B) over 15 days in Healthy *Pleurosigma* sp. (red) and Cocultures of *Pleurosigma* sp. and *P. isakeiti* (green). Grey ribbons around lines are the 95% confidence intervals around the predicted value from the glm

4.4 Detection of Chemical Differences in Parasitized *Pleurosigma* sp.

The fourth objective, to determine whether chemical differences could be detected among healthy and parasitized *Pleurosigma* sp. cultures were resolved using LC-MS, which revealed measurable chemical variances (Figure 12). Clearly, compounds were detected in parasitized cultures that could not be found in healthy cultures; however, the origin of the variance remains unknown. Without LC-MS data of extracts from isolated *P. isakeiti* to compare healthy and parasitized *Pleurosigma* sp. extracts against, it is unclear if compounds found in the coculture were produced by the parasite, the host, or a bacterial cohabitant. Several differences in chemical signatures were detected when comparing the spectra from extracts of healthy *Pleurosigma* sp., cocultures of *Pleurosigma* sp. *and P. isakeiti,* and controls of F/2 media diluted in 1:50 FSW. The delta area

under the curve between healthy *Pleurosigma* sp.*(red)* cultures and cocultures with *P. isakeiti* (blue) is represented with a green line below.
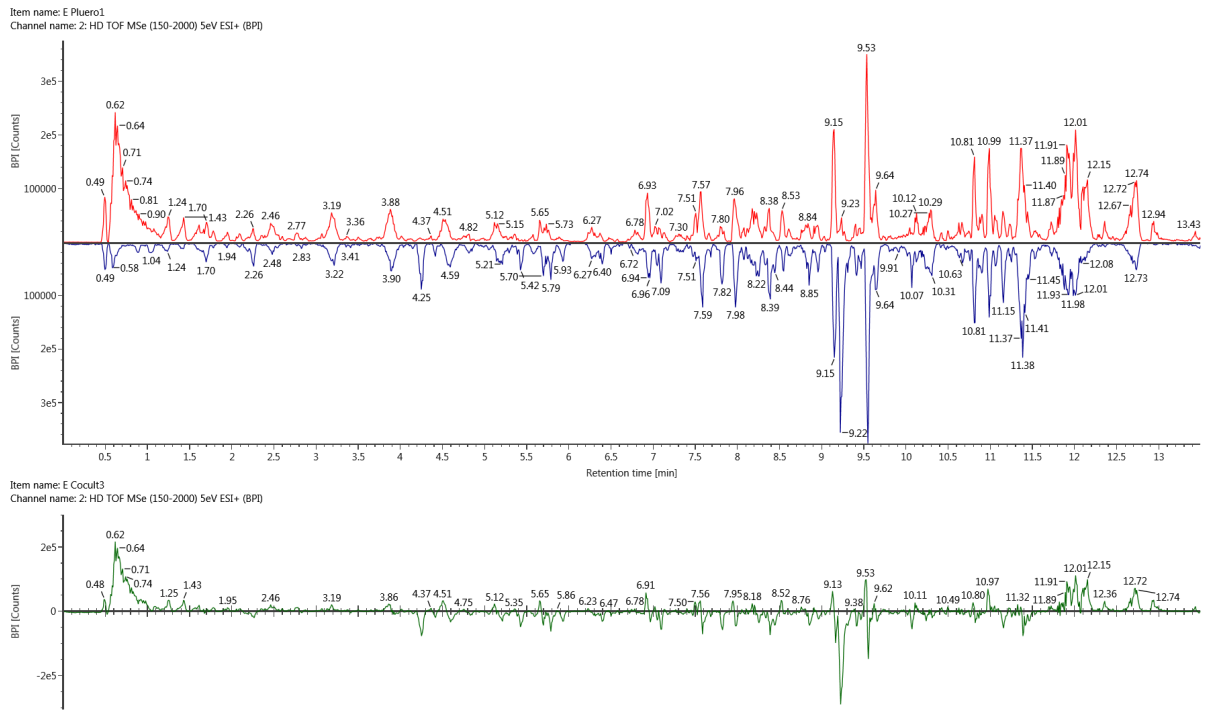
Figure 12 Chromatogram of TOF MSe (150-2000) 5eV ESI+ of base peak intensities of ethyl acetate extracts from healthy pennate diatom *Pleurosigma* sp. (red) and cocultures of *Pleurosigma* sp and *P. isakeiti* (blue). The difference between peak integrals (red and blue) is shown in the chromatogram below (green)

The two significantly different compounds that eluted from the coculture extracts in all three replicates at retention times 4.24 min and 9.23 min were not observed in the media controls or the healthy *Pleurosigma* sp. cultures (Figure 12). Analysis of variance revealed that the compound with retention time (R_t) 4.24 and *m/z* 278.2110 (Appendix 3), when compared to healthy *Pleurosigma* sp. and media controls, had a p-value of 2.4e-07, q-value of 7.61e-08 and power $\geq$ 0.9995 in variance analysis. The elemental composition was calculated as $C_{17}H_{27}NO_2$ ($[M+H]^+$) with an iFit score of 100%, *i.e.,* the experimental data had a perfect fit with theoretical data for this elemental composition. The compound that eluted at R_t 9.22 had a *m/z* of 325.1208 (Appendix 4) and p-value of 6.67e-05 and q-value of 6.67e-06 and power $\geq$ 0.9995 in variance analysis with healthy *Pleurosigma* sp. and controls. Its elemental composition, $C_{23}H_{16}O_2$ ($[M+H]^+$), also had an iFit score of 100%.

The unknown compound that appears at 4.24 minutes in cocultures is also present at low ion concentrations in the media control and healthy *Pleurosigma* sp. cultures, however; peaks detected in the control and healthy *Pleurosigma* sp. extracts are barely distinguishable from noise. There were several hits in marine literature databases for this elemental composition; however, it remains uncertain if any of these known natural products can be associated with *Pleurosigma* sp. or *P. isakeiti*. While the two compounds, $C_{17}H_{27}NO_2$ and $C_{23}H_{16}O_2$, were detected only in cocultures of *Pleurosigma* sp., without isolated biomass from *P. isakeiti*, determination of whether the compound was produced by the thraustochytrid to infect its host or the diatom to defend itself from parasitism cannot be distinguished.

4.5 Bioassay Results

Results from five different bioassays led to the rejection of the final null hypothesis that extracts from cocultures of *Pleurosigma* sp. and *P. isakeiti* contain no cytotoxic activity. No activity was observed against melanoma cells in the anti-cancer assay (Table 12). Thraustochytrid cultures showed limited activity against *Staphylococcus aureus* in the MIC assay (Table 13) and induced marginal LPS secretion of TNF-α in the anti-oxidant assay (Table 14). No activity was observed against *S. epidermidis* in the anti-biofilm assay (Table 15). The positive results of resin extracts from healthy *Pleurosigma* sp. cultures, cocultures with *P. isakeiti,* and media controls (Table 16) were not further investigated because media control results indicated that whatever activity was detected in the *Pleurosigma sp.* cultures and *P. isakeiti* cocultures could not be disassociated with the media extracts.

4.5.1 Anti-cancer Assay

Cell proliferation was not significantly affected by resin or ethyl acetate extracts of the *Pleurosigma* sp. coculture, healthy *Pleurosigma* sp. or media controls

Table 12 ~490 nm absorbance values directly proportion to cell concentration. Positive controls (10% DMSO) and Negative controls (media)

	Coculture w *P. iskeiti*			*Pleurosigma sp.*		
Concentration	1	2	3	1	2	3
250	0.8908	0.8605	0.8561	0.8131	0.8248	0.8433
125	0.8836	0.8513	0.8257	0.8283	0.8124	0.8197
62.5	0.9012	0.8381	0.829	0.8306	0.8338	0.882
31.25	0.9083	0.8437	0.8278	0.8167	0.821	0.8222
15.75	0.9019	0.8203	0.7904	0.8379	0.8236	0.8393
7.875	0.8998	0.8244	0.8216	0.8512	0.8434	0.8783

	Media Control			Positive Control	Negative Control	
Concentration	1	2	3	1	1	
250	0.9172	0.8563	0.8591	0.9166	0.2014	
125	0.9111	0.8286	0.847	0.9229	0.2206	
62.5	0.8955	0.8538	0.8657	0.9357	0.1972	
31.25	0.8405	0.8229	0.8104	0.9312	0.1963	
15.75	0.8512	0.8677	0.8512	0.9194	0.199	
7.875	0.9005	0.898	0.8769	0.9242	0.2102	

The absorbance values presented (Table 12) are directly proportional to the number of living cells in the culture. Cytotoxic activity against proliferating melanoma cancer cells produces results which reduce the tetrazolium compound (yellow color) to a formazan product (blue color).

4.5.2 Anti-bacterial MIC Assay

Table 13 Anti-bacterial results values are presented as optical density (OD) values at 600nm. Active extracts have OD-values under 0.25.

Extraction	Culture	Concentration	*Enterococcus faecalis*	*Escherichia coli*	*Staphylococcus aureus*	*Streptococcus agalactiae*	*Pseudomonas aeruginosa*
Resin	*Pleurosigma* sp.	High	0.36	0.56	0.34	0.35	0.64
Resin	*Pleurosigma* sp.	Medium	0.29	0.51	0.28	0.36	0.6
Resin	*Pleurosigma* sp.	Low	0.31	0.51	0.26	0.38	0.6
Resin	*Pleurosigma* sp. + *P. Isakeiti*	High	0.23	0.49	0.25	0.37	0.5
Resin	*Pleurosigma* sp. + *P. Isakeiti*	Medium	0.29	0.49	0.24	0.34	0.51
Resin	*Pleurosigma* sp. + *P. Isakeiti*	Low	0.34	0.49	0.28	0.36	0.55
Resin	Media Control	High	0.36	0.51	0.36	0.39	0.53
Resin	Media Control	Medium	0.28	0.46	0.25	0.34	0.51
Resin	Media Control	Low	0.29	0.45	0.26	0.36	0.49
Ethyl Acetate	*Pleurosigma* sp.	High	0.29	0.56	0.24	0.4	0.66
Ethyl Acetate	*Pleurosigma* sp.	Medium	0.31	0.51	0.23	0.36	0.63
Ethyl Acetate	*Pleurosigma* sp.	Low	0.31	0.51	0.25	0.36	0.64
Ethyl Acetate	*Pleurosigma* sp. + *P. Isakeiti*	High	0.3	0.55	0.24	0.36	0.58
Ethyl Acetate	*Pleurosigma* sp. + *P. Isakeiti*	Medium	0.27	0.51	0.25	0.37	0.63
Ethyl Acetate	*Pleurosigma* sp. + *P. Isakeiti*	Low	0.28	0.49	0.26	0.37	0.58
Ethyl Acetate	Media Control	High	0.29	0.5	0.28	0.36	0.67
Ethyl Acetate	Media Control	Medium	0.3	0.48	0.27	0.38	0.58
Ethyl Acetate	Media Control	Low	0.3	0.48	0.25	0.38	0.61

Anti-bacterial activity was detected in resin and extracts of *Pleurosigma* sp. + *P. isakeiti* at medium concentrations among *S. aureus*. Ethyl acetate extractions of healthy *Pleurosigma* sp. cultures *and Pleurosigma* sp. + *P. isakeiti* cocultures were active against *S. aureus* at high and medium concentrations.

4.5.3 Anti-oxidant Assay

The antioxidant assay showed resins extractions to have marginal free radical absorption capacity (Table 14). Activity outside of the calibration curve was observed in all of the resin extractions.

Table 14 Irradiance at 485-520nm of Trolox (TE) equivalent units of resin and ethyl acetate extractions of healthy Pleurosigma sp. Cultures, *Pleurosigma* sp. with *P. isakeiti* cocultures, and media controls

Resin Extraction			Ethyl Acetate Extraction		
Pleurosigma sp.	Coculture	Media Control	Pleurosigma sp.	Coculture	Media Control
30.53691367	31.8011573	32.1457396	7.84646321	24.0667278	16.18661341
Negative Control (Concentration µg/ml)			Positive Control (Concentration µg/ml)		
0 µg/ml	1.56 µg/ml	3.125 µg/ml	6.25 µg/ml	12.5 µg/ml	25 µg/ml
-2.293065948	2.27795029	4.47498735	7.55399915	11.4207351	15.60045415

4.5.4 Anti-bacterial Biofilm Assay

No biofilm degradation activity was detected in either the methanolic resin or ethyl acetate extractions of the coculture, healthy *Pleurosigma* sp.*,* or media controls against *S. epidermis* (Table 15).

Table 15 Anti-bacterial results values are presented as optical density (OD) values at 600nm. Active extracts have OD-values under 0.25.

Extraction	Culture	Concentration	*S. epidermidis*
Resin	*Pleurosigma* sp.	High	0.39
Resin	*Pleurosigma* sp.	Medium	0.32
Resin	*Pleurosigma* sp.	Low	0.33
Resin	*Pleurosigma* sp. + *P. Isakeiti*	High	0.38
Resin	*Pleurosigma* sp. + *P. Isakeiti*	Medium	0.38
Resin	*Pleurosigma* sp. + *P. Isakeiti*	Low	0.39
Resin	Media Control	High	0.38
Resin	Media Control	Medium	0.39
Resin	Media Control	Low	0.33
Ethyl Acetate	*Pleurosigma* sp.	High	0.3
Ethyl Acetate	*Pleurosigma* sp.	Medium	0.3
Ethyl Acetate	*Pleurosigma* sp.	Low	0.26
Ethyl Acetate	*Pleurosigma* sp. + *P. Isakeiti*	High	0.4
Ethyl Acetate	*Pleurosigma* sp. + *P. Isakeiti*	Medium	0.48
Ethyl Acetate	*Pleurosigma* sp. + *P. Isakeiti*	Low	0.49
Ethyl Acetate	Media Control	High	0.53
Ethyl Acetate	Media Control	Medium	0.45
Ethyl Acetate	Media Control	Low	0.39

4.5.5 Anti-inflammatory Assay

Anti-inflammatory activity was detected in the *Pleurosigma sp.,* coculture, and media extracts at levels higher than the calibration curve. No follow-up was pursued because any activity could not be attributed to the cultures because it was detected at such high levels in the media controls (Table 16). Ethyl acetate extracts of *Pleurosigma* sp. and *P. isakeiti* cocultures showed some inhibition of LPS induced secretion of TNF-α at concentrations of 31.3 μg/ml.

Table 16 Values presented below are shown in endotoxin units/ml

Sample	Concentration							
	1000	500	250	125	62.5	31.3	15.6	0
Ethyl Acetate Coculture	1.5733	1.778	1.6546	1.7237	2.0517	2.1544	0.0779	0.0782
Ethyl Acetate Pleurosigma	1.3862	1.3942	1.6885	1.7984	1.7934	1.9568	0.0788	0.0765
Ethyl Acetate Media	1.211	1.3154	1.3354	1.4964	1.4081	1.6666	0.0788	0.0783
Resin Coculture	0.0768	0.0755	0.074	0.0758	0.074	0.0759	0.0763	0.077
Resin Pleurosigma	0.0755	0.0744	0.0736	0.0752	0.0762	0.0764	0.0778	0.0772
Resin Media	0.0742	0.0745	0.0775	0.0759	0.0753	0.0751	0.0758	0.0755
Positive Control	1.9446	2.2259	2.1824	0.0761	0.0764	0.077	0.0764	0.0777
Negative Control	0.0884	0.0788	0.0845	0.076	0.0764	0.0767	0.0769	0.0777

5 Discussion

No direct observations suggest that the proliferation of the amorphic ameboid stages of *P. isakeiti* form a long-term or reiterative resting stage for the thraustochytrid protist; however, their ability to survive extended winter seasons at 69.6492° N, 18.9553° E (*e.i.,* Tromsø, Norway) raises questions about whether they can live saprotrophically as facultative parasites without a host. As host concentrations dip in winter months in the absence of light, it remains curious how they persist through dramatic seasonal variance.

Findings from this work support the local depletion of silicate by diatoms and diatom thraustochytrid cocultures. Silicate concentration varies considerably throughout the ocean (Tréguer et al. 1995) and parasites can affect local silicate concentration gradients along coastal regions (Raven and Waite 2004). As silicate is reduced in the sea, diatoms loose setae, decreasing their motility, control of buoyancy, and natural defense systems (Flynn and Martin-Jézéquel, 2000; Figure 3). Loss of buoyancy may be a community protection method to prevent parasitic spread and aid in nutrient uptake (Gemmell et al. 2016). Buoyancy control allows diatoms to reach photon rich surface waters for photosynthesis while dropping lower in the water column to take up nitrogen, phosphorus, and silicate in deeper, nutrient rich waters (Armbrust 2009; Gemmell et al. 2016). *Pleurosigma* sp., which tends to adhere to surfaces, especially during the winter, is not continuously living in the water column and cannot always rely on buoyancy protection from parasitism when resting on the sea floor.

Reduced silicate increases rate of infection and decreases the rate of division of *Pleurosigma* sp. during coculturing with *P. isakeiti*. As increased division occurs in silicate stressed conditions, future generations of the diatom may become less robust, with thinner silica walls, and greater vulnerability to other microbial parasites. When infected cells divide, in response to parasitism, local silicate decreases as result of the increased silicate uptake under division, perpetuating a cycle of diatom vulnerability to thraustochytrid parasites. Moreover, infection and division rates are cofounded with silicate uptake, and thus codependent (Figure 13).
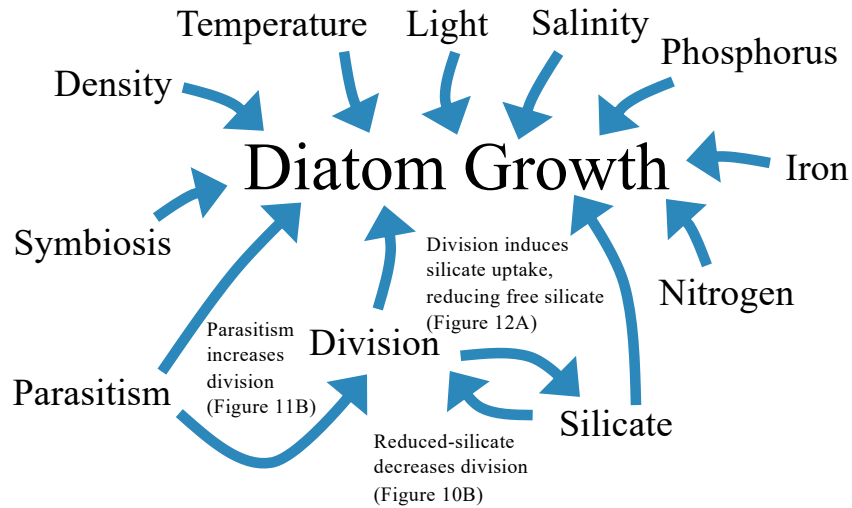
Figure 13 Schematic of diatom growth factors and the role of parasitism, division, silicate reduction**,** and uptake in the relationship between parasite *P. isakeiti* and *Pleurosigma* sp.

Contrarily, laboratory observations of the proportion of dividing *Pleurosigma* sp. may not be an adequate measure of biomass accumulation or growth in the environment (Passche 1973). Algal growth is most often measured using chlorophyll a rather than observations of division (Wang et al. 2017). Measures of chlorophyll a over the same period of time can estimate how accurate the rate of division is as a metric of predicting overall increases in biomass (Furnas 1990). Cells may be dividing at an increased rate; however, their division may take longer under reduced silicate conditions. In these experiments, prolonged division or arrested division in a response to parasitism may have led to over-represented observations of dividing cells. Yet, converting the incidence of division over time to doublings per day to chlorophyll a absorbance values may not be an accurate way to associate intrinsically different growth metrics. Additionally, increased incidence of division without adequate silicate to build cell walls may not result in a healthy photosynthesizing population of diatoms (Lippemeier et al. 1999).

Once silicate is incorporated into a diatom cell wall, it is no longer available to be incorporated into newly dividing diatoms. When diatoms are infected and overwhelmed by the parasite, the silica they sequester into their frustules sinks to the bottom of the ocean, or in the case of this study, to the bottom of the flasks, excluded from future utilization. During nutrient analysis sampling, this silica 'sink' of dead diatoms is removed via filter before analysis. Bacteria, or a saprotrophic

form of the thraustochytrid, may degrade empty silicate shells and reintroduce silicate back into the flask environment. Marine bacteria also have been observed to dramatically increased silicate dissolution in two taxa of lysed marine diatoms relative to bacteria-free controls (Bidle and Azam 1999). If chitin/silica degrading prokaryotic bacteria were present, the results from the nutrient analysis experiments should be re-examined. Moreover, observations have been made of the silica shell being penetrated by the parasite (Hassett 2020).

Slight increases in nitrate were observed in both healthy and infected *Pleurosigma* sp. cultures suggesting that diatoms are not taking up nitrate as was originally hypothesized. A rise in nitrate over time is uncommon in similar experiments using healthy diatoms (Fawcett and Ward 2011). The observed rise in nitrate could have been a result of the internal contents of the compromised diatom shell spilling into the culture media. Therefore, nitrate may be introduced into the cultures from moribund cells' uncontrolled excreting of lysed cytoplasmic contents – amino acids, proteins, and nucleic acids. Clear observations of thraustochytrid penetrations of the cell wall suggest that once their cell wall has been infiltrated, and sporangium have formed, host cell proteins of the cytoplasm, that cannot be easily utilized by the parasite, are released into the culture medium (Appendix 1). These proteins are eventually detected in greater abundance as the host culture is weakened and dead cells dominate the culture flask (Figure 9C). It remains unclear why nitrate also increased over time in healthy *Pleurosigma* sp. cultures.

Division among parasitized diatoms in silicate rich environments appears to have a prolonged response of division in comparison to reduced-silicate conditions (Figure 11C).The parasitism process of *P. isakeiti* in the laboratory culturing flask is effective (Hassett 2020; Figure 9A; Figure 10A); however, the dispersal of diatoms in the marine environment from currents, tides, upwelling, and wind shearing in shallow waters may disperse zoospores to a greater extent, decreasing the possibility of contact with host diatoms (Cermeño and Falkowski 2009).

While recent studies have linked diatoms and thraustochytrids to docosahexaenoic acid (Wang et al. 2018) and eicosapentaenoic acid production (Kobayashi et al. 2011), neither PUFA was detected freely in the ethyl acetate or resin extractions in the LC-MS experiment (Figure 12). As diatoms stop dividing, they stop forming phospholipids, disrupting the inclusion of PUFAs into

the cell wall (Jónasdóttir 2019), preventing potential lipid defense mechanisms (Sabharwal et al. 2017; Damare et al. 2020). In the present study, division increased in response to parasitism (Figure 10A; Figure 10C), suggesting a possible continued production of defensive phospholipids. Membrane fatty acids and aldehydes may be released in seawater following diatom cell lysis (Ribalet et al. 2014) and could also act against parasites –as a community scale defense response.

Although none of the extracts used in the bioassays demonstrated bioactivity of high potency, more strategic screening may yield different results. If any defense lipids or polyunsaturated aldehydes were released, they were only marginally effective at inhibiting the parasitism process under the present laboratory conditions (Figures 10A and 11A); however, in the natural environment, compounds, such as $C_{23}H_{16}O_2$ or $C_{17}H_{27}NO_2$ could play critical roles in parasitism or defense, or participate in signaling surrounding diatom cells to continue dividing or to begin incorporating silicate inside the cell to increase density (Poulson et al. 2009). $C_{23}H_{16}O_2$ and $C_{17}H_{27}NO_2$ could be integral to direct attachment, degradation, or invasion of the *Pleurosigma* sp. cell wall.

In the present study, in all cultures, some healthy diatoms continued to persist despite overwhelming zoospores and massive infection rates in infected cultures (Figures 10A and 11A). These persistent diatoms may have developed a resilience to the parasite (Scholz et al. 2017); however, to determine whether some *Pleurosigma sp.* acquired a resistance would require a reseeding of new culture flasks with the resilient diatoms and a replication of the infection counting experiments. Ultimately, parasites that totally kill their host are unable to proliferate; however, no evidence exists to suggest there is an internal mechanism, feedback loop or control in which *P. isakeiti* resists infecting all *Pleurosigma* sp. cells to persist longer.

Ultra-high performance-liquid chromatography in combination with resolution mass spectrometry gave highly complex chromatograms. However, there were subtle differences between healthy *Pleurosigma sp.* cultures, cocultures with *P. isakeiti,* and media controls (Figure 12). Two compounds characterized the major differences between healthy and parasitized extracts. One eluted at retention time 4.2422 min (*m/z* 278.20923; $C_{17}H_{27}NO_2$) and the second at retention time 9.2357 (m/z 325.12084; $C_{23}H_{16}O_2$). Molecular formulas of both compounds had iFit-scores of 100% confirming their elemental compositions calculated from variance between accurate masses

and isotope intensities (Hancock et al. 2006). Both compounds returned hits when queried among marine chemistry literature databases; however, their identities remain uncertain without compound isolation and structural elucidation using nuclear magnetic resonance. One distinguishing characteristic of $C_{17}H_{27}NO_2$ is the presence of nitrogen, indicating an alkaloid nature of the compound. Compound $C_{23}H_{16}O_2$ has a higher ratio of C:H, suggesting a possible polycyclic structure. In order to characterize the compounds further, they need to be isolated and structurally elucidated, which will require an upscaling of the cultivations in order to provide more biomass.

6   Future Perspectives

The non-distinctive evolutionary history of thraustochytrids, sharing both fungal and algal characteristics, suggests they may produce metabolic chemicals that can bridge different signaling pathways responsible for their parasitic success (Leyland 2017). The metabolism of algal defense and genetic regulation of PUFAs has been studied in recent years (Ward and Singh 2005); however, questions remain – including the ability of thraustochytrids to compete with algae and marine bacteria for nutrients while they invade and compromise the cell wall of their algal hosts (Scholz et al. 2016; Nagano et al 2011; Song et al. 2018).

If cocultures of *P. isakeiti* parasitizing a different host could be collected, comparison between healthy and parasitized host metabolic profiles could determine which organism produces the coculture-specific compounds. Further, bioassays conducted without individual extracts from both isolated host and parasite, prevent determination of which organisms is ultimately responsible for the bioactive results. The inherent life strategy of putative biotrophs makes metabolomic analyses a challenge and such an experimental dilemma limits deep investigation into positive bioactivity results. However, the basic observations of infection, division, and nutrient uptake in the present study, may contribute to the foundation of available knowledge for future examinations of the thraustochytrid-diatom, parasite-host relationship. Further, it remains plausible that the variances in LC-MS data among healthy *Pleurosigma sp.* cultures and *P. isakeiti* coculture extracts could be associated with physiological processes unrelated to parasitism, unintentionally induced by laboratory conditions.

In retrospect, objectives 2 and 3 could have been evaluated more concertedly by collecting division rate, infection rate, nutrient analysis, and chlorophyll a from parasitized and healthy culturing conditions under treatments of standard and reduced silicate in a single experiment, rather than collecting this information in two experiments. Nutrient analysis data was not collected on healthy and parasitized cultures under reduced silicate conditions limiting the juxtaposition of the silicate and nitrate uptake under these different nutrient conditions. Conducting such time-series experiments could elucidate the differences in effects of available silicate levels on silicate:nitrate retention and division during infection. The statistical modeling for percentage dividing over time in response to silicate treatment could be developed further. Splines modelling (Perperoglou 2019) could be used to compare multiple generalized linear models in Figure 11B to determine statistical differences between each slope. Effectively, this method could determine differences in variance in slopes modeled at different increments of the time-series to determine which part of the trend is most robustly different.

Counting experiments are time consuming and can be prone to bias. Despite committed discipline to sampling, in the infection and division rate experiments under different silicate treatments (Figure 4) only 31 timepoints were observed with 10 replicates and 3 controls under two silicate treatments. Concerns about pseudo-replication arose when two dilutions were necessary for the NA calibration requiring data cleaning and consolidation between experiments. Randomization of field of views during observations and sampling could have been biased by a single data collector (Figure 4-6). Counting experiment sampling required long periods of focused attention over a microscope that may have introduced bias. Throughout this study, silicate and nitrate depletion has been attributed primarily to *Pleurosigma* sp. metabolism due to the greater relative size of the diatom cell compared to the parasite; however, this assumption may have been overly simplistic. The presumption that thraustochytrid *P. isakeiti* does not significantly contribute to nutrient depletion requires further testing.

7 Conclusion

P. isakeiti has only been observed as an obligate parasite. After exposure to the parasite, observations of the incidence of infected diatom *Pleurosigma sp.* host cells increased over time and in response to reduced-silicate treatments. The proportion of dividing diatom *Pleurosigma sp.*

host cells during infection by *P. isakeiti* increased over time under standard and reduced silicate treatments. During the infection, available silicate decreased while available nitrate increased. Available nitrate:silicate ratio in standard F/2 1:50 FSW culture media increased in parasitized cultures of *Pleurosigma sp.* Two compounds with elemental formulas of $C_{17}H_{27}NO_2$ and $C_{23}H_{16}O_2$ were eluted from cocultures of *Pleurosigma sp.* with *P. isakeiti.* that were not present in healthy diatom or media controls. Limited bioactivity was detected in anti-inflammation and anti-bacterial MIC assays. No bioactivity was observed in the anti-cancer or biofilm assays. The present research is multidisciplinary, spanning the fields of ecology and biodiscovery to yield novel, fundamental knowledge on a newly described species, *P. isakeiti* and describe the interaction with its host, *Pleurosigma* sp., an ecologically important diatom species.

8 Literature Cited

Abida, H., Ruchaud, S., Rios, L., Humeau, A., Probert, I., De Vargas, C., Bach, S., Bowler, C., 2013. Bioprospecting Marine Plankton. Marine Drugs 11, 4594–4611. https://doi.org/10.3390/md11114594

Admiraal, W., Breugem, P., Jacobs, D.M.L.H.A., De Ruyter Van Steveninck, E.D., 1990. Fixation of dissolved silicate and sedimentation of biogenic silicate in the lower river Rhine during diatom blooms. Biogeochemistry 9, 175–185. https://doi.org/10.1007/BF00692170

Adolph, S., Bach, S., Blondel, M., Cueff, A., Moreau, M., Pohnert, G., Poulet, S.A., Wichard, T., Zuccaro, A., 2004. Cytotoxicity of diatom-derived oxylipins in organisms belonging to different phyla. Journal of Experimental Biology 207, 2935–2946. https://doi.org/10.1242/jeb.01105

Alves-de-Souza, C., Pecqueur, D., Floc'h, E.L., Mas, S., Roques, C., Mostajir, B., Vidussi, F., Velo-Suárez, L., Sourisseau, M., Fouilland, E., Guillou, L., 2015. Significance of Plankton Community Structure and Nutrient Availability for the Control of Dinoflagellate Blooms by Parasites: A Modeling Approach. PLOS ONE 10, e0127623. https://doi.org/10.1371/journal.pone.0127623

Amo, Y.D., Brzezinski, M.A., 1999. The Chemical Form of Dissolved Si Taken up by Marine Diatoms. Journal of Phycology 35, 1162–1170. https://doi.org/10.1046/j.1529-8817.1999.3561162.x

Armbrust, E.V., 2009. The life of diatoms in the world's oceans. Nature 459, 185–192. https://doi.org/10.1038/nature08057

Bahnweg, G., Sparrow, F.K., 1974. Four New Species of Thraustochytrium from Antarctic Regions, with Notes on the Distribution of Zoosporic Fungi in the Antarctic Marine Ecosystems. American Journal of Botany 61, 754–766. https://doi.org/10.1002/j.1537-2197.1974.tb12298.x

Baldauf, S.L., 2003. The Deep Roots of Eukaryotes. Science 300, 1703–1706. https://doi.org/10.1126/science.1085544

Bennett, R.M., Honda, D., Beakes, G.W., Thines, M., 2017. Labyrinthulomycota, in: Archibald, J.M., Simpson, A.G.B., Slamovits, C.H. (Eds.), Handbook of the Protists. Springer International Publishing, Cham, pp. 507–542. https://doi.org/10.1007/978-3-319-28149-0_25

Bhattarai, H.D., Ganti, V.S., Paudel, B., Lee, Y.K., Lee, H.K., Hong, Y.-K., Shin, H.W., 2007. Isolation of antifouling compounds from the marine bacterium, Shewanella oneidensis SCH0402. World J Microbiol Biotechnol 23, 243–249. https://doi.org/10.1007/s11274-006-9220-7

Bidle, K.D., Azam, F., 1999. Accelerated dissolution of diatom silica by marine bacterial assemblages. Nature 397, 508–512. https://doi.org/10.1038/17351

Billen, G., Lancelot, C., Meybeck, M., Mantoura, R.F.C., Martin, J.M., Wollast, R., 1991. N, P and Si retention along the aquatic continuum from land to ocean. https://doi.org/null

Bochdansky, A.B., Clouse, M.A., Herndl, G.J., 2017. Eukaryotic microbes, principally fungi and labyrinthulomycetes, dominate biomass on bathypelagic marine snow. The ISME Journal. https://doi.org/10.1038/ismej.2016.113

Bondoc, K.G.V., Heuschele, J., Gillard, J., Vyverman, W., Pohnert, G., 2016. Selective silicate-directed motility in diatoms. Nature Communications 7, 1–7. https://doi.org/10.1038/ncomms10540

Bongiorni, L., Jain, R., Raghukumar, S., Aggarwal, R.K., 2005. Thraustochytrium gaertnerium sp. nov.: a New Thraustochytrid Stramenopilan Protist from Mangroves of Goa, India. Protist 156, 303–315. https://doi.org/10.1016/j.protis.2005.05.001

Bouwman, A.F., Beusen, A.H.W., Billen, G., 2009. Human alteration of the global nitrogen and phosphorus soil balances for the period 1970–2050. Global Biogeochemical Cycles 23. https://doi.org/10.1029/2009GB003576

Bower, S.M., 1987. Labyrinthuloides haliotidis n.sp. (Protozoa: Labyrinthomorpha), a pathogenic parasite of small juvenile abalone in a British Columbia mariculture facility. Can. J. Zool. 65, 1996–2007. https://doi.org/10.1139/z87-304

Bower, S.M., McLean, N., Whitaker, D.J., 1989. Mechanism of infection by Labyrinthuloides haliotidis (Protozoa: Labyrinthomorpha), a parasite of abalone (Haliotis kamtschatkana) (Mollusca: Gastropoda). Journal of Invertebrate Pathology 53, 401–409. https://doi.org/10.1016/0022-2011(89)90106-7

Bremer, G., Talbot, G., 1995. Cellulolytic Enzyme Activity in the Marine Protist Schizochytrium aggregatum. https://doi.org/10.1515/botm.1995.38.1-6.37

Brevnova, E., Flatt, J., Gandhi, C., Rajgarhia, V., Mcbride, J., Warner, A., 2010. Isolation and Characterization of Schizochytrium Aggregatum Cellobiohydrolase I (cbh 1).

Brunner, E., Lutz, K., Sumper, M., 2004. Biomimetic synthesis of silica nanospheres depends on the aggregation and phase separation of polyamines in aqueous solution. Phys. Chem. Chem. Phys. 6, 854–857. https://doi.org/10.1039/B313261G

Brzezinski, M.A., 1985. The Si:C:N ratio of marine diatoms: interspecific variability and the effect of some enviornmental variables. Journal of Phycology 21, 347–357. https://doi.org/10.1111/j.0022-3646.1985.00347.x

Byreddy, A.R., 2016. Thraustochytrids as an alternative source of omega-3 fatty acids, carotenoids and enzymes. Lipid Technology 28, 68–70. https://doi.org/10.1002/lite.201600019

Caldwell, G.S., 2009. The Influence of Bioactive Oxylipins from Marine Diatoms on Invertebrate Reproduction and Development. Marine Drugs 7, 367–400. https://doi.org/10.3390/md7030367

Cavalier-Smith, T., 1998. A revised six-kingdom system of life. Biol Rev Camb Philos Soc 73, 203–266. https://doi.org/10.1017/s0006323198005167

Cermeño, P., Falkowski, P.G., 2009. Controls on diatom biogeography in the ocean. Science 325, 1539–1541. https://doi.org/10.1126/science.1174159

Chamberlain, A.H., Moss, S.T., 1988. The thraustochytrids: a protist group with mixed affinities. BioSystems 21, 341–349. https://doi.org/10.1016/0303-2647(88)90031-7

Chamberlain, A.H.L., 1980. Cytochemical and ultrastructural studies on the cell walls of Thraustochytrium spp. Botanica marina.

Chambouvet, A., Morin, P., Marie, D., Guillou, L., 2008. Control of Toxic Marine Dinoflagellate Blooms by Serial Parasitic Killers. Science 322, 1254–1257. https://doi.org/10.1126/science.1164387

Choudhury, A.K., Bhadury, P., 2015. Relationship between N : P : Si ratio and phytoplankton community composition in a tropical estuarine mangrove ecosystem. Biogeosciences Discuss. 12, 2307–2355. https://doi.org/10.5194/bgd-12-2307-2015

Coleman, N.K., Vestal, J.R., 1987. An epifluorescent microscopy study of enzymatic hydrolysis of fluorescein diacetate associated with the ectoplasmic net elements of the protist *Thraustochytrium striatum*. Can. J. Microbiol. 33, 841–843. https://doi.org/10.1139/m87-147

Conley, D., Schelske, C., Stoermer, E., 1993. Modification of the biogeochemical cycle of silica with eutrophication. Marine Ecology Progress Series 101, 179–192. https://doi.org/10.3354/meps101179

Consul, P.C., 1990. On some properties and applications of quasi-binomial distribution. Communications in Statistics - Theory and Methods 19, 477–504. https://doi.org/10.1080/03610929008830214

Corinaldesi, C., Barone, G., Marcellini, F., Dell'Anno, A., Danovaro, R., 2017. Marine Microbial-Derived Molecules and Their Potential Use in Cosmeceutical and Cosmetic Products. Marine Drugs 15, 118. https://doi.org/10.3390/md15040118

Damare, V., Raghukumar, S., 2006. Morphology and physiology of the marine straminipilan fungi, the aplanochytrids isolated from the equatorial Indian Ocean. IJMS Vol.35(4).

Damare, V., Raghukumar, S., 2008. Abundance of thraustochytrids and bacteria in the equatorial Indian Ocean, in relation to transparent exopolymeric particles (TEPs). FEMS Microbiol Ecol 65, 40–49. https://doi.org/10.1111/j.1574-6941.2008.00500.x

Damare, V.S., 2019. Chapter 30 - Advances in isolation and preservation strategies of ecologically important marine protists, the thraustochytrids, in: Meena, S.N., Naik, M.M. (Eds.), Advances in Biological Science Research. Academic Press, pp. 485–500. https://doi.org/10.1016/B978-0-12-817497-5.00030-6

Damare, V.S., D'Costa, P.M., Shivaramu, M.S., Borges, V., Fernandes, M., Fernandes, C., Cardozo, S., 2020. Preliminary study on the response of marine fungoid protists, the thraustochytrids, to lipid extracts of diatoms. Aquat Ecol 54, 355–367. https://doi.org/10.1007/s10452-020-09747-z

Darley, W.M., Porter, D., Fuller, M.S., 1973. Cell wall composition and synthesis via Golgi-directed scale formation in the marine eucaryote, Schizochytrium aggregatum, with a note on Thraustochytrium sp. Archiv. Mikrobiol. 90, 89–106. https://doi.org/10.1007/BF00414512

Darley, W.M., Volcani, B.E., 1969. Role of silicon in diatom metabolism: A silicon requirement for deoxyribonucleic acid synthesis in the diatom Cylindrotheca fusiformis Reimann and Lewin. Experimental Cell Research 58, 334–342. https://doi.org/10.1016/0014-4827(69)90514-X

De Caralt, S., Bry, D., Bontemps, N., Turon, X., Uriz, M.-J., Banaigs, B., 2013. Sources of Secondary Metabolite Variation in Dysidea avara (Porifera: Demospongiae): The Importance of Having Good Neighbors. Mar Drugs 11, 489–503. https://doi.org/10.3390/md11020489

del Campo, J., Guillou, L., Hehenberger, E., Logares, R., López-García, P., Massana, R., 2016. Ecological and evolutionary significance of novel protist lineages. European Journal of Protistology, Current trends in protistology – results from the VII ECOP - ISOP Joint Meeting 2015 55, 4–11. https://doi.org/10.1016/j.ejop.2016.02.002

Dell'Aquila, G., Ferrante, M.I., Gherardi, M., Cosentino Lagomarsino, M., Ribera d'Alcalà, M., Iudicone, D., Amato, A., 2017. Nutrient consumption and chain tuning in diatoms exposed to storm-like turbulence. Sci Rep 7. https://doi.org/10.1038/s41598-017-02084-6

Devasia, V.L.A., Muraleedharan, U.D., 2012. Polysaccharide-degrading enzymes from the marine protists, Thraustochytrids. URL https://www.semanticscholar.org/paper/Polysaccharide-degrading-enzymes-from-the-marine-Devasia-Muraleedharan/bea2f93fe5a1908ebfa9937caebcddebdf69f8d5 (accessed 5.13.20).

Dick, M.W., 1997. Fungi, flagella and phylogeny. Mycological Research 101, 385–394. https://doi.org/10.1017/S0953756296003267

Dick, M.W., 2001. Straminipilous Fungi. Springer Netherlands, Dordrecht. https://doi.org/10.1007/978-94-015-9733-3

Dortch, Q., Whitledge, T.E., 1992. Does nitrogen or silicon limit phytoplankton production in the Mississippi River plume and nearby regions? Continental Shelf Research 12, 1293–1309. https://doi.org/10.1016/0278-4343(92)90065-R

Drebes, G., Schnepf, E., 1982. Phagotrophy and development ofPaulsenella cf.chaetoceratis (Dinophyta), an ectoparasite of the diatomStreptotheca thamesis. Helgolander Meeresunters 35, 501–515. https://doi.org/10.1007/BF01999138

Dutkiewicz, S., Cermeno, P., Jahn, O., Follows, M.J., Hickman, A.E., Taniguchi, D.A.A., Ward, B.A., 2020. Dimensions of marine phytoplankton diversity. Biogeosciences 17, 609–634. https://doi.org/10.5194/bg-17-609-2020

Dybdahl, M.F., Lively, C.M., 1998. Host-Parasite Coevolution: Evidence for Rare Advantage and Time-Lagged Selection in a Natural Population. Evolution 52, 1057–1066. https://doi.org/10.1111/j.1558-5646.1998.tb01833.x

Egge, J., Aksnes, D., 1992. Silicate as regulating nutrient in phytoplankton competition. Marine Ecology Progress Series 83, 281–289. https://doi.org/10.3354/meps083281

Falkowski, P., Knoll, A.H., 2011. Evolution of Primary Producers in the Sea. Academic Press.

Fawcett, S.E., Ward, B.B., 2011. Phytoplankton succession and nitrogen utilization during the development of an upwelling bloom. Marine Ecology Progress Series 428, 13–31. https://doi.org/10.3354/meps09070

Field, C., Behrenfeld, M., Randerson, J., Falkowski, P., 1998. Primary production of the biosphere: integrating terrestrial and oceanic components. Science 281, 237–240. https://doi.org/10.1126/science.281.5374.237

Flynn, K.J., Blackford, J.C., Baird, M.E., Raven, J.A., Clark, D.R., Beardall, J., Brownlee, C., Fabian, H., Wheeler, G.L., 2012. Changes in pH at the exterior surface of plankton with ocean acidification. Nature Climate Change 2, 510–513. https://doi.org/10.1038/nclimate1489

Flynn, K.J., Martin-Jézéquel, V., 2000. Modelling Si–N-limited growth of diatoms. J Plankton Res 22, 447–472. https://doi.org/10.1093/plankt/22.3.447

Fontana, A., d'Ippolito, G., Cutignano, A., Miralto, A., Ianora, A., Romano, G., Cimino, G., 2007. Chemistry of oxylipin pathways in marine diatoms. Pure and Applied Chemistry 79, 481–490. https://doi.org/10.1351/pac200779040481

Fossier Marchan, L., Lee Chang, K.J., Nichols, P.D., Mitchell, W.J., Polglase, J.L., Gutierrez, T., 2018. Taxonomy, ecology and biotechnological applications of thraustochytrids: A review. Biotechnology Advances 36, 26–46. https://doi.org/10.1016/j.biotechadv.2017.09.003

Furnas, M., 1978. Influence of temperature and cell size on the division rate and chemical content of the diatom Chaetoceros curvisetum Cleve. Journal of Experimental Marine Biology and Ecology 34, 97–109. https://doi.org/10.1016/0022-0981(78)90034-5

Garvetto, A., Nézan, E., Badis, Y., Bilien, G., Arce, P., Bresnan, E., Gachon, C.M.M., Siano, R., 2018. Novel Widespread Marine Oomycetes Parasitising Diatoms, Including the Toxic Genus Pseudo-nitzschia: Genetic, Morphological, and Ecological Characterisation. Front. Microbiol. 9. https://doi.org/10.3389/fmicb.2018.02918

Gemmell, B.J., Oh, G., Buskey, E.J., Villareal, T.A., 2016. Dynamic sinking behaviour in marine phytoplankton: rapid changes in buoyancy may aid in nutrient uptake. Proc Biol Sci 283. https://doi.org/10.1098/rspb.2016.1126

Gilpin, L.C., Davidson, K., Roberts, E., 2004. The influence of changes in nitrogen: silicon ratios on diatom growth dynamics. Journal of Sea Research 51, 21–35. https://doi.org/10.1016/j.seares.2003.05.005

Grossi, V., Beker, B., Geenevasen, J.A.J., Schouten, S., Raphel, D., Fontaine, M.-F., Sinninghe Damsté, J.S., 2004. C25 highly branched isoprenoid alkenes from the marine benthic diatom Pleurosigma strigosum. Phytochemistry 65, 3049–3055. https://doi.org/10.1016/j.phytochem.2004.09.002

Guillard, R.R.L., 1975. Culture of Phytoplankton for Feeding Marine Invertebrates, in: Smith, W.L., Chanley, M.H. (Eds.), Culture of Marine Invertebrate Animals: Proceedings — 1st Conference on Culture of Marine Invertebrate Animals Greenport. Springer US, Boston, MA, pp. 29–60. https://doi.org/10.1007/978-1-4615-8714-9_3

Gupta, A., Barrow, C.J., Puri, M., 2012. Omega-3 biotechnology: Thraustochytrids as a novel source of omega-3 oils. Biotechnology Advances 30, 1733–1745. https://doi.org/10.1016/j.biotechadv.2012.02.014

Gupta, A., Wilkens, S., Adcock, J.L., Puri, M., Barrow, C.J., 2013. Pollen baiting facilitates the isolation of marine thraustochytrids with potential in omega-3 and biodiesel production. J. Ind. Microbiol. Biotechnol. 40, 1231–1240. https://doi.org/10.1007/s10295-013-1324-0

Gupta, H., Kao, S.-J., Dai, M., 2012. The role of mega dams in reducing sediment fluxes: A case study of large Asian rivers. Journal of Hydrology 464–465, 447–458. https://doi.org/10.1016/j.jhydrol.2012.07.038

Gutiérrez, M.H., Jara, A.M., Pantoja, S., 2016. Fungal parasites infect marine diatoms in the upwelling ecosystem of the Humboldt current system off central Chile: Fungal parasites on marine diatoms in upwelling ecosystems. Environ Microbiol 18, 1646–1653. https://doi.org/10.1111/1462-2920.13257

Haefner, B., 2003. Drugs from the deep: marine natural products as drug candidates. Drug Discovery Today 8, 536–544. https://doi.org/10.1016/S1359-6446(03)02713-2

Hagestad, O.C., Andersen, J.H., Altermark, B., Hansen, E., Rämä, T., 2019. Cultivable marine fungi from the Arctic Archipelago of Svalbard and their antibacterial activity. Mycology 0, 1–13. https://doi.org/10.1080/21501203.2019.1708492

Hamm, C.E., Merkel, R., Springer, O., Jurkojc, P., Maier, C., Prechtel, K., Smetacek, V., 2003. Architecture and material properties of diatom shells provide effective mechanical protection. Nature 421, 841–843. https://doi.org/10.1038/nature01416

Hancock, P., Goshawk, J., McMillan, D., Rontree, S., 2006. Advanced software for multi-analyte screening of TOF-MS data using library searching and accurate mass confirmation 1.

Harel, M., Ben-Dov, E., Rasoulouniriana, D., Siboni, N., Kramarsky-Winter, E., Loya, Y., Barak, Z., Wiesman, Z., Kushmaro, A., 2008. A new Thraustochytrid, strain Fng1, isolated from the surface mucus of the hermatypic coral Fungia granulosa. FEMS Microbiology Ecology 64, 378–387. https://doi.org/10.1111/j.1574-6941.2008.00464.x

Harwood, D.M., Nikolaev, V.A., Winter, D.M., 2007. Cretaceous Records of Diatom Evolution, Radiation, and Expansion. The Paleontological Society Papers 13, 33–59. https://doi.org/10.1017/S1089332600001455

Hassett, B.T., 2020. A Widely Distributed Thraustochytrid Parasite of Diatoms Isolated from the Arctic Represents a gen. and sp. nov. J. Eukaryot. Microbiol. jeu.12796. https://doi.org/10.1111/jeu.12796

Hildebrand, M., Dahlin, K., Volcani, B.E., 1998. Characterization of a silicon transporter gene family in Cylindrotheca fusiformis: sequences, expression analysis, and identification of homologs in other diatoms. Mol Gen Genet 260, 480–486. https://doi.org/10.1007/s004380050920

Hildebrand, M., Volcani, B.E., Gassmann, W., Schroeder, J.I., 1997. A gene family of silicon transporters. Nature 385, 688–689. https://doi.org/10.1038/385688b0

Honda, D., Yokochi, T., Nakahara, T., Raghukumar, S., Nakagiri, A., Schaumann, K., Higashihara, T., 1999. Molecular phylogeny of labyrinthulids and thraustochytrids based on the sequencing of 18S ribosomal RNA gene. J. Eukaryot. Microbiol. 46, 637–647. https://doi.org/10.1111/j.1550-7408.1999.tb05141.x

Humborg, C., Conley, D.J., Rahm, L., Wulff, F., Cociasu, A., Ittekkot, V., 2000. Silicon Retention in River Basins: Far-reaching Effects on Biogeochemistry and Aquatic Food Webs in Coastal Marine Environments. AMBIO: A Journal of the Human Environment 29, 45–50. https://doi.org/10.1579/0044-7447-29.1.45

Imhoff, J., 2016. Natural Products from Marine Fungi—Still an Underrepresented Resource. Marine Drugs 14, 19. https://doi.org/10.3390/md14010019

Ittekkot, V., Humborg, C., Schäfer, P., 2000. Hydrological Alterations and Marine Biogeochemistry: A Silicate Issue? BioScience 50, 776. https://doi.org/10.1641/0006-3568(2000)050[0776:HAAMBA]2.0.CO;2

Iwata, I., Honda, D., 2018. Erratum to "Nutritional Intake by Ectoplasmic Nets of Schizochytrium aggregatum (Labyrinthulomycetes, Stramenopiles" [Protist 169 (November (5)) (2018) 727–743]. Protist 169, 978–979. https://doi.org/10.1016/j.protis.2018.11.005

Iwata, I., Kimura, K., Tomaru, Y., Motomura, T., Koike, Kanae, Koike, Kazuhiko, Honda, D., 2017. Bothrosome Formation in Schizochytrium aggregatum (Labyrinthulomycetes, Stramenopiles) during Zoospore Settlement. Protist 168, 206–219. https://doi.org/10.1016/j.protis.2016.12.002

Jain, R., Raghukumar, S., Tharanathan, R., Bhosle, N.B., 2005. Extracellular Polysaccharide Production by Thraustochytrid Protists. Mar Biotechnol 7, 184–192. https://doi.org/10.1007/s10126-004-4025-x

Jónasdóttir, S.H., 2019. Fatty Acid Profiles and Production in Marine Phytoplankton. Mar Drugs 17. https://doi.org/10.3390/md17030151

Kafouris, S., Smeti, E., Spatharis, S., Tsirtsis, G., Economou-Amilli, A., Danielidis, D.B., 2019. Nitrogen as the main driver of benthic diatom composition and diversity in oligotrophic coastal systems. Sci. Total Environ. 694, 133773. https://doi.org/10.1016/j.scitotenv.2019.133773

Kanchana, R., Muraleedharan, U.D., Raghukumar, S., 2011. Alkaline lipase activity from the marine protists, thraustochytrids. World J Microbiol Biotechnol 27, 2125–2131. https://doi.org/10.1007/s11274-011-0676-8

Käse, L., Geuer, J.K., 2018. Phytoplankton Responses to Marine Climate Change – An Introduction, in: Jungblut, S., Liebich, V., Bode, M. (Eds.), YOUMARES 8 – Oceans Across Boundaries: Learning from Each Other. Springer International Publishing, Cham, pp. 55–71. https://doi.org/10.1007/978-3-319-93284-2_5

Kimura, H., Naganuma, T., 2001. Thraustochytrids: A neglected agent of the marine microbial food chain. Aquatic Ecosystem Health & Management 4, 13–18. https://doi.org/10.1080/146349801753569243

Knoll, A. h, Javaux, E. j, Hewitt, D., Cohen, P., 2006. Eukaryotic organisms in Proterozoic oceans. Philosophical Transactions of the Royal Society B: Biological Sciences 361, 1023–1038. https://doi.org/10.1098/rstb.2006.1843

Kobayashi, T., Sakaguchi, K., Matsuda, T., Abe, E., Hama, Y., Hayashi, M., Honda, D., Okita, Y., Sugimoto, S., Okino, N., Ito, M., 2011. Increase of Eicosapentaenoic Acid in Thraustochytrids through Thraustochytrid Ubiquitin Promoter-Driven Expression of a Fatty Acid Δ5 Desaturase Gene. Appl. Environ. Microbiol. 77, 3870–3876. https://doi.org/10.1128/AEM.02664-10

Kooistra, W.H.C.F., Gersonde, R., Medlin, L.K., Mann, D.G., 2007. The Origin and Evolution of the Diatoms: Their Adaptation to a Planktonic Existence, in: Evolution of Primary Producers in the Sea. Elsevier, pp. 207–249. https://doi.org/10.1016/B978-012370518-1/50012-6

Kröger, N., Lorenz, S., Brunner, E., Sumper, M., 2002. Self-Assembly of Highly Phosphorylated Silaffins and Their Function in Biosilica Morphogenesis. Science 298, 584–586. https://doi.org/10.1126/science.1076221

Kumar, C.R., 1978. Physiology of infection of the marine diatom Licmophora by the fungus Ectrogella perforans. Veroff. Inst. Meeresforsch. Bremerhaven 17, 1–14.

Leander, C.A., Porter, D., 2001. The Labyrinthulomycota is comprised of three distinct lineages. https://doi.org/10.1080/00275514.2001.12063179

Lechner, C.C., Becker, C.F.W., 2015. Silaffins in Silica Biomineralization and Biomimetic Silica Precipitation. Mar Drugs 13, 5297–5333. https://doi.org/10.3390/md13085297

Lee, S.D., Park, J.S., Yun, S.M., Lee, J.H., 2014. Critical criteria for identification of the genus Chaetoceros(Bacillariophyta) based on setae ultrastructure. I. Subgenus Chaetoceros. Phycologia 53, 174–187. https://doi.org/10.2216/13-154.1

Leflaive, J., Ten-Hage, L., 2009. Chemical interactions in diatoms: role of polyunsaturated aldehydes and precursors. New Phytologist 184, 794–805. https://doi.org/10.1111/j.1469-8137.2009.03033.x

Levasseur, M.E., Therriault, J.-C., 1987. Phytoplankton biomass and nutrient dynamics in a tidally induced upwelling: the role of the NO3 :S i 0 4ratio. Mar. Ecol. Prog. Ser. 11.

Lewis, T.E., Nichols, P.D., McMeekin, T.A., 1999. The Biotechnological Potential of Thraustochytrids. Mar. Biotechnol. 1, 580–587. https://doi.org/10.1007/PL00011813

Lewis, William M., 1985. Nutrient Scarcity as an Evolutionary Cause of Haploidy. The American Naturalist 125, 692–701. https://doi.org/10.1086/284372

Leyland, B., Leu, S., Boussiba, S., 2017. Are Thraustochytrids algae? Fungal Biology 121, 835–840. https://doi.org/10.1016/j.funbio.2017.07.006

Li, H.-Y., Lu, Y., Zheng, J.-W., Yang, W.-D., Liu, J.-S., 2014. Biochemical and Genetic Engineering of Diatoms for Polyunsaturated Fatty Acid Biosynthesis. Mar Drugs 12, 153–166. https://doi.org/10.3390/md12010153

Li, Q., Wang, X., Liu, X., Jiao, N., Wang, G., 2013. Abundance and Novel Lineages of Thraustochytrids in Hawaiian Waters. Microb Ecol 66, 823–830. https://doi.org/10.1007/s00248-013-0275-3

Li, W., Cai, C.-H., Guo, Z.-K., Wang, H., Zuo, W.-J., Dong, W.-H., Mei, W.-L., Dai, H.-F., 2015. Five new eudesmane-type sesquiterpenoids from Chinese agarwood induced by artificial holing. Fitoterapia 100, 44–49. https://doi.org/10.1016/j.fitote.2014.11.010

Lippemeier, S., 1999. Direct impact of silicate on the photosynthetic performance of the diatom Thalassiosira weissflogii assessed by on- and off-line PAM fluorescence measurements. Journal of Plankton Research 21, 269–283. https://doi.org/10.1093/plankt/21.2.269

Liu, X., Ashforth, E., Ren, B., Song, F., Dai, H., Liu, M., Wang, J., Xie, Q., Zhang, L., 2010. Bioprospecting microbial natural product libraries from the marine environment for drug discovery. J Antibiot 63, 415–422. https://doi.org/10.1038/ja.2010.56

Liu, Y., Ma, J., Wang, Y., Donkor, P.O., Li, Q., Gao, S., Hou, Y., Xu, Y., Cui, J., Ding, L., Zhao, F., Kang, N., Chen, L., Qiu, F., 2014. Eudesmane-Type Sesquiterpenes from Curcuma phaeocaulis and Their Inhibitory Activities on Nitric Oxide Production in RAW 264.7 Cells. European Journal of Organic Chemistry 2014, 5540–5548. https://doi.org/10.1002/ejoc.201402465

Liu, Y., Singh, P., Liang, Y., Li, J., Xie, N., Song, Z., Daroch, M., Leng, K., Johnson, Z.I., Wang, G., 2017. Abundance and molecular diversity of thraustochytrids in coastal waters of southern China. FEMS Microbiol Ecol 93. https://doi.org/10.1093/femsec/fix070

Martin-Jézéquel, V., Lopez, P.J., 2003. Silicon--a central metabolite for diatom growth and morphogenesis. Prog. Mol. Subcell. Biol. 33, 99–124. https://doi.org/10.1007/978-3-642-55486-5_4

McLean, N., Porter, D., 1982. The Yellow-Spot Disease of Tritonia diomedea Bergh, 1894 (Mollusca: Gastropoda: Nudibranchia): Encapsulation of the Thraustochytriaceous Parasite by Host Amoebocytes. The Journal of Parasitology 68, 243. https://doi.org/10.2307/3281182

Medlin, L.K., 2002. Why Silica or Better yet Why Not Silica? Speculations as to Why the Diatoms Utilise Silica as Their Cell Wall Material. Diatom Research 17, 453–459. https://doi.org/10.1080/0269249X.2002.9705562

Meyer, N., Rettner, J., Werner, M., Werz, O., Pohnert, G., 2018. Algal Oxylipins Mediate the Resistance of Diatoms against Algicidal Bacteria. Marine Drugs 16, 486. https://doi.org/10.3390/md16120486

Moss, M.O., 1986. The Biology of Marine Fungi. CUP Archive.

Muehlstein, L.K., Porter, D., Short, F.T., 1988. Labyrinthula sp., a marine slime mold producing the symptoms of wasting disease in eelgrass, Zostera marina. Mar. Biol. 99, 465–472. https://doi.org/10.1007/BF00392553

Nagano, N., Matsui, S., Kuramura, T., Taoka, Y., Honda, D., Hayashi, M., 2010. The Distribution of Extracellular Cellulase Activity in Marine Eukaryotes, Thraustochytrids. Marine Biotechnology. https://doi.org/10.1007/s10126-010-9297-8

Naganuma T., Kimura H., Karimoto R., Pimenov N.V., 2006. Abundance of planktonic thraustochytrids and bacteria and the concentration of particulate ATP in the Greenland and Norwegian Seas 20, 37–45.

Nilsson, R.H., Tedersoo, L., Abarenkov, K., Ryberg, M., Kristiansson, E., Hartmann, M., Schoch, C.L., Nylander, J.A.A., Bergsten, J., Porter, T.M., Jumpponen, A., Vaishampayan, P., Ovaskainen, O., Hallenberg, N., Bengtsson-Palme, J., Eriksson, K.M.,

Larsson, K.-H., Larsson, E., Kõljalg, U., 2012. Five simple guidelines for establishing basic authenticity and reliability of newly generated fungal ITS sequences. MycoKeys 4, 37–63. https://doi.org/10.3897/mycokeys.4.3606

Nygaard, K., Hessen, D.O., 1994. Diatom kills by flagellates. Nature 367, 520–520. https://doi.org/10.1038/367520a0

Oelsner, G.P., Stets, E.G., 2019. Recent trends in nutrient and sediment loading to coastal areas of the conterminous U.S.: Insights and global context. Science of The Total Environment 654, 1225–1240. https://doi.org/10.1016/j.scitotenv.2018.10.437

Officer, C.B., Ryther, J.H., 1980. The Possible Importance of Silicon in Marine Eutrophication. Marine Ecology Progress Series 3, 83–91.

Okafor, N., 2011. Environmental Microbiology of Aquatic and Waste Systems. Springer Science & Business Media.

Paasche, E., 1973. Silicon and the ecology of marine plankton diatoms. I. Thalassiosira pseudonana (Cyclotella nana) grown in a chemostat with silicate as limiting nutrient. Marine Biology 19, 117–126. https://doi.org/10.1007/BF00353582

Pan, J., del Campo, J., Keeling, P.J., 2017. Reference Tree and Environmental Sequence Diversity of Labyrinthulomycetes. J. Eukaryot. Microbiol. 64, 88–96. https://doi.org/10.1111/jeu.12342

Pančić, M., Torres, R.R., Almeda, R., Kiørboe, T., 2019. Silicified cell walls as a defensive trait in diatoms. Proc. R. Soc. B 286, 20190184. https://doi.org/10.1098/rspb.2019.0184

Pascaline Rahelivao, M., Lübken, T., Gruner, M., Kataeva, O., Ralambondrahety, R., Andriamanantoanina, H., P. Checinski, M., Bauer, I., Knölker, H.-J., 2017. Isolation and structure elucidation of natural products of three soft corals and a sponge from the coast of Madagascar. Organic & Biomolecular Chemistry 15, 2593–2608. https://doi.org/10.1039/C7OB00191F

Patel, A., Liefeldt, S., Rova, U., Christakopoulos, P., Matsakas, L., 2020. Co-production of DHA and squalene by thraustochytrid from forest biomass. Scientific Reports 10, 1992. https://doi.org/10.1038/s41598-020-58728-7

Pernice, M.C., Forn, I., Gomes, A., Lara, E., Alonso-Sáez, L., Arrieta, J.M., del Carmen Garcia, F., Hernando-Morales, V., MacKenzie, R., Mestre, M., Sintes, E., Teira, E., Valencia, J., Varela, M.M., Vaqué, D., Duarte, C.M., Gasol, J.M., Massana, R., 2015. Global abundance of planktonic heterotrophic protists in the deep ocean. The ISME Journal 9, 782–792. https://doi.org/10.1038/ismej.2014.168

Perperoglou, A., Sauerbrei, W., Abrahamowicz, M., Schmid, M., 2019. A review of spline function procedures in R. BMC Medical Research Methodology 19, 46. https://doi.org/10.1186/s12874-019-0666-3

Pohnert, G., 2000. Wound-Activated Chemical Defense in Unicellular Planktonic Algae. Angewandte Chemie International Edition 39, 4352–4354. https://doi.org/10.1002/1521-3773(20001201)39:23<4352::AID-ANIE4352>3.0.CO;2-U

Pohnert, G., 2005. Diatom/copepod interactions in plankton: the indirect chemical defense of unicellular algae. Chembiochem 6, 946–959. https://doi.org/10.1002/cbic.200400348

Porter, D., Margulis, L., Corliss, O., Melkonian, M., Chapman, J., 1990. Phylum Labyrinthulomycota. In: Handbook of Protoctista. Jones and Bartlett, Boston.

Poulson, K.L., Sieg, R.D., Kubanek, J., 2009. Chemical ecology of the marine plankton. Nat. Prod. Rep. 26, 729. https://doi.org/10.1039/b806214p

Rad-Menéndez, C., Gerphagnon, M., Garvetto, A., Arce, P., Badis, Y., Sime-Ngando, T., Gachon, C.M.M., 2018. Rediscovering Zygorhizidium affluens Canter: Molecular Taxonomy, Infectious Cycle, and Cryopreservation of a Chytrid Infecting the Bloom-Forming Diatom Asterionella formosa. Appl. Environ. Microbiol. 84. https://doi.org/10.1128/AEM.01826-18

Raghukumar, C., 1986. Thraustochytrid fungi associated with marine algae. IJMS Vol.15(2) [June 1986].

Raghukumar, S., 1990. Speculations on niches occupied by fungi in the sea with relation to bacteria. Proc. Indian Acad. Sci. (Plant Sci.) 100, 129–138. https://doi.org/10.1007/BF03053437

Raghukumar, S., 1992. Bacterivory: a novel dual role for thraustochytrids in the sea. Marine Biology 113, 165–169. https://doi.org/10.1007/BF00367650

Raghukumar, S., 2002. Ecology of the marine protists, the Labyrinthulomycetes (Thraustochytrids and Labyrinthulids). European Journal of Protistology 38, 127–145. https://doi.org/10.1078/0932-4739-00832

Raghukumar, S., 2008. Thraustochytrid Marine Protists: production of PUFAs and Other Emerging Technologies. Mar. Biotechnol. 10, 631–640. https://doi.org/10.1007/s10126-008-9135-4

Raghukumar, S., Damare, V.S., 2011. Increasing evidence for the important role of Labyrinthulomycetes in marine ecosystems. Botanica Marina 54, 3–11. https://doi.org/10.1515/bot.2011.008

Raghukumar, S., Ramaiah, N., Raghukumar, C., 2001. Dynamics of thraustochytrid protists in the water column of the Arabian Sea. Aquatic Microbial Ecology 24, 175–186. https://doi.org/10.3354/ame024175

Raghukumar, S., Sharma, S., Raghukumar, C., Sathe-Pathak, V., Chandramohan, D., 1994. Thraustochytrid and fungal component of marine detritus. IV. Laboratory studies on decomposition of leaves of the mangrove Rhizophora apiculata Blume. Journal of Experimental Marine Biology and Ecology 183, 113–131. https://doi.org/10.1016/0022-0981(94)90160-0

Raposo, M., De Morais, R., Bernardo de Morais, A., 2013. Bioactivity and Applications of Sulphated Polysaccharides from Marine Microalgae. Marine Drugs 11, 233–252. https://doi.org/10.3390/md11010233

Rapp, J.Z., Fernández-Méndez, M., Bienhold, C., Boetius, A., 2018. Effects of Ice-Algal Aggregate Export on the Connectivity of Bacterial Communities in the Central Arctic Ocean. Front. Microbiol. 9, 1035. https://doi.org/10.3389/fmicb.2018.01035

Raven, J.A., Waite, A.M., 2004. The evolution of silicification in diatoms: inescapable sinking and sinking as escape? New Phytologist 162, 45–61. https://doi.org/10.1111/j.1469-8137.2004.01022.x

Ribalet, F., Bastianini, M., Vidoudez, C., Acri, F., Berges, J., Ianora, A., Miralto, A., Pohnert, G., Romano, G., Wichard, T., Casotti, R., 2014. Phytoplankton Cell Lysis Associated with Polyunsaturated Aldehyde Release in the Northern Adriatic Sea. PLOS ONE 9, e85947. https://doi.org/10.1371/journal.pone.0085947

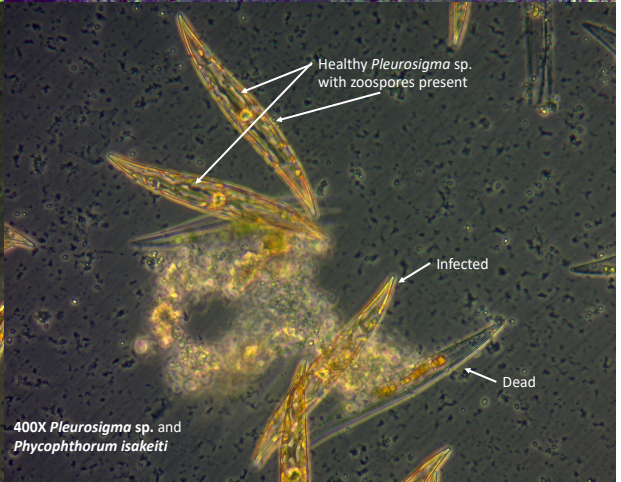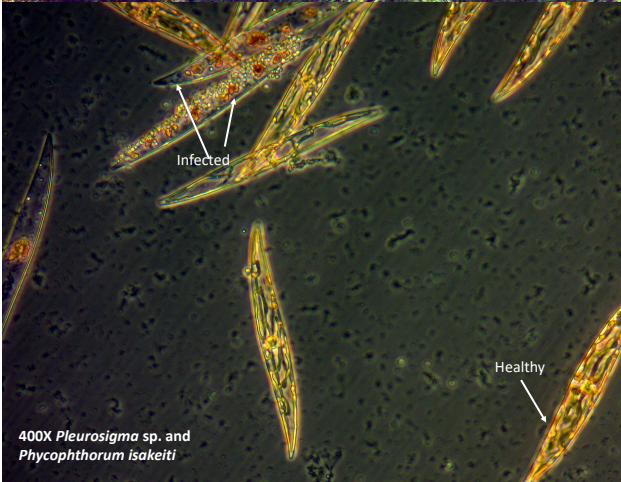Rocha, C.L.D.L., Passow, U., 2004. Recovery of Thalassiosira weissflogii from nitrogen and silicon starvation. Limnology and Oceanography 49, 245–255. https://doi.org/10.4319/lo.2004.49.1.0245
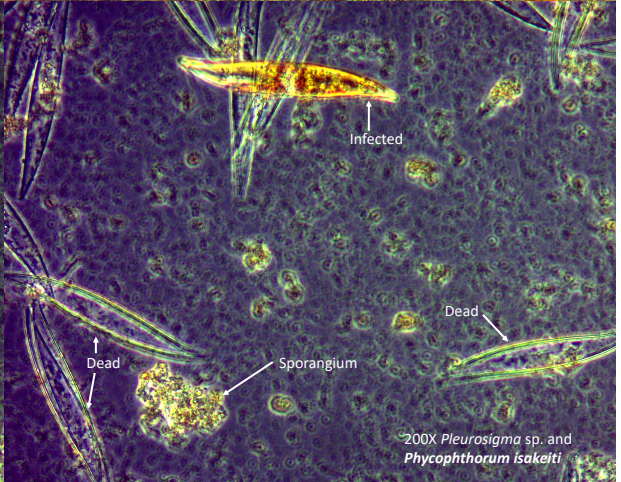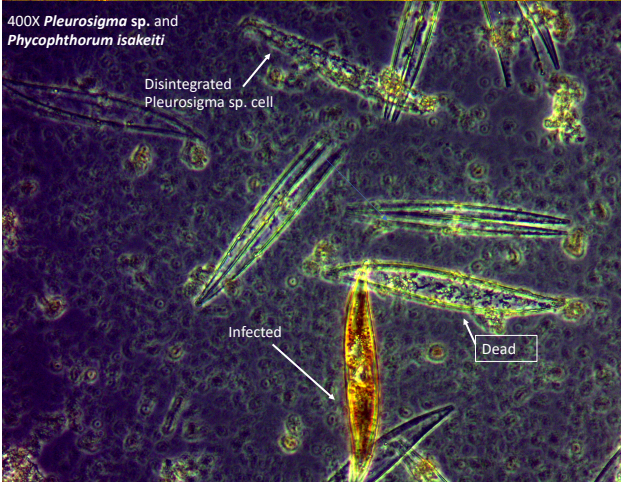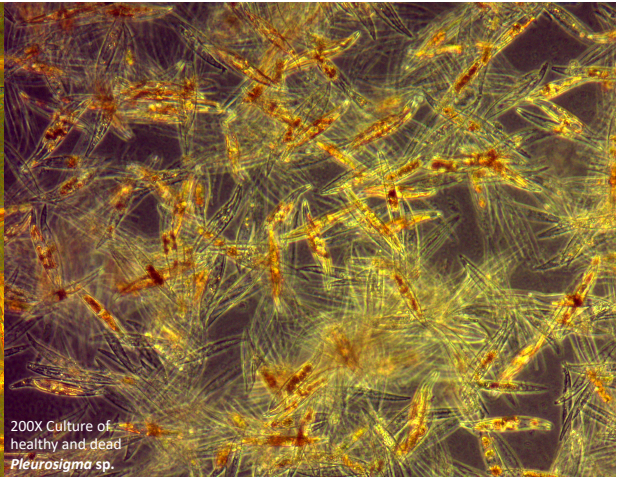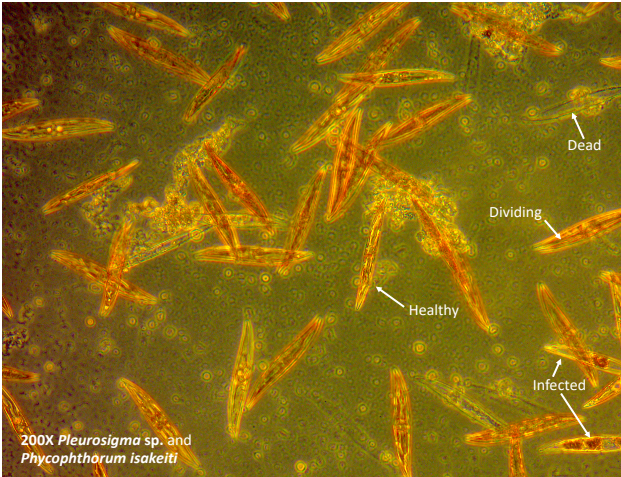
Roncel, M., González-Rodríguez, A.A., Naranjo, B., Bernal-Bayard, P., Lindahl, A.M., Hervás, M., Navarro, J.A., Ortega, J.M., 2016. Iron Deficiency Induces a Partial Inhibition of the Photosynthetic Electron Transport and a High Sensitivity to Light in the Diatom Phaeodactylum tricornutum. Front. Plant Sci. 7. https://doi.org/10.3389/fpls.2016.01050

Rosa, S.M., Galvagno, M.A., Vélez, C.G., 2011. Adjusting culture conditions to isolate thraustochytrids from temperate and cold environments in southern Argentina. Mycoscience 52, 242–252. https://doi.org/10.1007/S10267-010-0091-2

Rowland, S.J., Allard, W.G., Belt, S.T., Massé, G., Robert, J.-M., Blackburn, S., Frampton, D., Revill, A.T., Volkman, J.K., 2001. Factors influencing the distributions of polyunsaturated terpenoids in the diatom, Rhizosolenia setigera. Phytochemistry 58, 717–728. https://doi.org/10.1016/S0031-9422(01)00318-1

Sabharwal, T., Sathasivan, K., Mehdy, M.C., 2017. Defense related decadienal elicits membrane lipid remodeling in the diatom Phaeodactylum tricornutum. PLOS ONE 12, e0178761. https://doi.org/10.1371/journal.pone.0178761

Sarkar, Deepayan. 2008. Lattice: Multivariate Data Visualization with R. Springer, New York. ISBN 978-0-387-75968-5

Schärer, L., Knoflach, D., Vizoso, D.B., Rieger, G., Peintner, U., 2007. Thraustochytrids as novel parasitic protists of marine free-living flatworms: Thraustochytrium caudivorum sp. nov. parasitizes Macrostomum lignano. Mar Biol 152, 1095–1104. https://doi.org/10.1007/s00227-007-0755-4

Schmid, A.-M.M., 2003. Endobacteria in the Diatom Pinnularia Bacillariophyceae Scattered ct nucleoids explained: Journal of Phycology 39, 122–138. https://doi.org/10.1046/j.1529-8817.2003.02084.x

Schnepf, E., Deichgräber, G., Drebes, G., 1978. Development and ultrastructure of the marine, parasitic Oomycete,Lagenisma coscinodisci Drebes (Lagenidiales): Formation of the primary zoospores and their release. Protoplasma 94, 263–280. https://doi.org/10.1007/BF01276776

Scholz, B., Guillou, L., Marano, A.V., Neuhauser, S., Sullivan, B.K., Karsten, U., Küpper, F.C., Gleason, F.H., 2016. Zoosporic parasites infecting marine diatoms – A black box that needs to be opened. Fungal Ecology 19, 59–76. https://doi.org/10.1016/j.funeco.2015.09.002

Scholz, B., Küpper, F.C., Vyverman, W., Ólafsson, H.G., Karsten, U., 2017. Chytridiomycosis of Marine Diatoms—The Role of Stress Physiology and Resistance in Parasite-Host Recognition and Accumulation of Defense Molecules. Mar Drugs 15. https://doi.org/10.3390/md15020026

Sharma, S., Raghukumar, C., Raghukumar, S., Sathe-pathak, V., Chandramohan, D., 1994. Thraustochytrid and fungal component of marine detritus II. Laboratory studies on decomposition of the brown alga Sargassum cinereum J. Ag. Journal of Experimental Marine Biology and Ecology 175, 227–242. https://doi.org/10.1016/0022-0981(94)90028-0

Shrestha, R.P., Hildebrand, M., 2015. Evidence for a Regulatory Role of Diatom Silicon Transporters in Cellular Silicon Responses. Eukaryotic Cell 14, 29–40. https://doi.org/10.1128/EC.00209-14

Sime-Ngando, T., 2012. Phytoplankton Chytridiomycosis: Fungal Parasites of Phytoplankton and Their Imprints on the Food Web Dynamics. Front. Microbio. 3. https://doi.org/10.3389/fmicb.2012.00361
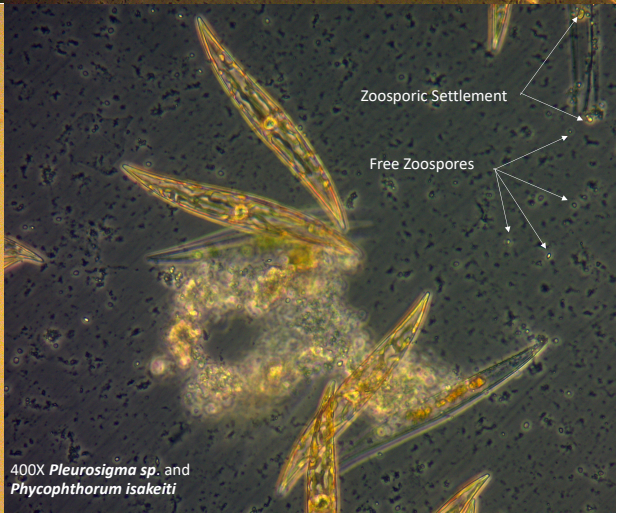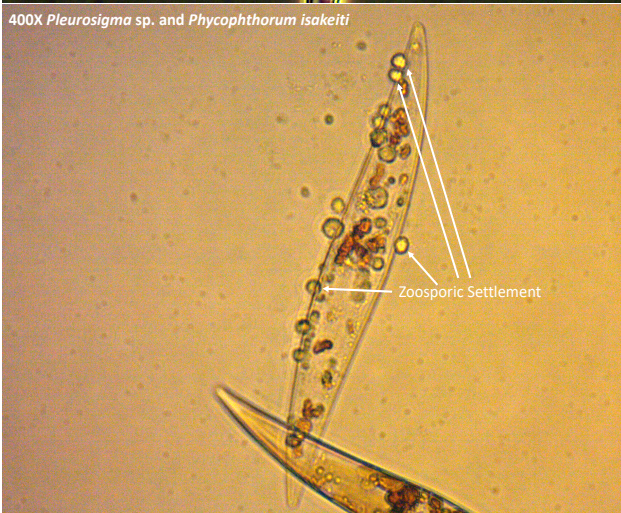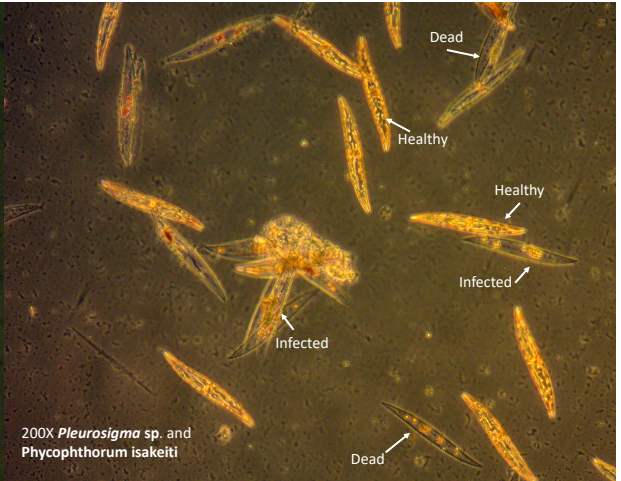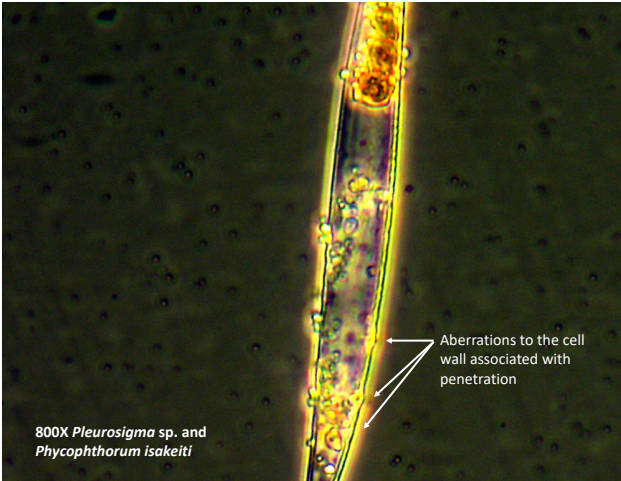
Simms, E.L., Taylor, D.L., Povich, J., Shefferson, R.P., Sachs, J.L., Urbina, M., Tausczik, Y., 2006. An empirical test of partner choice mechanisms in a wild legume–rhizobium interaction. Proc. R. Soc. B. 273, 77–81. https://doi.org/10.1098/rspb.2005.3292

Simpson, T.L., Volcani, B.E. (Eds.), 1981. Silicon and Siliceous Structures in Biological Systems. Springer New York, New York, NY. https://doi.org/10.1007/978-1-4612-5944-2

Sims, P.A., Mann, D.G., Medlin, L.K., 2006. Evolution of the diatoms: insights from fossil, biological and molecular data. Phycologia 45, 361–402. https://doi.org/10.2216/05-22.1

Smetacek, V., 1998. Diatoms and the silicate factor. Nature 391, 224–225. https://doi.org/10.1038/34528

Song, Z., Stajich, J.E., Xie, Y., Liu, X., He, Y., Chen, J., Hicks, G.R., Wang, G., 2018. Comparative analysis reveals unexpected genome features of newly isolated Thraustochytrids strains: on ecological function and PUFAs biosynthesis. BMC Genomics 19, 541. https://doi.org/10.1186/s12864-018-4904-6

Sparmann, S.F., Leander, B.S., Hoppenrath, M., 2008. Comparative morphology and molecular phylogeny of Apicoporus n. Gen.: a new genus of marine benthic dinoflagellates formerly classified within Amphidinium. Protist 159, 383–399. https://doi.org/10.1016/j.protis.2007.12.002

Sparrow, F.K., 1936. Biological observations on the marine fungi of Woods Hole waters. The Biological Bulletin 70, 236–263. https://doi.org/10.2307/1537470

Spilling, K., Olli, K., Lehtoranta, J., Kremp, A., Tedesco, L., Tamelander, T., Klais, R., Peltonen, H., Tamminen, T., 2018. Shifting Diatom—Dinoflagellate Dominance During Spring Bloom in the Baltic Sea and its Potential Effects on Biogeochemical Cycling. Front. Mar. Sci. 5. https://doi.org/10.3389/fmars.2018.00327

Subrahmanyan, R., 1945. On the cell-division and mitosis in some South Indian Diatoms. Proc. Ind. Acad. Sa., B, 22, 347–349.

Sumper, M., Kröger, N., 2004. Silica formation in diatoms: the function of long-chain polyamines and silaffins. J. Mater. Chem. 14, 2059–2065. https://doi.org/10.1039/B401028K

Svenson, J., 2013. MabCent: Arctic marine bioprospecting in Norway. Phytochem Rev 12, 567–578. https://doi.org/10.1007/s11101-012-9239-3

Taoka, Y., Nagano, N., Okita, Y., Izuminda, H., Sugimoto, S., Hayashi, M., 2009. Extracellular Enzymes Produced by Marine Eukaryotes, Thraustochytrids. Bioscience, Biotechnology, and Biochemistry 73, 180–182. https://doi.org/10.1271/bbb.80416

Tillmann, U., Hesse, K.-J., Tillmann, A., 1999. Large-scale parasitic infection of diatoms in the Northfrisian Wadden Sea. Journal of Sea Research 42, 255–261. https://doi.org/10.1016/S1385-1101(99)00029-5

Tréguer, P., Nelson, D.M., Van Bennekom, A.J., DeMaster, D.J., Leynaert, A., Queguiner, B., 1995. The Silica Balance in the World Ocean: A Reestimate. Science 268, 375–379. https://doi.org/10.1126/science.268.5209.375

Tréguer, P.J., De La Rocha, C.L., 2013. The world ocean silica cycle. Ann Rev Mar Sci 5, 477–501. https://doi.org/10.1146/annurev-marine-121211-172346

Tsui, C.K.M., Marshall, W., Yokoyama, R., Honda, D., Lippmeier, J.C., Craven, K.D., Peterson, P.D., Berbee, M.L., 2009. Labyrinthulomycetes phylogeny and its implications for the evolutionary loss of chloroplasts and gain of ectoplasmic gliding. Molecular Phylogenetics and Evolution 50, 129–140. https://doi.org/10.1016/j.ympev.2008.09.027

Ueda, M., Nomura, Y., Doi, K., Nakajima, M., Honda, D., 2015. Seasonal dynamics of culturable thraustochytrids (Labyrinthulomycetes, Stramenopiles) in estuarine and coastal waters. Aquat. Microb. Ecol. 74, 187–204. https://doi.org/10.3354/ame01736

Vargas, C.A., Martínez, R.A., Cuevas, L.A., Pavez, M.A., Cartes, C., GonzÁlez, H.E., Escribano, R., Daneri, G., 2007. The relative importance of microbial and classical food webs in a highly productive coastal upwelling area. Limnology and Oceanography 52, 1495–1510. https://doi.org/10.4319/lo.2007.52.4.1495

Wang, Li, Wang, X., Jin, X., Xu, J., Zhang, H., Yu, J., Sun, Q., Gao, C., Wang, Lingbin, 2017. Analysis of algae growth mechanism and water bloom prediction under the effect of multi-affecting factor. Saudi Journal of Biological Sciences, Computational Intelligence Research & Approaches in Bioinformatics and Biocomputing 24, 556–562. https://doi.org/10.1016/j.sjbs.2017.01.026

Wang, Q., Ye, H., Sen, B., Xie, Y., He, Y., Park, S., Wang, G., 2018. Improved production of docosahexaenoic acid in batch fermentation by newly-isolated strains of Schizochytrium sp. and Thraustochytriidae sp. through bioprocess optimization. Synth Syst Biotechnol 3, 121–129. https://doi.org/10.1016/j.synbio.2018.04.001

Ward, O.P., Singh, A., 2005. Omega-3/6 fatty acids: Alternative sources of production. Process Biochemistry 40, 3627–3652. https://doi.org/10.1016/j.procbio.2005.02.020

Wasmund, N., Nausch, G., Feistel, R., 2013. Silicate consumption: an indicator for long-term trends in spring diatom development in the Baltic Sea. Journal of Plankton Research 35, 393–406. https://doi.org/10.1093/plankt/fbs101

Whyte, S., Cawthorn, R., McGladdery, S., 1994. QPX (Quahaug Parasite X), a pathogen of northern quahaug Mercenaria mercenaria from the Gulf of St. Lawrence Canada. Dis. Aquat. Org. 19, 129–136. https://doi.org/10.3354/dao019129

Wickham et al., 2019. Welcome to the tidyverse. Journal of Open Source Software, 4(43), 1686, https://doi.org/10.21105/joss.01686

Xie, Y., Sen, B., Wang, G., 2017. Mining terpenoids production and biosynthetic pathway in thraustochytrids. Bioresource Technology, SI:Algal Biorefinery 244, 1269–1280. https://doi.org/10.1016/j.biortech.2017.05.002

Zhang, P., Li, J., Lang, J., Jia, C., Niaz, S.-I., Chen, S., Liu, L., 2018. Two new sesquiterpenes derivatives from marine fungus Leptosphaerulina Chartarum sp. 3608. Natural Product Research 32, 2297–2303. https://doi.org/10.1080/14786419.2017.1408102

Zhao, J., Wu, J., Yan, F., 2014. A new sesquiterpenoid from the rhizomes of Homalomena occulta. Natural Product Research 28, 1669–1673. https://doi.org/10.1080/14786419.2014.934238

Zhou, P.-P., Lu, M.-B., Li, W., Yu, L.-J., 2010. Microbial production of docosahexaenoic acid by a low temperature-adaptive strain Thraustochytriidae sp. Z105: screening and optimization. J. Basic Microbiol. 50, 380–387. https://doi.org/10.1002/jobm.200900378

9   Appendix

200X *Pleurosigma* sp. and *Phycophthorum isakeiti*

200X Culture of healthy and dead *Pleurosigma* sp.

400X *Pleurosigma* sp. and *Phycophthorum isakeiti*

200X *Pleurosigma* sp. and *Phycophthorum isakeiti*

400X *Pleurosigma* sp. and *Phycophthorum isakeiti*

400X *Pleurosigma* sp. and *Phycophthorum isakeiti*

800X *Pleurosigma* sp. and *Phycophthorum isakeiti*

Aberrations to the cell wall associated with penetration

200X *Pleurosigma* sp. and *Phycophthorum isakeiti*

Dead
Healthy
Healthy
Infected
Infected
Dead

400X *Pleurosigma* sp. and *Phycophthorum isakeiti*

Zoosporic Settlement

400X *Pleurosigma sp.* and *Phycophthorum isakeiti*

Zoosporic Settlement

Free Zoospores

Dividing

200X *Pleurosigma sp.* and *Phycophthorum isakeiti*

Sporangium among infected and dead cells

400X *Pleurosigma* sp. and *Phycophthorum isake*
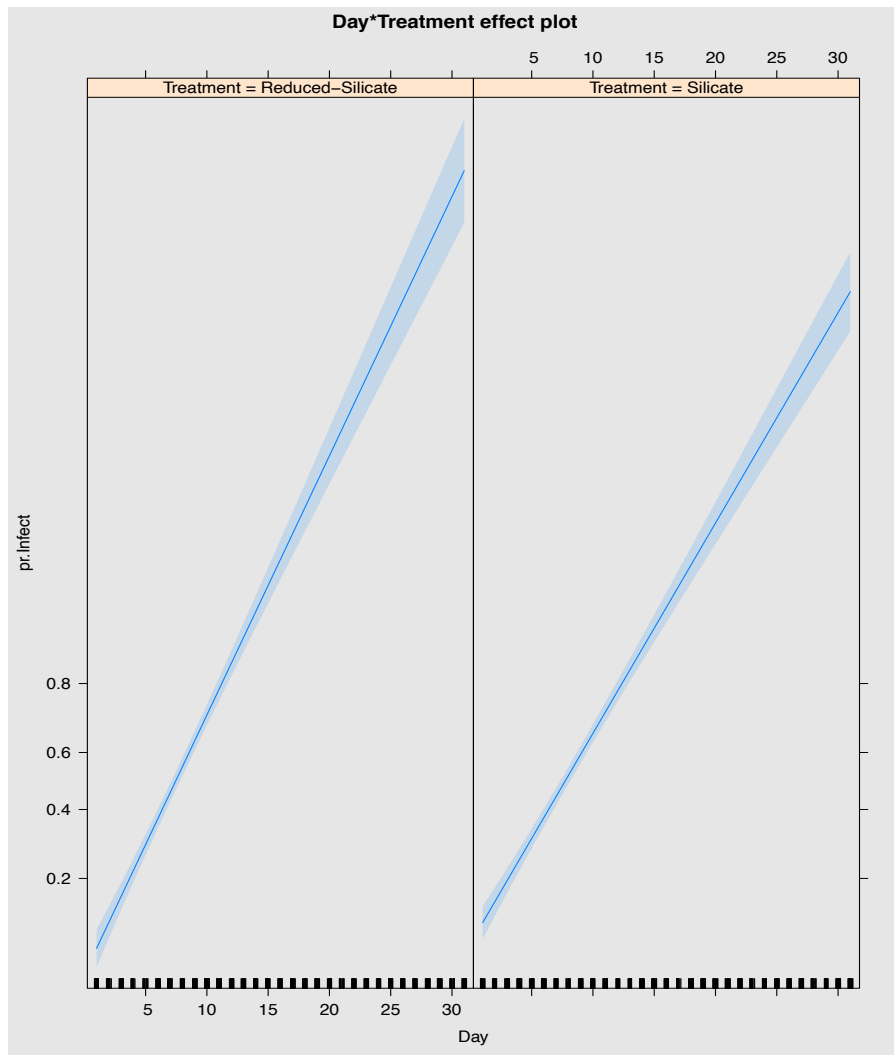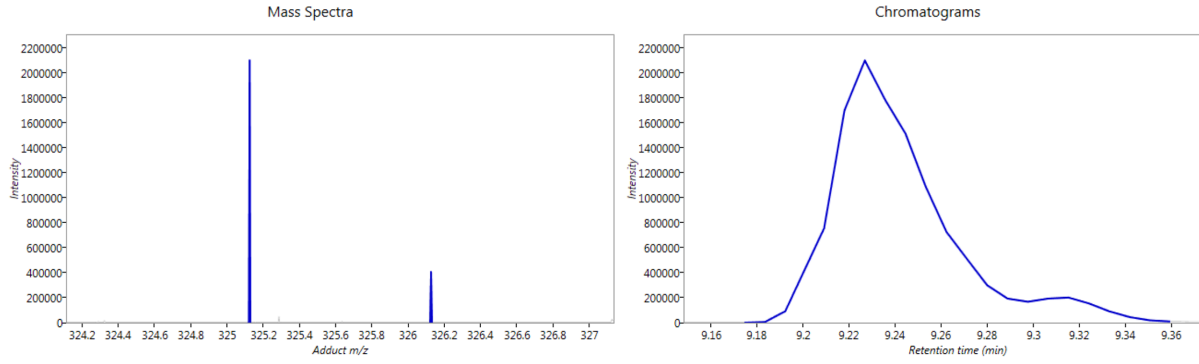
Appendix 1 Table of observational examples of health status (healthy, infected, dividing and dead) of *Pleurosigma* sp. under standard and reduced silicate media during infection by *P. isakeiti* from counting and nutrient analysis sampling


*Appendix 2 Rate of infection (log) in GGEffect (Pr.infect~Day*Silicate)*

Appendix 3 Compound eluted at retention time 4.2422 min (m/z 278.20923; $C_{17}H_{27}NO_2$) in extracts of infected *Pleurosigma* sp by *P. isakeiti* not detected in healthy *Pleurosigma* sp. cultures and media control extracts
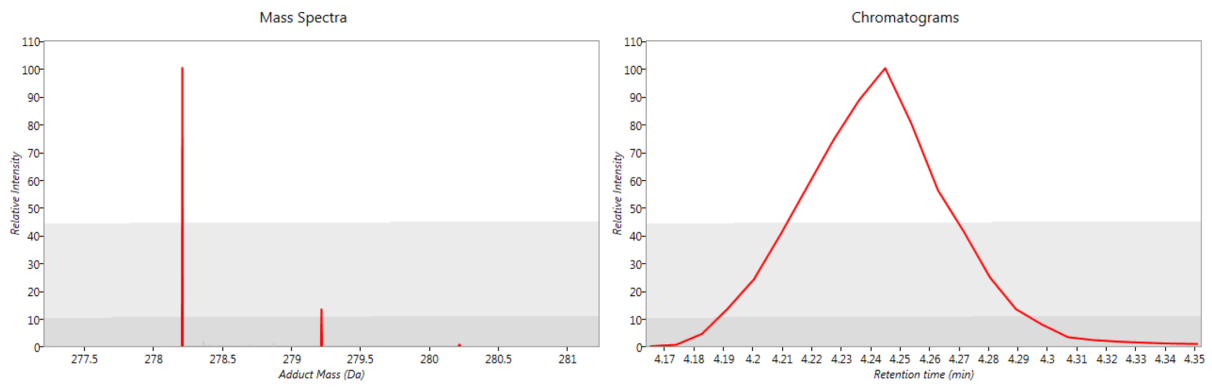
Appendix 4 Compound eluted at retention time 9.2357 (m/z 325.12084; $C_{23}H_{16}O_2$) in extracts of infected *Pleurosigma* sp by *P. isakeiti* not detected in healthy *Pleurosigma* sp. cultures and media control extracts
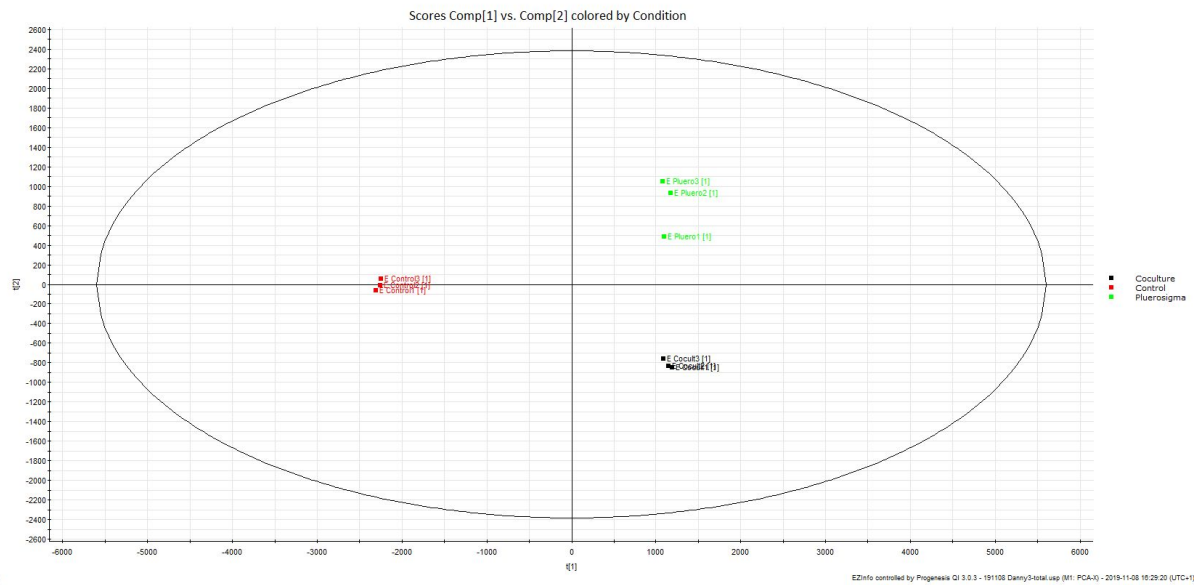
Appendix 5 PCA of healthy and parasitized *Pleurosigma* sp. extracts by P. *isakeiti*, and media controls

```
#Import and calculate proportions of infected and dividing
dt <- read.delim("thraustochytridinfection.txt", header = T)
dt$pr.Infect <- dt$Infect / (dt$Health + dt$Infect)
dt$pr.Divide <- dt$Divide / (dt$Health)
#Clean data
dt <- dt[dt$Rep != "Control",]
dt.corr=dt[which(dt$pr.Divide<=1),]
#Create models
Infmod <- glm(pr.Infect ~ Day * Treatment, data = dt.corr, family = "quasibinomial")
Divmod <- glm(pr.Divide ~ Day * Treatment, data = dt.corr, family = "quasibinomial")
#visualize models
plot(effects::allEffects(Infmod))
plot(effects::allEffects(Divmod))
#Extract model summaries
summary(Infmod)
summary(Divmod)
##Objective 3##
#How are the cells division and infection affected by silicate and nitrate uptake in infected and healthy
  cultures?
##Import data
NAt <- read.delim("NAt.corr.txt", header = T)
#Calculate Proportions
NAt$Infect <- NAt$Dead
NAt$pr.Infect <- NAt$Infect / (NAt$Health + NAt$Infect)
NAt$pr.Divide <- NAt$Divide / (NAt$Health)
NAt$NS <- NAt$NAtNO3.NO3 / (NAt$Silicate)
##Divide Cultures
NAtCoc=NAt[which(NAt$Culture=="Coculture"),]
NAtPl=NAt[which(NAt$Culture=="Pluerosigma"),]
##Create models##
#Coculture
Infmodco <- glm(pr.Infect ~ Day * Silicate, data = NAtCoc, family = "quasibinomial")
Divmodco <- glm(pr.Divide ~ Day * Silicate, data = NAtCoc, family = "quasibinomial")
InfmodcoN <- glm(pr.Infect ~ Day * NAtNO3.NO3, data = NAtCoc, family = "quasibinomial")
DivmodcoN <- glm(pr.Divide ~ Day * NAtNO3.NO3, data = NAtCoc, family = "quasibinomial")
InfmodcoNS <- glm(pr.Infect ~ Day * NS, data = NAtCoc, family = "quasibinomial")
DivmodcoNS <- glm(pr.Divide ~ Day * NS, data = NAtCoc, family = "quasibinomial")
#Healthy Pluerosigma culture
Divmodpl <- glm(pr.Divide ~ Day * Silicate, data = NAtPl, family = "quasibinomial")
DivmodplN <- glm(pr.Divide ~ Day * NAtNO3.NO3, data = NAtPl, family = "quasibinomial")
DivmodplNS <- glm(pr.Divide ~ Day * NS, data = NAtPl, family = "quasibinomial")
##Visualize models
plot(effects::allEffects(Infmodco))
plot(effects::allEffects(Divmodco))
plot(effects::allEffects(InfmodcoN))
plot(effects::allEffects(DivmodcoN))
plot(effects::allEffects(InfmodcoNS))
plot(effects::allEffects(DivmodcoNS))
plot(effects::allEffects(Divmodpl))
plot(effects::allEffects(DivmodplN))
```

```
plot(effects::allEffects(DivmodplNS))
##Extract model summaries
summary(Infmodco)
summary(Divmodco)
summary(InfmodcoN)
summary(DivmodcoN)
summary(InfmodcoNS)
summary(DivmodcoNS)
summary(Divmodpl)
summary(DivmodplN)
summary(DivmodplNS)
```

Appendix 6 R script for data analysis